8-1-1990

Distortion Induced Cracking in Steel Bridge Members

John W. Fisher

Jian Jin

David C. Wagner

Ben T. Yen

ADVANCED TECHNOLOGY FOR
LARGE
STRUCTURAL SYSTEMS

Lehigh University

DISTORTION INDUCED CRACKING IN STEEL BRIDGE MEMBERS

by

John W. Fisher
Jian Jin
David C. Wagner
Ben T. Yen

ATLSS Report No. 90 - 07

August, 1990

An NSF Sponsored Engineering Research Center

Acknowledgment

This work was sponsored by the American Association of State Highway and Transportation Officials, in cooperation with the Federal Highway Administration, and was conducted in the National Cooperative Highway Research Program which is administered by the Transportation Research Board of the National Research Council.

Disclaimer

12/28(6)

DISTORTION INDUCED CRACKING IN STEEL BRIDGE MEMBERS

FINAL REPORT

Prepared for

National Cooperative Highway Research Program
Transportation Research Board
National Research Council

John W. Fisher, Jian Jin, David C. Wagner, and Ben T. Yen
Center for Advanced Technology for Large Structural Systems
117 ATLSS Drive
Lehigh University
Bethlehem, Pennsylvania 18015

August 1990

Table of Contents

LIST OF TABLES

LIST OF FIGURES

ACKNOWLEDGMENTS

The research reported herein was performed under NCHRP Project 12-28(6) at the Fritz Engineering Laboratory, Lehigh University, Bethlehem, Pennsylvania. John W. Fisher, Joseph T. Stuart Professor of Civil Engineering, was principal investigator. The other authors of this report are Ben T. Yen, Professor of Civil Engineering; Jian Jin, former Research Assistant (engineer with City of Philadelphia); and David C. Wagner, former Research Assistant (engineer with Gilbert Associates).

Special thanks are extended to ATLSS staff members Richard Sopko, who was responsible for photographic coverage, and John M. Gera who assisted with the illustrations. Thanks are due ATLSS and Fritz Laboratory foremen Robert Dales and Charles Hittinger and their staff for assistance during the test setups and experimentations.

Thanks are also due Dr. George R. Irwin for his review and comments.

SUMMARY

The research described in this report is the result of a review of existing experimental field studies and experimental work performed in the laboratory under NCHRP Project 12-28(6). It provides a detailed review of the experimental studies undertaken on a variety of bridges that had experienced fatigue cracking as a result of web gap distortion. This review provided information of girder-floorbeam bridges, multigirder bridges, box girder bridges and tied-arch bridges with box girder tension ties.

The review of field measurements indicated that floorbeam-girder connection plates provided about the highest cyclic stresses in the web gap adjacent to the top flange. Floor beams connected to box tie girder members in tied arch bridges also resulted in relatively large web gap cyclic stresses as a result of internal diaphragms that were not positively attached to the flanges.

Multigirder bridges without staggered diaphragms were found to have cyclic stress about half the magnitude of the floorbeam-girder bridges. As a result cracking took longer to develop and was not as extensive as was observed in the floorbeam-girder bridges.

Structures with lateral bracing web gusset plates that were not provided with a positive attachment between the gusset plates and the transverse stiffeners were found to be very susceptible to distortion in the gap between the gusset and transverse connection plate. Cyclic stresses were observed to approach 30 ksi (207 MPa) in these gaps.

The experimental laboratory data from the transverse connection plate web gaps and the lateral gusset plate web gaps demonstrated that the fatigue resistance from the web gap was equivalent to Category C of the AASHTO Fatigue Resistance Curves. For the transverse connection plate web gap, cracking generally developed first at the end of the connection plate. For the lateral gusset plate web gap, cracking only occurred along the web welded toe of the transverse connection plate.

The study demonstrated that an accurate prediction of web gap cyclic stress was not likely from design models of the structure. Hence, rules providing for positive attachment of transverse connection plates to the flanges were necessary in order to minimize web gap distortion and cracking.

The study also indicated that welded connections were more resistant to web gap distortion than bolted connections. As a result, an increase in the size of web gap was recommended for bolted connections.

Recommendations are provided in this report for changes in the provisions for end connections for stringers and floorbeams. These recommendations provide an extension compatible with the provisions adopted by AASHTO for transverse connection plates at diaphragms.

CHAPTER ONE
INTRODUCTION AND RESEARCH APPROACH

PROBLEM STATEMENT AND BACKGROUND

During the past seventeen years, extensive fatigue cracking has developed in a wide variety of steel bridges due to unanticipated out-of-plane distortions. These cracks often occurred after only a few years of service because of the high distortion-induced stress ranges which developed under normal traffic loadings.

Several hundred bridges have developed fatigue cracks as a result of out-of-plane distortion in small gaps *(1, 2, 3, 4, 5, 6, 7)*. Most often this was a segment of a girder web. When distortion-induced cracking develops in a bridge, the structural features which are causing it are usually repeated in the bridge structure, and large numbers of cracks may form before corrective action is taken. Early detection of distortion cracking is therefore desirable. This permits more complete assessment of cracking damage and allows other potential cracking locations to be identified. Retrofit methods which assist repair of regions with observed cracking can be employed to prevent cracking at these other locations. In this way development of widespread cracking damage in the bridge can be prevented.

Displacement induced fatigue cracking has developed in many types of bridges, including trusses, suspension bridges, girder floorbeam bridges, multibeam bridges, tied arch bridges and box girder bridges. Cracks have mainly formed in planes parallel to the stresses from loading, and so these cracks have not been detrimental to the performance of the structure providing they were discovered and retrofitted before turning perpendicular to the applied stresses from loads. In some structures the cracks have arrested in low stress areas and thus have served to relieve local restraint conditions.

Conditions which resulted in web gap cracks have often developed because of the desire to avoid welding transverse stiffeners, that serve as connection plates, to the tension flanges. Figure 1 shows a schematic of a condition that exists in floorbeam-girder bridges. Figure 2 is typical of the cracks observed at a floorbeam web gap.

Other examples of web gaps abound. They include diaphragm connection plates in multibeam bridges and internal diaphragms in box girders including box tie girders.

Current designs are required by the AASHTO Specifications to provide a positive attachment between the transverse connection plate for diaphragms and X-frames and both girder flanges *(8)*. This decreases the web gap distortion to acceptable levels providing the web gaps at the copes are at least 2 in. (51 mm) or four times the web plate thickness whichever is larger.

In addition to the web gaps at the ends of transverse connection plates, cracking has also been observed in the web gaps of lateral gusset plate details *(3, 5, 7)*. In order to distribute transverse wind loads, lateral bracing is often placed between adjacent girders on longer span structures. Earlier specifications required such bracing for spans over 125 ft.

(38.1 m) long. However, current specifications *(8)* have increased the governing span length and provided additional design criteria. The attachment of bracing members is often made through gusset plates which are connected to the web plates. The lateral bracing system may be designed to interact with the main girders or to simply transfer the forces generated by wind. If the system is intended to interact with the main load carrying members, then the lateral bracing may be subjected to the same stress cycles as the main girder.

Regardless of interaction with main members, lateral gusset plate attachments result in a detail with low fatigue resistance. The welded connection accommodates the small out-of-plane displacements necessary to induce relatively high stress ranges in web gaps. These displacements, though often on the order of only 0.004 in. (0.1 mm), are accommodated within the segment of web plate bounded by the transverse stiffener weld toe and the inside of the gusset plate edge as illustrated in Figure 3. The out-of-plane deflections generate, in the unstiffened gaps, secondary bending stresses which are often sufficient to initiate cracking at weld toes. These secondary stresses are not calculated in normal rating procedures nor accounted for in the current design process. Thus, fatigue provisions have not been applied to this type of cracking.

The longitudinal web gap, present in most gusset plate connections for lateral bracing, typically ranges from 0.25 in. to 4 in. (6.4 to 101.6 mm) in length. Details which include the smaller gaps increase the risk of cracking at the intersection of the transverse stiffener weld and the longitudinal gusset plate weld. Restraint due to large shrinkage strains along these welds, elevates the local stresses within the smaller gap. Further problems may arise from lack of fusion or slag inclusions which may exist at such intersections. Larger gaps are more flexible and can better accommodate out-of-plane displacements. The magnitude of distortion-induced fatigue cracking is directly related to the length of web plate over which the distortions must be absorbed.

With damage accumulating for each stress excursion above the detail's fatigue limit, a crack may initiate at the toe of a weld after only a brief period in service. The initial crack will grow perpendicular to the largest cyclic stresses. At longitudinal web gaps, the greatest restraint is provided by the boundaries at the ends of the web plate adjacent to the stiffener weld and the inner edge of the gusset plate as was shown in Figure 3. This restraint generates large secondary stresses. Consequently, gusset plate web gaps must undergo the simultaneous effects of primary, in-plane bending stresses and secondary, out-of-plane displacement-induced stresses. Thus, the horizontal gaps are very susceptible to fatigue crack growth and pose a serious threat to the servicability of the bridge. This was confirmed by observations on several bridge structures as detailed in References 5 and 7.

OBJECTIVES AND SCOPE

The work in this project was directed toward the creation of a database to aid in the development of guidelines for the prevention and repair of distortion-induced fatigue cracking at transverse connection plate and lateral gusset plate details. Due to the lack of laboratory information on the types and behavior of fatigue cracks which form within or adjacent to these details, this work focuses primarily on experimental studies. With the

information compiled on the stress magnitudes actually experienced by a number of bridge structures while in service *(5, 9)*, the experimental studies simulated detail behavior under controlled conditions. These studies involved altering and examining the numerous variables associated with distortion-induced fatigue cracking.

Transverse Connection Plate Details

The available experimental data was not well defined nor was it known if it was directly applicable to actual bridge structures. The small simulated test specimen was known to provide an upper bound to fatigue strength. The available full scale tests were not applicable to details that had been cracked and then retrofitted with drilled holes when out-of-plane deformations continued.

The objectives of the transverse connection plate study reported here were:

1. To provide experimental data to define the fatigue strength of web gaps comparable in size to the range of 1½ in. (38 mm) and 3 in. (76 mm). This is most common in bridges.
2. To determine whether or not drilled holes would effectively stop crack growth at web gap cracks.
3. To determine the influence the in-plane stress range has on web gap cracking behavior.
4. To evaluate the fatigue behavior of drilled retrofit holes when supplemented by a direct attachment of the transverse connection plate with a bolted tee connection to the girder flange. An alternate condition of removing part of the connection plate to soften the web gap region was also assessed.

During the experimental research program, 12 full size girders were fabricated from ASTM A36 steel and fatigue tested to determine their fatigue strength and behavior at the transverse connection plate web gaps and to further evaluate techniques intended to extend their fatigue life so that the web gap cracking would not adversely impact the girders in-plane bending resistance.

The beams were tested in pairs under two levels of constant amplitude cyclic loading. After cracks developed in the web gap at a particular connection plate defining its fatigue life, this connection plate web gap was retrofitted by drilling holes at the crack tips and the test proceeded to ascertain the effectiveness of the drilled holes and other supplemental changes to further the fatigue life of the cracked girder web.

Lateral Gusset Plate Details

Classification of a lateral detail's severity is based on the structural variables which influence the degree of distortion-induced cracking, as well as the geometry and nature of the detail itself. A careful correlation of the following variables with those values and with magnitudes reported in field studies permitted such a classification:

1. The in-plane stress range generated at the level of the lateral gusset plate under a prescribed loading.
2. The specific horizontal web gap geometry.
3. The means of gusset plate attachment and degree of physical displacement.
4. The magnitude of the transverse forces which depends on:
    a. The system by which the driving force is transmitted to the gusset plate.
    b. The actual magnitude of the resulting driving force.
5. The magnitude of the secondary stress range induced within the web plate by lateral displacement.

Since the gusset plate is often coped to fit around the stiffener or connection plate, an unrestrained web gap may exist depending upon the means by which the gusset plate is connected to the transverse plate. Many existing structures have made use of gusset plates with no positive connection to the stiffener. However, more bridges include gusset plates that are attached to the transverse connection plate with welded or bolted parts. This research study investigates the behavior of three lateral gusset plate connections:

1. A gusset plate welded to the girder web and the transverse connection plate (Detail A).
2. A gusset plate welded to the girder web and bolted to the transverse connection plate (Detail B).
3. A gusset plate free of attachment to the transverse connection plate, but welded to the girder web (Detail C).

These details are shown in Figure 4.

Thus,details including positive attachment were studied as well as a connection free of such lateral restraint. After a degree of fatigue crack development had been experienced, retrofit procedures were examined. These included the introduction of drilled holes at the leading crack tips within the horizontal web gap and further lateral restraint through the introduction of additional positive attachment between the gusset plate and the transverse plate.

This investigation provides valuable insight into the behavior of lateral gusset plate attachments which have been found to be susceptible to distortion-induced fatigue cracking. A better understanding of secondary distortion should minimize the use of poor details in new structures as well as permit retrofit schemes to be developed.

RESEARCH APPROACH

Available experimental field measurements were examined and evaluated to ascertain the magnitude of out-of-plane distortion and the resulting web gap stresses at the weld boundaries. The most comprehensive measurements were provided by the studies reported in References 9, 13, and 18 which described the measurements and analysis carried out on the PennDOT study on Causes of Deformation Induced Cracking and in References 14, 16, 19,

and 20 from other test programs. These studies are reviewed in Chapter 3. The review included floorbeam-girder bridges, multiple girder bridges with diaphragms and floorbeam-box tie girder systems. These measurements are always in a region with substantial stress gradient. Hence, it is necessary to extrapolate from the measured values and to obtain approximations of the stresses at the weld toes where the fatigue cracks initially form. The results of this review were used to establish the stress range levels for the experimental study.

Laboratory Tests

Altogether 18 full size welded girders were tested during this research project. Twelve of the girders had transverse connection plates attached to the girder webs and were tested in pairs in order to impose out-of-plane distortion in the web gap. The other 6 girders had transverse connection plates and lateral gusset plates attached to the girder webs. Each girder consisted of a 10 ft. (3048 mm) test section and two 8 ft. (2438 mm) end connections that were bolted to the test section as illustrated in Figure 5.

The 10 ft. (3048 mm) test section for the transverse connection plate tests can be seen in Figure 6. The girders were 36 in. (914 mm) deep and had 3/8 in. (9.5 mm) thick web plates. The connection plates were welded to the girder web and top flange and had 1 1/2 in. (38 mm) and 3 in. (76 mm) web gaps adjacent to the bottom flange. The end sections were 42 in. (1067 mm) deep built-up sections with a secondary flange to accommodate the test girders and can be seen in Figure 7. The 10 ft. (3048 mm) test sections for the gusset plate test are detailed in Figure 8. All girders were tested on a 25 ft. (7620 mm) span.

The gusset plate connections had three configurations as illustrated in Figure 4. The three details were identified as Details A, B, and C. Detail A was a 18×14×1/2-in. (457×356×12.7-mm) gusset plate welded to the web and the transverse stiffener with 5/16 in. (7.9 mm) welds. The interior corners were coped 2 in. (51 mm). Detail B had the gusset plate cut to fit around the transverse stiffener and was provided with 1 1/2 in (38 mm) and 3 in (76 mm) nominal web gaps on each side of the transverse connection plate. A positive attachment was provided between the gusset plate and the transverse stiffener by bolting a structural T-section (WT5 x 6) to both gusset plate and transverse stiffener as illustrated in Figure 9. Detail C included a 6 in. (152 mm) deep cut rounded to prevent contact with the 5 in. (127 mm) stiffener. Nominal web gap sizes of 1 in. (25 mm) and 3 in. (76 mm) resulted and no positive attachment was provided between the gusset plate and the stiffener. All bolted attachments were connected with 7/8 in. (22 mm) A325 high strength bolts.

Coupon tension specimens taken from the girder flanges (ASTM A370) gave average yield points of 36 ksi (248 MPa) and tensile strength of 58 ksi (400 MPa).

For this test program, the girders with transverse connection plates were subjected to two levels of nominal flexural stress range in the girder flange: 6 ksi and 12 ksi (41.4 and 82.8 MPa) over the center 5 ft. (1524 mm) containing the test details (see Figure 5). Figure 10 shows the factorial experimental arrangement of the details and test girders. The six pairs of girders were tested in compliance with the scheme shown in Figure 11. As can be seen in Figure 10, the out-of-plane distortion stress range corresponded to three levels designated as

low, intermediate, and high. The actual stress range was based on measured strains in the web gap region and their extrapolation to the weld toe.

The girder gusset plates were all subjected to a single level of stress range of 6 ksi (41.4 MPa), due to in-plane bending at the lateral gusset plate level, as the same 5 ft. (1524 mm) constant moment region was utilized for these girders. Since only six girders (3 pairs) with two gusset plates were tested, it was apparent that replicas would not be possible since three types of gusset plates were being examined. Figure 12 (a) shows the partial factorial for web gap size and detail type. The paired test girders and their details are shown in Figure 12 (b). The out-of-plane web gap stress range was "low", i.e., in the range 10 to 15 ksi (69 to 104 MPa) or "high" in the range of 18 to 31.5 ksi (124 to 217 MPa).

All girders were fabricated by Lehigh Structural Steel Co. at a local fabrication shop in Allentown, Pa. The fabricator was instructed to use normal bridge fabrication and inspection procedures. The web-flange weld area was preheated to 100 ° F (38 ° C) before the welded connection was made. E7018 electrodes were used to attach the stiffeners and lateral gusset plates to the girder webs and other attachment points. No holes were cut in the gusset plates at time of fabrication. This work was carried out in the laboratory after the bracing properties and bolt patterns were fixed. Five of the girders had excessive web distortion from the welding process. These were corrected by local heating.

Test Procedures

All girders were tested on the dynamic test bed in the Fritz Engineering Laboratory at Lehigh University. Figure 13 shows two girders under test in the dynamic test bed. The cyclic loading was applied to each girder by two Amsler jacks (see Figure 5) 5 ft. (1524 mm) apart. Either four 55 k (245 kN) jacks or four 100 k (445 kN) jacks were used to apply the cyclic load with a pair of Amsler variable stroke hydraulic pulsators. Loading was applied at a constant frequency of 260 cycles per minute (cpm). The minimum applied stress was always tensile but generally less than 1 ksi (6.9 MPa). All testing was carried out at room temperatures between 60 ° F and 90 ° F (15 ° C to 33 ° C).

Prior to subjecting the test girders to cyclic loading, the members were gaged to determine the in-plane bending stress with strain gages on the girder flanges. In addition each web gap region was instrumented with either strip gages for small gaps or several discrete gages for larger web gaps. From 45 to 60 strain gages were installed on each pair of test girders. Heavy sections were clamped to the bottom tension flanges between the adjacent girders below the transverse connection plates. These struts prevented the tension flanges from rotating or translating out of the plane of the web plate. This restraint is similar to the restraint provided by an overlaying concrete deck in the negative moment region of a girder. Figure 14 shows the heavy sections clamped to the girder tension flanges and the adjustable steel rods used to impose out-of-plane distortion.

The adjustable steel rods shown in Figure 14 were fabricated from 2½ in. (63.5 mm) and 3 in. (76 mm) steel pipe. The 3 in. (76 mm) pipe was used as sleeve and was threaded for 9 in. (229 mm) with 8 threads per inch. The 2½ in. (63.5 mm) pipe was machined and

threaded to fit into the sleeve. This permitted the rod length to be adjusted so that the length and angle could be changed to control the magnitude of the out-of-plane distortion. Figure 15 shows a schematic of the test girder cross-section with the strut, lateral bracing, and driving rods in place. Each rod was gaged and calibrated to permit the measurement of the cyclic rod force being introduced into the girder by the vertical deflection from the jacks. Two lateral tee's were used between the gusset plates as illustrated in Figures 4 and 9. This provided symmetry and prevented uncontrolled twisting of the gusset plates.

Static calibration tests were carried out prior to cyclic loading and at periodic intervals during the fatigue tests. Strains and web gap distortion were recorded for seven to ten load increments up to the maximum jack load. The tension flange strains and vertical girder deflection were used to control the magnitude of the in-plane bending stresses. Because the driving rods reacted directly against the jack loads, the measured girder stresses were necessary for control of the experiments.

A finite element model was used to provide an indication of the desired angle of the driving rod necessary to produce the desired level of distortion induced stress. This expedited the test set-up and minimized the experimental adjustments.

The pairs of test girders shown in Figures 11 and 12 (b) had adjacent details assigned on the basis of the number of detail types, the web gap size, and the degree of anticipated web gap lateral distortion each might undergo. They were matched between adjacent test girder sections as much as practical (see Figures 10, 11, and 12). The pairs of girders were cycled until a crack was detected at one or more details or until at least ten million cycles had been applied to the girders. As cracks developed at a given detail they were permitted to propagate through the web thickness before an appropriate retrofitting procedure was used to stop crack growth and allow continued testing of the girders.

Retrofitting Procedures

The fatigue cracks that formed in the various web gaps always developed at a weld toe as surface cracks. Since each gap was instrumented, changes in the gage response helped in the crack detection. Generally the cracks were between 1 and 1.4 in. (25 to 35 mm) long at the time of detection. Initially 3/4 in. (19 mm) holes were drilled at the crack tips when the crack length was 2 to 6.8 in. (50 to 170 mm) long. Cyclic load was continued to determine the effectiveness of the retrofit holes and observe changes in the flexibility of the web gap. Generally the driving rod force was observed to decrease as a result of the cracked web gap.

When the crack re-initiated at the retrofit holes, further holes were installed of larger diameter from 1 in. (25 mm) to 1 1/2 in. (37.5 mm). It was observed that the stress range below the hole increased at the gusset plate details which tended to lead to rapid re-initiation of the crack. A bolted attachment was introduced to decrease the stress range below the hole and this generally prevented further crack re-initiation.

CHAPTER TWO
FINDINGS

The findings of the review of web gap cracking and the experimental studies of NCHRP Project 12-28(6) are summarized in this chapter. A detailed evaluation of the experimental data is given in Chapter Three. The documentation of the test results is provided in Appendices A and B.

LITERATURE SURVEY OF LABORATORY AND FIELD TESTS

A limited amount of laboratory testing has focused on distortion-induced fatigue cracking. The only known study was reported in *NCHRP Report 206 (10)*. Testing was conducted on five full scale welded girders with multiple stiffeners. Web cracking within the transverse gaps at stiffeners was introduced by an externally applied load (displacement) with the girder flat, and under no in-plane loading. The adequacy of a retrofit procedure was then tested under in-plane bending stresses only, with no further distortion introduced. The study deformed the web gap using deflection control and provided no direct measurement of out-of-plane bending stress. No in-plane stress was combined with out-of-plane distortion.

The only other experimental data were tests made on small specimens to simulate the flange-web boundary of plate girders *(11, 12)*. These experiments were used to assess the potential for fatigue cracking from pumping of the plate girder web. Figure 16 shows the results of these experiments in the form of the classical *S–N* curve.

These tests on small T-type specimens simulating the web-flange connection indicated that out-of-plane web bending stresses provided a fatigue resistance compatible with Category C.

The review of available experimentation on bridge structures developing web gap cracking have verified that out-of-plane distortion is the cause of the web gap cracks. These studies indicated that floorbeam-girder web gaps adjacent to the top flange generally experienced the largest out-of-plane movement. The displacements were equal to 0.02 to 0.04 in. (0.5 to 1 mm) with corresponding stress ranges between 20 and 40 ksi (138 to 276 MPa). When no cracks formed at the floorbeam-girder web gap, the distortion was generally less than 0.004 in. (0.1 mm) and the cyclic stress was generally less than 10 ksi (69 MPa) *(5)*. The measurements indicated that web gap regions are always subjected to gradients from the out-of-plane distortion. This resulted in high cyclic stresses at web gap weld toes.

Multigirder bridges without staggered diaphragms were found to experience distortions less than 0.02 in. (0.5 mm) which caused cyclic stresses between 10 and 20 ksi (69 to 138 MPa) *(7, 9)*. Measurements were not available on staggered diaphragms but the degree of cracking in actual bridges appeared comparable to floorbeam girder bridges. Also, the bottom flange web gap often cracked in structures with staggered diaphragms.

At lateral gusset plate connections which framed around transverse connection plates at floorbeams, two types of details have available measurements. In one case no attachment

was provided between the lateral gusset plate and the transverse connection plate. The resulting web gaps were found to be 0.25 to 1 in. (6 to 25 mm). The maximum stress ranges were found to vary between 15 and 20 ksi (105 to 138 MPa) at the weld toes *(5, 7)*. In a second structure high strength bolts were used to connect the welded gusset plate to the transverse connection plate *(13)*. The web gaps were about 1½ in. (38 mm) and maximum stress ranges at the transverse weld toe were observed between 13 and 27 ksi (93 to 186 MPa). These stresses resulted from the floorbeam end rotation and the lateral members restraining forces.

The limited measurements at lateral gusset plates which frame around transverse connection plates demonstrate that large web gap bending stresses result when there is no positive attachment between the lateral gusset plate and the transverse connection plate.

Box girder components subjected to web gap distortion, such as internal diaphragms at tie girder-floorbeam connections, were observed to provide cyclic stresses nearly as large as the floorbeam-girder structures. This led to early cracking in these structures. These types of details were not examined in this study.

DISTORTION CRACKING IN THIS STUDY

Visual inspection with a 10X magnification during the experimental study helped reveal the presence of cracks in the web gap regions. These observations were augmented with the strain gage measurements. These gages, which were sensitive to the crack development and sudden changes, were used to focus the visual examination.

The short web gaps of the transverse connection plate details tended to promote cracking through the weld bead which extended beyond the end of the connection plate. When the gap was greater than 1½ in. (37 mm) the cracks tended to form at the weld toe.

At the lateral gusset plate details cracking developed only along the weld toe of the transverse connection plates. At the transverse connection plate web gap adjacent to the flange, cracks formed first mostly at the end of the connection plate.

FATIGUE BEHAVIOR OBSERVED AT WEB GUSSET PLATES

No fatigue cracking developed at either end of the fillet welds connecting the gusset plates to the web. The direct addition of in-plane and out-of-plane bending stresses provides a stress range which over-estimates the seriousness of the detail. In-plane loading alone provides a fatigue resistance equal to Category E as was demonstrated in *NCHRP Report 227 (14)*. At the exterior weld ends the combined stress was well above the fatigue limit for Category E yet no cracks developed.

Cracking in the web gap between the transverse connection plate and the gusset plate always developed along the transverse connection plate weld. The experimental results demonstrated that the fatigue strength of the web gap was consistent with the fatigue strength provided by Category C of the AASHTO Specifications *(8)*.

None of the Detail A and Detail B lateral gusset plates developed web gap cracking when the distortion induced stress range was less than 15.5 ksi (107 MPa) even though subjected to 10 to 20 million stress cycles. The level of stress range was well above the fatigue limit for Category E. Cracking occurred at all four C details and at Type B detail when cyclic web gap stresses exceeded 19.5 ksi (134 MPa).

Finite element models of the gusset plate, transverse connection plate, and girder provided web gap stress gradients that were compatible with measured results. A higher web gap stress was produced at the transverse connection plate weld than at the end of the gusset plate weld. This predicted behavior was in general consistent with the experimental measurements.

The experimental studies and the finite element models both indicated that it was desirable for lateral gusset-transverse connection plates to have a positive attachment when they intersect.

FATIGUE BEHAVIOR OBSERVED AT TRANSVERSE CONNECTION PLATES

Fatigue cracks usually formed at the ends of the transverse connection plates when subjected to web gap distortion. Thirteen of 15 details cracked at the connection plate end during the course of this study.

The fatigue strength of the web gap was consistent with the fatigue strength provided by Category C for the transverse connection plate details.

Although the measured stress range was often higher at the web-flange weld, the unusually smooth weld profile of that region resulted in much higher fatigue resistance. As a result only two cracks formed at the web-flange weld.

RETROFITTING PROCEDURES DURING THIS STUDY

Placement of holes at crack tips was an effective means of arresting fatigue cracks originating from transverse connection plate ends when the cyclic stress was less than 15 ksi (105 MPa). A positive attachment between the transverse connection plate and the beam flange was necessary when the cyclic stress in the web gap exceeded 15 ksi (105 MPa). Holes placed at the crack tip then insure that no further crack extension will develop.

When lateral gusset plates frame around a transverse connection plate, web gap distortion and cracking will occur if no positive attachment is provided. Holes drilled at the crack will only temporarily arrest crack growth unless a direct attachment is provided between the gusset and transverse connection plate.

During this study it was observed that drilled holes at the crack tip which satisfied the relationship $\Delta K/\sqrt{\rho} < 4\sqrt{\sigma_y}$ developed in Reference 14 were found capable of preventing re-initiation of the distortion induced fatigue cracks. ΔK is the stress intensity range for the through thickness crack, ρ is the radius of the drilled hole, and σ_y is the yield point of the web

plate. This resulted in a limiting value of $\Delta K/\sqrt{\rho} <$ 24 ksi (166 MPa).

CHAPTER THREE
RESULTS AND EVALUATION OF EXPERIMENTAL DATA

The results of the literature review, analytical studies, and laboratory experiments are summarized in this chapter. The fatigue characteristics of two types of web gaps were examined in this study. It includes the behavior of gusset plates welded to the web of welded girders and framed around a transverse connection plate. This resulted in web gaps susceptible to distortion. Three types of gusset plate details were examined in this study. The second type of detail examined was at the end of transverse connection plates where a web gap exists between the end of the connection plates and the web-flange fillet welds.

Each of these two web gap details were subjected to out-of-plane cyclic stress and concurrent in-plane cyclic stress. The stress range in the web gap resulted in web gap cracking in about half of the details that were tested. After cracks developed in the web gaps and had propagated through the web thickness, the cracked details were retrofitted in order to permit continued cyclic loading of the test girders. This permitted the uncracked details to be subjected to significant numbers of additional stress cycles and also allowed the retrofit procedure to be evaluated for effectiveness.

Among the procedures used to arrest crack growth and extend the fatigue life were drilled holes at the crack tips and introduction of a positive attachment to reduce web gap distortion.

LITERATURE REVIEW

Floor Beam Connection Plates

Extensive cracking has developed in web plates at the ends of floor beam connection plates. Studies indicate the cracking to be the direct result of cyclic, secondary bending stresses which are generated through relative out-of-plane movements. These displacements, though often less than only 0.005 in. (0.13 mm), concentrate in gaps between the floor beam connection plate and the girder tension flange as illustrated in Figures 1 and 2.

This mode of fatigue cracking was found at numerous web gaps on the web of main girders on the Woodrow Wilson Bridge *(15)*. The structure consists of ten approach units, a 212 ft. (64.6 m) span, and another eight approach units. The multiple, continuous girder spans range from 62 ft. (18.9 m) to 184 ft. (56.1 m) in length. Floor beams supporting longitudinal stringers are 25.7 ft. (7.8 m) long and 36 in. (914 mm) deep. An investigation of strain measurements indicates the magnitude of stresses within a typical distorted web gap. No positive attachment was made between either flange and the connection plate. The original deck slab was cast directly on the outside main girder, but supported by stringers and floor beams within the interior. Thus, the slab restrained the top flange of the main girders and resulted in out-of-plane distortion within the web gap as the transverse floor beam deforms. When the measured stresses were extrapolated to the longitudinal weld toe at the top of gap, a stress of 10 to 12 ksi (69 to 83 MPa) often resulted based on surface strains

measured 0.65 in. (16.5 mm) away from the connection plate. Finite element analysis demonstrated that the stresses within the gap can be two to three times greater than those recorded outside the local region *(16)*.

The stress range spectrum for a gage in the gap indicated that maximum stress range often exceeded 12 ksi (83 MPa) and a Miner's effective stress range of 3 ksi (20.7 MPa) was common. The Miner's effective stress range is defined as $S_{re} = \left(\sum \gamma_i S_{ri}^{\ 3} \right)^{1/3}$ where γ_i is the percentage frequency of occurrence of stress range S_{ri}.

Similar cracking developed in main girder web gaps at the floor beam connection plates of the Poplar Street Bridge, East St. Louis, Illinois *(17)*. The two girder structure has both straight and curved spans. Six continuous spans range from 75 ft. (22.9 m) to 100 ft. (30.5 m) in length. In the negative moment region, the floor beam connection plates are attached to the compression flange. The corresponding stiffener on the exterior face of the girder is only fitted to the compression flange and cut 5/8 in. (16 mm) short of the tension flange. The floor beam attachment in the positive moment region is similar except that the bottom flange is in tension. At piers, floor beams are connected directly to bearing stiffeners, which are tightly fitted to both top and bottom flanges and welded only to the girder web. Cracks developed in the web gaps of each of these three types of connection plates.

Nine bearing stiffener-to-floor beam connections were monitored. Web gap gages were mounted directly opposite each other on the web. The measurements indicated that the web gap was undergoing out-of-plane bending. A summary of selected field measurements is presented in Table 1. The web gap stresses have been adjusted to the flange-to-web weld toe for the maximum values measured and for those recorded during typical truck traffic.

Further cracking developed in the web gaps located at the first-interior floor beam connections. A listing of crack length and the corresponding maximum displacements measured under normal traffic is presented in Table 2. The general trend indicated a direct relationship between the out-of-plane displacement and the length of the existing crack. The measured displacements at the uncracked sites are on the order of those recorded at the bearing stiffener gaps, while at the cracked locations, sufficient flexibility allows displacements 10 to 20 times larger than those at the bearing stiffeners.

Under controlled loading, a 1/2 in. (12.7 mm) web gap experienced cyclic double curvature. Gages mounted on opposite surfaces of the web plate within the gap revealed both tensile and compressive stresses of 9 ksi (62.1 MPa) at the longitudinal weld toe. The exterior face was in tension at the horizontal flange-to-web weld. A corresponding out-of-plane displacement of 0.025 in. (0.64 mm) was measured. Review of field data indicates that the magnitude of this displacement and the corresponding stresses of the web are typical of floor beam connection plate gaps in the range of 1/4 in. to 3/4 in. (6.4 to 19.1 mm). Similar connections with the connection plate tightly fit to the tension flange during fabrication have smaller out-of-plane displacements, but the corresponding stresses could still be relatively high. Stresses of 22 ksi (151.7 MPa) with a simultaneous out-of-plane displacement of only 0.008 in. (0.2 mm) have been recorded at such sites.

The Canoe Creek Bridge in Clarion County, Pennsylvania also experienced cracking at

the floor beam connection plates cut short of the top flange in the negative moment regions *(13)*. The structure consists of separate bridges for the east and west bound traffic. Each bridge is a twin girder-floor beam type structure consisting of five continuous spans and a simply supported multi-girder end span. The continuous span structure consists of two 135 ft. (41.5 m) end spans and three 162 ft. (49.4 m) spans. Extensive cracking had developed in the top web gaps and had been temporarily arrested a number of times with drilled holes. Strain measurements adjacent to retrofit holes 6 in. (152.4 mm) from the top flange along the transverse connection plate and 4 in. (101.6 mm) along the web-flange weld provided stress range values between 15 ksi (105 MPa) and 25 ksi (175 MPa) and large numbers of smaller secondary cycles during a truck passage, which resulted in cracks reinitiating at the retrofit holes.

Multiple Girder Diaphragm Connection Plates

Similar web gaps exist at the junction of longitudinal girder flanges and the transverse connection plates of diaphragms or cross-bracing in multi-girder bridges. The transverse connection plate is often cut short of the tension flange. The gap formed by this geometry undergoes cyclic out-of-plane distortion induced through the differential vertical movement of adjacent girders. As the girders deflect, the diaphragms transfer lateral forces sufficient to cause the transverse connection plate to displace and rotate out of the plane of the web plate. If the lateral bracing members are of considerable depth or stiffness, the displacements and rotations may become substantial. The magnitude of the out-of-plane movements and rotations are governed by the girder spacing, skewness of the bridge, and the geometry and rigidity of the diaphragm.

Cracks develop in the web plate within the gap along the web-flange weld toe and across the ends of the transverse connection plate welds in both the positive and negative moment regions. An inspection of the connection plates on the continuous span Beaver Creek Bridge in Clarion County, Pennsylvania proved such cracks to exist in the negative moment regions where a 1 in. (25.4 mm) web gap existed *(18)*. Figure 17 shows cracks at the end of the stiffener weld and at the web-flange weld.

This type of fatigue cracking in welded multi-girder bridges was detected in the I-79 bridge #2680 over Big Sandy Creek in West Virginia *(19)*. The 476 ft. (145.1 m) long bridge has two 108 ft. (32.9 m) side spans and two 130 ft. (39.6 m) interior spans. The deck is supported by six 5 ft. (1.5 m) deep main girders which were shop welded and field spliced.

Upon inspection, small cracks were found along both the web-flange weld and the transverse connection plate weld in many diaphragm connection plate web gaps. The cracks were parallel to the longitudinal axis of the main girder, and therefore are parallel to the primary bending stresses in the web plate. The gap lengths ranged from 1/2 in. (12.8 mm) to 5/8 in. (15.9 mm). The maximum observed web gap stress was 20 ksi (138 MPa). No stress reversal was observed during the passage of trucks. Thus the maximum live load stress range is equal to the maximum live load stress. At all locations, measured strains revealed the development of double-curvature in the web gap. Strain gradients indicate the diaphragm is distorting the web and inducing cyclic, secondary bending stresses with the passage of live

load.

Box Member Diaphragms

Cracks have been detected in web plates of tied arch box girders at gaps of internal diaphragms opposite floor beams which are attached to the box girders. The diaphragm is often bolted to one web of the box and welded to the other. When the diaphragm plate is not connected to the top or bottom flanges, four gaps are formed between the internal diaphragms and the flanges. Furthermore backup bars are often utilized at the junction of a vertical or slanted web plate and the horizontal flange. Numerous cases of lack of fusion at the backup bar have been detected. When the fusion is poor, a discontinuity is built in. The combination of out-of-plane displacement and rotation within the gap and the existence of relatively large initial flaws can cause fatigue cracks in the gap.

This type of distortion-induced cracking has been investigated within the 750 ft. (228.6 m) long I-79 tie girder structure at Neville Island *(20)*. Cracks were found to exist in the welded connection between the diaphragm and outside web of the 42 in. × 150 in. (1067 mm × 3810 mm) box. Results of web gap strain measurements show that major stress cycles occur when trucks pass over the 92 ft. (28 m) long floor beam. Consequently, the diaphragm and all web gaps are subjected to higher magnitude stress cycles that include stress reversal. The maximum stress range within such gaps varies between 8 and 11 ksi (55.2 to 75.8 MPa), with Miner's effective stress ranges of 3 to 4 ksi (20.7 to 27.6 MPa).

As a result of out-of-plane displacement, significant stress gradients were generated within the web gap. Extrapolation to the backup bar root indicated the stresses to be three times as great as the measured values.

Throughout the review of the cases involving box distortion and the subsequent fatigue cracking, double curvature has always been introduced in the web plate gaps. Because the curvature and cyclic bending stresses were induced by end restraint of the floor beam at tie-girder connections and diaphragms, the entire box is distorted at the diaphragm. All four box corners at each floor beam connection are therefore susceptible to fatigue cracking. The distortion is only a partial cause of the cracking. Consideration must also be given to the quality of the welds at the backup bar. Field measurements indicate that these lack of fusion areas behind the backup bar often serve as a notch condition at the root of the weld. The notch is perpendicular to the forces transferred at the diaphragms and enhances crack growth in the direction of the main axis of the box. When the crack propagation changes direction in accordance with the stress field around the diaphragm-to-web connection, undesirable conditions could result. Early detection of these cracks is therefore of paramount importance.

Lateral Bracing Gusset Plates

In order to distribute transverse wind load, lateral bracing is often placed between adjacent girders. The attachment of bracing members is made through gusset plates which are connected to the web plates. The lateral bracing gusset plates are subjected to out-of-

plane forces from the bracing members and undergo small out-of-plane movements.

The gusset plate may be welded, bolted, or cut free of the transverse stiffener in addition to being welded at the web. Figure 18 shows the case of two separate plates welded only to the web. Within the gap bounded by the transverse stiffener weld toe and the inside of the gusset plate edge, the out-of-plane displacement is accommodated by the short length of the web plate. The resulting out-of-plane cyclic bending stresses have caused crack development and growth. The web gap is less than 1/4 in. (6.4 mm) in length, and the displacement is sufficient to generate large stresses.

Cracking at the lateral gusset plate gaps developed in I-79 Bridge #2682 over Big Sandy Creek in West Virginia *(19)*. The twin roadway is supported by two main steel girders with four stringers resting on 10 ft. (3.1 m) long floor beams. The continuous girders have three spans of 120 ft.-130 ft.-120 ft. (36.6-39.6-36.6 m). The lateral bracing is bolted to a gusset plate which is welded to the girder web, but not to the floor beam connection plate. The gusset plate detail is shown in Figure 19. The web gaps vary from 1/4 in. to 1 in. (6.4 to 25.4 mm) in length. The prevailing condition has resulted in the formation of vertical cracks along the outside (facia) transverse stiffener weld toes.

Strain measurements of main girder flanges verified the composite behavior of the girder sections. A maximum in-plane bending stress range of 3 to 5 ksi (20.7 to 34.5 MPa) was recorded and is typical of stresses in other bridges of comparable span length. Strains recorded on the laterals indicated a maximum stress range of 2 to 3 ksi (13.8 to 20.7 MPa) in both members framing into a gusset plate. The equivalent maximum forces were 7.5 and 8.5 kips (33.4 and 37.8 kN). Additional strain-time records indicated that each primary stress cycle is associated with a truck passing over the region.

Strains were measured at the transverse connection plate weld toe within the gusset plate gap and along the toes of the outside (facia) stiffener. Evaluation of stresses indicated the outer stiffener weld toes to be the critical location for crack growth. Stress ranges of 8 to 12 ksi (55.2 to 82.7 MPa) were calculated at the weld toe on the outer surface of the web directly opposite the gusset plate gap. The stress range within the gap was found to be 3 ksi (20.7 MPa), but when extrapolated to the transverse weld the range was closer to 7 ksi (48.3 MPa). Maximum stresses of 9 to 15 ksi (62.1 to 103.4 MPa) were induced at the transverse weld in the gap.

Positive attachment may be made by framing the lateral bracing member directly to the transverse stiffener or connection plate. Rigid attachment tends to reduce the magnitude of out-of-plane displacement, but may increase the magnitude of loads in the components. In such an attachment the intersection of the gusset longitudinal weld and the transverse stiffener weld must be avoided. Weld shrinkage strains will produce severe restraint in the region and the possibility of discontinuity and inclusions at the intersection is increased.

Similar cracking was investigated on the Canoe Creek Bridge in Clarion County, Pennsylvania *(13)*. Figure 20 shows the gusset plate detail which resulted in 1 1/2 in. (38 mm) web gaps between the transverse connection plate and the weld bars on the girder web. High strength bolts were used to attach the gusset plates to the welded connection plates.

Stress ranges up to 27 ksi (186 MPa) were extrapolated within 1½ in. (38 mm) lateral gusset plate web gaps to the transverse stiffener weld toe on the outside web surface. Strain measurements also indicated the stresses in the laterals to be of opposite sign and out of phase during the passage of vehicles. This condition again implies that the lateral connection plate was forced to rotate out-of-plane. Such rotations reduced the stress at one weld toe, but elevated the stress at the other.

ANALYTICAL ASSESSMENT OF TEST SPECIMENS

In order to evaluate the lateral bracing requirements as well as the needed lateral loading and restraint necessary for the web gap out of plane distortion, the test girders, gusset and transverse connection plates, the restraint struts, and the driving rods were modeled with a series of finite element models. The analytical results were compared with the experimental results so that adjustments could be made in both test specimen and computer model.

Gusset Plate Detail Without Positive Attachment

Because of the specimen's symmetry, only one-half of the plate girder was modeled. A central region with a 41 in. (1041 mm) depth and a 13 ft (3960 mm) length was discretized first. This depth extended from the center of the top flange to the center of the bottom flange. The elements simulating the flanges were then superimposed on the plane. This overlay resulted in a 42.0 in. (1066.8 mm) deep section with an accurate distribution of stiffness. The loading stiffener and transverse connection plate elements were then superimposed on the web's mesh. Finally, a rectangular plate was discretized in the third dimension at the level of the gusset plate. A computer-generated plot of the finite element model is shown in Figure 21.

All flanges were modeled with truss elements to provide for the transfer of axial forces. To restrain lateral motion of the tension flange during testing, a heavy structural section was clamped between adjacent girders. The model simulated this restraint through the "locking" of out-of-plane translational and rotational degrees of freedom.

From the left edge of the model, to a length of 118 in. (2997 mm) along the girder's longitudinal axis, 99 plane stress elements form the web plate. These elements are large at a considerable distance from the gusset plate detail. Triangular plane stress elements provided a transition to smaller scale elements. Plane stress implies a lack of lateral deflections and subsequent out-of-plane bending moments. The magnitude of the out-of-plane displacements at the gusset plate web gaps was expected to be in the order of 0.02 in. (0.51 mm). Previous research indicates that these displacements decrease rapidly and are usually insignificant within several inches of the weld toe *(16)*. Thus, prohibiting lateral deflections within the region defined by plane stress elements does not have a detrimental effect on the local analysis results.

The model's remaining 38 in. (965.2 mm) length was formulated with 289 plate-bending elements. These elements develop transverse moments as a result of lateral

distortion. The out-of-plane behavior of each region of elements is refined by the addition of smaller plates. Therefore, the mesh is reduced to an ordered collection of 1 in. × 1 in. (25.4 mm × 25.4 mm) elements in the local region surrounding the web gaps and connection plate. This discretization captures the strain gradient within large web gaps from which displaced shapes may then be plotted. The elements' dimensions were within an aspect ratio of 4 to 1. Each node was given all six degrees of freedom, except the column which defines the girder's vertical centerline. Due to symmetry, the girder's centerline can only undergo vertical deflections. These nodes can not rotate or undergo longitudinal translation. They may, however, experience lateral motion under the influence of plate element distortion.

The concentrated load stiffener and transverse connection plate were also modeled with beam elements. Each element has the properties of a pair of stiffener plates separated by a thin web plate.

The gusset plate was modeled with plane stress elements. Since the cracks develop in the specimen's web plate, the gusset plate is considered to be a means through which lateral distortion is introduced. Within the vicinity of the transverse connection plate, the discretization is fully compatible with that of the local web region. The discretization allowed for a change in the nominal web gap length from 1 in. (25.4 mm) to 3 in. (127 mm) by 1 in. (25.4 mm) increments.

Secondary members, specifically the "driving" rod and the lateral braces, were simulated with truss elements. The overall testing layout is symmetrical about a centerline between the pair of girders. The lateral brace's cross-sectional area was altered until acceptable behavior resulted. In this manner a suitable lateral brace section was selected for the laboratory test. Three truss elements were used to form each brace. Two of these elements overlap the plane stress elements of the gusset plate. Several nodes were common to both the truss and plane stress elements, thereby simulating a bolt line. The actual braces transmit restraining forces in the plane of the gusset plate and provide constraint necessary to induce curvature within the web's plate-bending elements.

The rod was assumed to behave as a simple compression member. The actual rod is pinned to both the transverse connection plate and the surrounding test frame. Member length, as well as angular orientation, was varied by changing the nodal coordinates. Cross-sectional area was also a variable. This analysis resulted in the selection of a section area on the basis of the force developed in the rod and the lateral displacement introduced in the web gap region.

The finite element analysis results for Detail C are summarized in Figures 22 and 23 for a 3 in. (76.2 mm) web gap and a rod angle of 20 °. The model was loaded to the jack's capacity of 55 kip (245 kN). The out-of-plane displaced shape along the gusset plate is plotted in Figure 22. The lateral translation of the plate's outer edges is 0.001 in. (0.025 mm). However, the rigidity of the braces restrains the deflection to 0.0005 in. (0.013 mm) at their point of attachment. The inner edges of the gusset plate translate 0.0012 in. (0.03 mm), while the driving rod forces the stiffener to undergo a lateral displacement of 0.0082 in. (0.208 mm). Thus, the web gap experiences a relative distortion of 0.007 in. (0.18 mm) within the unrestrained web plate.

The combined stress distribution is illustrated in Figure 23. This plot is a superposition of both primary and secondary stresses associated with in-plane loading and lateral distortion respectively. The stress is 5.2 ksi (35.9 MPa) at the outer edge of the gusset and -4.8 ksi (-33.1 MPa) at the inner edges. The transverse connection plate weld toes are exposed to a combined stress of 18.7 ksi (129 MPa) produced by double-curvature of the web gap.

Gusset Plate Detail With Positive Attachment

The bolted attachment of the gusset plate and the transverse connection plate (Detail B) made use of a structural section identical to those serving as lateral braces. The section provides additional lateral resistance to the opposing force developed in the rod.

The member was modeled with four truss elements whose properties are identical to those described for the lateral braces. The inner element shares a common end node with the transverse connection plate. This element's other defining node is at the inner boundary of the gusset plate. The remaining three elements overlap the gusset plate's plane stress elements and share nodes along the member's longitudinal axis. Therefore, a single line of elements has been fixed to both the gusset plate and the connection plate.

The finite element analysis results of Detail B are presented for the case of a 3 in. (76.2 mm) web gap and a rod angle of 20 degrees. The load was 55 kip (245 kN).

The out-of-plane displaced shape along the gusset plate is plotted in Figure 24. The lateral displacement of the plate's outer edges was 0.003 in. (0.076 mm). The inner edges, those serving as the outer boundaries of the web gaps, displaced 0.0025 in. (0.064 mm). A relative distortion of 0.0033 in. (0.084 mm) was been induced within the unrestrained web plate gap.

The distributions associated with the primary, in-plane bending stresses and the secondary, displacement-induced stresses are shown in Figure 25. The sudden variation in the primary membrane stress occurs at the points of lateral brace attachment. This reduction is due to the restraint offered by these rigid components. The nominal primary stress is 5.8 ksi (40 MPa) at the level of the gusset plate. The distortion-induced stresses clearly reveals the development of double-curvature within the web gap. The plate's outer edges are exposed to stresses of less than 1 ksi (6.9 MPa), while the inner edges undergo secondary stresses of -4.5 to -5 ksi (-31 to -34.5 MPa) on one side of the web plate. Distortion-induced stresses of 6.4 ksi (44.1 MPa) are developed at the transverse connection plate weld toes. These values are comparable in magnitude to the prevailing primary membrane stresses.

The combined stress distribution is illustrated in Figure 26. The transverse connection plate weld toes are exposed to a combined longitudinal stress of 11 ksi (75.8 MPa).

The analysis of a 3 in. (76 mm) web gap for Details B and C indicated that the worst condition occurred during the maximum load of 55 kip (245 kN) and at a rod angle of 15 °. The average primary stress remains relatively constant for each detail at the three web gap sizes because the vertical deflections are nearly unaffected by detail.

The difference in the lateral displacements of a web gap's boundaries is defined as the

gap's relative distortion. This distortion increases from 0.0027 in. (0.069 mm) to 0.0064 in. (0.163 mm) for Detail C as the web gap approaches 3 in. (76.2 mm). The relative distortion ranges from 0.0013 in. (0.033 mm) to 0.003 in. (0.076 mm) for the detail which includes bolted positive attachment. Similar to the absolute, lateral displacement, the distortion grows with the gap size due to enhanced plate flexibility. However, the degree of distortion in the largest web gap of Detail B is the almost identical to that of the smallest gap in Detail C. The bolted positive attachment reduced the relative distortion by a factor of two for each web gap size investigated.

The force developed in the rod was observed to decrease slightly for each detail with a corresponding increase in web gap size. The force is larger in the positive attachment case due to the inherent rigidity of the connection.

The proceeding analysis resulted in the following observations which were used for the experimental studies:

1. Larger web gaps accommodate larger absolute, out-of-plane displacements in both details, and progressively increase the force developed in the positive attachment while decreasing that developed in lateral braces.
2. The gap size has no effect on the girder's vertical deflection. The detail which includes positive attachment will slightly decrease such deflections due to the enhanced local stiffness.
3. The primary membrane stress at the gusset plate level is not effected by web gap distortion (symmetrical).
4. Larger web gaps accommodate greater degrees of relative distortion without elevating the secondary bending moments at the gap boundaries (all other conditions remaining constant).
5. The unrestrained plate within web gaps may experience only tensile or compressive stresses on one side of the plate (single-curvature). However, double-curvature of the web plate will occur within a short distance beyond the gap.
6. Positive attachment provides a means for the lateral transfer of forces transmitted through the gusset plate. This increases the axial thrust in the lateral braces.
7. Positive attachment reduces the magnitude of out-of-plane displacements experienced by the girder's web plate. This reduces the subsequent secondary stresses along the detail.
8. The secondary, distortion-induced stress levels dominate the resultant total stresses. The primary membrane stress is virtually constant.
9. The stress at the gusset plate's outer edge is effected by lateral displacements to a lesser degree than the regions within the web gap. Although distortion-induced stresses are still present, they are on the outer reaches of the lateral displacement field and are reduced.

EXPERIMENTAL RESULTS ON WEB GUSSET PLATES

The experiments were carried out with paired girders as illustrated in Figures 12 and 13 so that adjacent details at a section could be subjected to comparable distortion induced stresses. The gusset plate details were subjected to cyclic stresses from in-plane and out-of-plane loading that were in three stress range regions: low (10 to 15 ksi (69 to 103.5 MPa)), intermediate (15 to 23 ksi (103.5 to 141 MPa)), and high (greater than 26 ksi (180 MPa)).

Six details (one on each girder) with web gap between 1½ and 3 in. (38 and 76 mm) were evaluated in the low stress range regime. These details are summarized in Table 3. None of the details subjected to low levels of stress range in the web gap developed fatigue cracks. This included the two Type A and three Type B details. Figure 27 shows the web gap region for Detail T5-6 (Type B) which was subjected to 10×10^6 cycles at 10 ksi (69 MPa) without detectable cracking.

Fatigue Behavior of Gusset Plates

Each web gap region was gaged to establish the strain gradient and magnitude. Figure 28 shows the stress gradient observed at Detail T5-1 which was subjected to a 15 ksi (103.5 MPa) stress range. The low distortion stress range details were all provided with a positive attachment (either welded or bolted) between the gusset plate and the transverse connection plate.

Two details without positive attachment to the vertical connection plate (Type C) and two details with bolted positive attachments (Type B) underwent intermediate degrees of out-of-plane distortion during testing. A web gap stress range of 15 to 23 ksi (103.5 to 151.8 MPa) was defined as an intermediate range. This corresponds to the level of cracking that would be expected after only a few years of service. Details T5-9 and T5-10 (Type C) include gaps of 0.2 in. (5.1 mm) and 0.3 in. (7.6 mm) lengths between weld toes. Only one of the Type B, bolted attachment details developed fatigue cracks (Detail T5-5). As can be seen in Table 3, Detail T5-8 was subjected to 20×10^6 cycles at 15.5 ksi (107 MPa) without detectable cracking. Detail T5-5 with a stress range of 19.5 ksi (134.6 MPa) was observed to have a small crack after 5×10^6 cycles. Both of the Type B details experienced stress gradients similar in shape to the Type A detail. Figure 29 shows the stress gradient for T5-5 which developed a fatigue crack. Figure 30 shows the small fatigue crack that was first detected after 5×10^6 cycles. A history of each gusset detail crack development and retrofit condition is provided in Appendix A.

Detail T5-10 (Type C) is shown in Figure 31. The detail is not connected to the transverse connection plate. A plot of the typical stress gradients across a pair of 0.2 in. (5.1 mm) gaps is shown in Figure 32.

The vertical connection plate weld toe experienced a stress range of 26 ksi (179.4 MPa) in a 0.2 in. (5.1 mm) web gap, and a range of 23 ksi (158.7 MPa) in a 0.3 in. (7.62 mm) web gap. The measured gradients extrapolated to ranges of over 17 ksi (117.3 MPa) at the toe of the gusset's inner edge weld for these same gaps. These values were all tensile and indicate

the development of single-curvature within the narrow, horizontal web gaps.

The weld terminations at the outer ends of the gusset plates were found to undergo a stress range of 9.5 ksi (64.9 MPa). These ranges result from a primary range of 6 ksi (41.4 MPa) and a secondary deformation-induced stress ranges were 3.5 ksi (24.2 MPa). No cracks developed at any of these exterior weld ends.

The initial relative distortion of the web gap was about 0.0015 in. (0.04 mm). This distortion remained about the same until the crack was about 1.5 in. (38 mm) long as shown in Figure 33. Thereafter, the out-of-plane distortion tended to increase as the crack extended.

Two Detail C-type connections were subjected to high degrees of out-of-plane distortion during testing. Detail T5-11 includes gaps of 2.4 in. (61 mm) and 2.6 in. (66 mm) length and can be seen in Figure 34.

A plot of the measured stress gradients across the gaps of Detail T5-12 is shown in Figure 35. Stress ranges of 30 to 31.5 ksi (207 to 217 MPa) developed along the vertical connection plate weld toe within the horizontal gaps. The measured gradients extrapolated to compressive stress ranges of 4 to 6 ksi (27.6 to 41.4 MPa) at the toe of the gusset weld for these gaps. The measured stresses indicated the development of double-curvature within unrestrained web plate gap.

The weld terminations at the outer edges of the gusset plates experienced a consistent stress range of 9 ksi (62.1 MPa). The corresponding point on the outside surface of the web plate underwent a range of 4 ksi (27.6 MPa). These values are based on a primary range of 6.5 ksi (44.9 MPa) and are evidence of the development of a secondary gradient through the web thickness. Therefore, a distortion-induced stress range of 2.5 ksi (17.25 MPa) was generated at the outer weld terminations.

Stress ranges at weld toes for Detail T5-12 were extrapolated from plotted gradients and scaled from the finite element analyses. The model provided stress ranges along the vertical connection plate weld toe within 13% of those measured. However, the double-curvature was more severe than accounted for by analysis, and the model predicted compressive stresses of one-half the magnitude of those measured. The computed stress range at the gusset's outer edge was within 20% of the experimental results.

The test results for all 12 gusset plate details are summarized in Table 3 for initial cracking. The test results are also plotted in Figure 36 and compared with the AASHTO Category C Fatigue Resistance Curve. The stress range plotted in Figure 36 is the extrapolated measured value at the transverse connection plate weld toe which developed a crack. It includes both in-plane and out-of-plane stress. Category C would be applicable to the transverse connection plate. It is readily apparent that all test data at the time of crack detection falls well above this resistance curve. A substantial number of details experienced no crack growth even though the fatigue limit for Category C was exceeded.

The results indicate that the web gap combined stresses are not as severe as in-plane bending alone. It is also apparent from all of the web gap measurements that the stress range at the transverse connection plate weld toe is substantially higher than the stress range at the

gusset plate weld end. This can be seen in Figures 28, 29, 32, and 35 for all three types of gusset plate details.

The experimental results were also examined for the web gap at the termination of the gusset plate detail. Figure 37 compares the experimental data with the AASHTO Category E Fatigue Resistance Curve for attachments greater than 8 in. (203 mm) long. The experimental results include the effects of in-plane bending stress equal to 6 ksi (41.4 MPa) for all gusset plate outer edges and the out-of-plane deformation induced stress. It can be seen that although many details exceeded the fatigue limit of 4.5 ksi (31.1 MPa), none exhibited cracking after 10 to 20 million cycles. The measurements also indicated that the web gap stress range tended to decrease as the crack length increased and retrofit holes were introduced. The strain gradients were more favorable to the gusset weld end.

It is also interesting to examine the outer ends of the lateral gusset plates. The strain gage measurements indicated that the stress range at the welded toe was about 50% greater than the in-plane bending stress range. The out-of-plane movement of the gusset plate had increased the weld toe stress. This did not result in cracks initiating from the gusset plate end, even though cyclic stress was well above the fatigue limit of 4.5 ksi (31.1 MPa). None of the lateral gusset plates developed fatigue cracks at the gusset plate ends after 10 to 20 million cycles were applied.

Retrofit of Gusset Plate Web Gaps

Retrofit holes were installed at the web gap crack tips after the cracks had extended above and below the web gap as illustrated in Figure 38. The hole diameter varied from 3/4 in. (19 mm) to 1 1/2 in. (31.8 mm). Table 4 summarizes the crack length, cycles to retrofit and the hole diameter for each initial retrofitted detail.

The retrofit holes were initially sized to satisfy the relationship *(14)*

$$\frac{\Delta K}{\sqrt{\rho}} < 4\sqrt{\sigma_y} \quad (\text{for } \sigma_y \text{ in ksi})$$

$$\frac{\Delta K}{\sqrt{\rho}} < 10.5\sqrt{\sigma_y} \quad (\text{for } \sigma_y \text{ in MPa})$$

where the hole diameter, ρ, was estimated from the in-plane bending and the stress intensity factor ΔK from the relationship $S_r\sqrt{\pi a_r}$ where a_r is defined in Figure 39 and S_r is the stress range at the hole. Sometimes only a single hole at the lower end of the crack was initially installed. A second hole was installed later if crack growth continued at the upper end.

The introduction of the retrofit holes tended to decrease the stress range in the web gap and at the end of the gusset plates by about 10%. This was due to the reduction in lateral restraint. The detailed test results are summarized in Appendix A and provide the progress of the crack as it sometimes re-initiated and was arrested again.

Figure 40 shows the holes installed in the web of Girder 18 Detail T5-10. The final set of retrofit holes were installed after 5×10^6 cycles at which time a bolted connection was also

provided between the lateral gusset plate and the transverse connection plate. This reduced the stress range below the retrofit hole by about 50% and prevented the crack from re-initiating during an additional 4.7×10^6 cycles. Figure 41 shows the retrofit hole and connection provided between the gusset plate and the transverse connection plate for Detail T5-11. The crack along the other side of the transverse connection plate was extensive as can be seen in Figure 42. 1¼ in. (31.8 mm) holes were installed along the vertical weld at the time the bolted attachment was made and an additional 6.7×10^6 cycles were applied without any apparent re-initiation. Appendix A provides a summary of the history of each of the 12 gusset plate details.

The test results demonstrated that for intermediate levels of stress range (< 20 ksi (138 MPa)), drilled holes are fully capable of arresting the crack and preventing its re-initiation at the gusset plate web gap. Higher levels of stress range require a positive attachment between the gusset plate and the transverse stiffener, even when a 3 in. gap exists.

EXPERIMENTAL RESULTS ON TRANSVERSE CONNECTION PLATES

The twelve welded girders tested in this phase of the program utilized the same loading scheme and restraint conditions to introduce distortion into the web gap between the end of transverse stiffener and the bottom flange of the test girders. Figure 14 shows the setup used to displace the transverse connection plates out-of-plane. The gusset plate girders had lateral members framing between the adjacent girders as shown in Figure 15. The transverse connection plates had no such comparable members other than the restraint girders attached to the bottom flange.

The twelve girders were arranged in test pairs as illustrated in Figure 11. The test factorial identifying the various web gap conditions and stress range conditions is provided in Figure 10.

The out-of-plane bending stress in the web gap region was determined from strain gages installed in the gap as illustrated in Figure 43. Strain gages were mounted on each side of the web plate.

Fatigue Behavior of Transverse Connection Plates

The fatigue cracks that developed in the transverse connection plate web gap first developed at the fillet weld toe of the transverse connection plate as illustrated in Figure 44. As can be seen in Figure 44, the crack extended for a distance up the girder web along the transverse weld toe and then grew away from the weld toe into the web plate.

Detection of crack growth was assisted by use of strain gages installed in the web gap. A close up view of the weld end in Figure 45 shows that the crack at the weld toe and its extension around the end of the weld up the girder web. At this detail the crack branched away from the weld toe about 1 in. (25 mm) above the end of the connection plate. At the smaller web gaps, where the welds on the transverse connection plates extended beyond the plate, cracks generally formed at the end of the plate through the weld as illustrated in Figure

46.

Of the 24 transverse connection plate web gaps examined in this study, fifteen developed cracks in the web gap. Most of the cracks developed at the end of the transverse connection plates as 13 of the fifteen details first developed cracks at that location. The other 2 details first developed cracks at the web-flange weld. Table 5 summarizes the test results for the diaphragm connection plates. Table 5 identifies the detail and girder, the gap size (nominal in parenthesis) and measured weld toe gap, the girder in-plane stress range in the beam flange, the measured (extrapolated) weld toe stress range at the detail that cracked, the cycles to to crack detection, and the cycles to retrofitting. It should be noted that the nominal gap size is the distance between the end of the connection plate and the surface of the flange. The actual value tabulated in Table 5 and shown in Figures 47 to 53 corresponds to the measured distance between the weld toes in the gap.

Figures 47 to 53 show the stress gradients that were observed in typical 1½ in. (38 mm) and 3 in. (76 mm) web gaps. Two plots are provided when cracks developed. The top plots show the stress gradients measured on each side of the web plate at the start of the test or before cracking occurred. The bottom plots show the gradients observed after the initial crack had formed. In each plot, the solid symbols show the results at the detail from the north side of web plate and the open symbols show the results from the south side of web plate. The two symbols for each side depict the minimum and maximum stress in the stress cycle. Hence, the difference between the two sets of data provides the stress range. The vertical dashed lines and symbols on each side of the plot provide the gage location and the length of the gap on each side of the web plate. The difference in the length of the dashed lines results from the different web gap length on each side of the web plate.

The measured web gap stresses for the 1½ in. (38 mm) details prior to cracking in general showed a single curvature response as can be seen in Figures 47 (a) to 49 (a) and 50. After cracking, the measurements generally showed a trend to double curvature and a re-distribution in the web gap. The strain measurements for the smaller web gaps generally indicated a cyclic tensile stresses on one face of the web and cyclic compression on the opposite web gap face. Cracks always formed initially at the weld toe subjected to cyclic tension. Eventually, the cracks propagated through the web thickness and were observed on both sides of the web.

The measured web gap stresses at the larger 3 in. (76 mm) details usually exhibited double curvature as can be seen in Figures 51 (a) to 53 (a). After cracking, some details retained their double curvature characteristics whereas others developed single curvature conditions. It is also apparent that the welded toe on each side of the web was subjected to a stress reversal and hence was more susceptible to crack growth from each side of the web plate.

The web gap measurements shown in Figures 47(a) to 53(a) demonstrated the wide variability in response that can be expected at web gaps. This variability makes it difficult to model web gap behavior.

The weld notch condition at the end of transverse connection plate welds was in general

more variable and severe than the machine made web-flange welds. Hence, a much higher fatigue strength existed along the web-flange weld toes than at the end of the transverse connection plates.

The test results at the cracked details are compared with the fatigue resistance provided by Categories C and D of the AASHTO Specifications in Figures 54 and 55. Crack detection provided a lower bound fatigue life corresponding to the Category D fatigue resistance curve as illustrated in Figure 54. This is consistent with other fatigue test data where fatigue cracks are generally observed at about 75% of their fatigue resistance. When the results were compared for cycles at the time of first retrofit, the fatigue strength generally exceeded Category C.

The results plotted in Figure 55 show the fatigue life at the first retrofit (usually by drilling holes) at which time the crack was through the web thickness and several inches long. At this stage of crack extension the fatigue life was comparable to other details used to define the AASHTO fatigue resistance curves. The four details that developed cracks below Category C fatigue limit were not retrofitted even though small cracks were detected. These details were subjected to an additional 10 to 17 million cycles of stress range. The cracks extended between 1 and 2 in. (25 to 50 mm) during these additional cycles. Hence, the results verify that Category C is a reasonable resistance curve for distortion induced fatigue cracking at the ends of transverse connection plates.

Also plotted in Figures 54 and 55 are the details which experienced no crack growth. When the end of the transverse connection plate were subjected to cyclic stress below 10 ksi (69 MPa) there was usually no evidence of crack growth. Many of the web gaps experienced higher stress range levels at the web-flange weld toe. The stress range had to exceed 15 ksi (105 MPa) before cracks developed at this location.

Retrofitting Transverse Connection Plate Web Gaps

The fatigue cracks that formed at the transverse connection plate web gap extended in length and penetrated through the web. These cracks were arrested by one or more retrofit procedures. Table 6 summarizes the various retrofit sequences carried out on each detail. The initial retrofit was carried out when the crack length exceeded 2 in. (50 mm). This involved either drilling one or two holes at the ends of the crack, providing a bolted attachment between the connection plate and the bottom flange, or removing part of the transverse connection plate to increase the web gap flexibility.

Figures 56 and 57 show examples of the holes drilled in the girder web at one end of the crack. In both of these cases, the crack has extended from the end of the transverse connection plate up the vertical weld toe for about 1 in. (25 mm) before moving out into the web following the principal tensile stress from the web gap distortion.

A positive attachment was provided with high strength bolts between the connection plate and beam flange with a structural tee as illustrated in Figure 58. Four bolts were installed in the flange on a stagger to minimize the section loss. Two bolts were installed in the connection plate and web of the tee. No retrofit holes were initially installed so that the

effectiveness of reducing the distortion could be assessed. As Table 6 illustrates, the bolted connection was effective in reducing or stopping the crack growth. Generally the crack extended a small amount in the longitudinal direction of the girder. Such extensions would be prevented altogether with crack arrest holes.

The removal of a portion of the transverse connection plate as illustrated in Figure 59 was found to soften the web gap and significantly reduce the crack growth rate. The connection plate was cut away along the plate weld toe so that only the welds and a small plate segment remained. This substantially reduced the crack growth. The total crack extension was 0.5 in. (12.5 mm) after an additional 6 million cycles. The crack remained parallel to the in-plane bending stress.

Seven of the girders details which developed cracks were not retrofitted. Six were known to have small cracks which were detected after 1.8 to 10.7 million cycles. Each of these details was subjected to 10 million or more additional cycles with only modest amounts of crack extension. The other detail was found to have a small crack after the detail was removed from the girder and more closely examined. The crack was about 1/4 in. (6 mm) long and confined to the weld end. All of these details had cyclic stresses at the connection plate weld end between 7.5 ksi (52 MPa) and 32.5 ksi (224 MPa) which was at or greater than their fatigue limit. The results from these seven details are summarized in Table 7. Most of these cracked details had Type II cracks.

The retrofit holes were effective in stopping crack growth in a plane perpendicular to the in-plane bending when the relationship developed in Reference 14:

$$\frac{\Delta K}{\sqrt{\rho}} < 4\sqrt{\sigma_y} \quad (\text{for } \sigma_y \text{ in ksi})$$

$$\frac{\Delta K}{\sqrt{\rho}} < 10.5\sqrt{\sigma_y} \quad (\text{for } \sigma_y \text{ in MPa})$$

was satisfied. In this equation, ΔK is the stress intensity range for the in-plane stress range at the hole with radius, ρ. The crack size was taken distance from the end of the connection plate to the edge of the hole as illustrated in Figure 60. This resulted in a stress intensity range estimate of $\Delta K = S_r\sqrt{\pi a_r}$.

The crack sometimes reinitiated at the toe of the transverse connection plate weld terminated at the hole. This occurred when the hole was at the weld toe (see Figure 57). Table 4 shows estimates of $\Delta K / \sqrt{\rho}$ for the test girders.

The girders tested at an in-plane bending stress range of 12 ksi (82.8 MPa), G11 and G12, were not tested beyond 3.04 million cycles because at such a large in-plane stress range, the cracks in the girder web could not be satisfactorily arrested. Testing was discontinued when the crack entered the girder flange. Girders G9 and G10 were tested to 6 million cycles at which time one of the girders fractured.

APPLICATION OF RESULTS

The findings from this study should be of value to structural engineers involved in the design of welded steel girders, researchers working in the subject area, and members of specification writing bodies. The suggested revisions to the AASHTO Standard Specifications can also be applied to other bridge specifications such as those of the American Railway Engineering Association. These finding result from a limited experimental effort, but are also augmented by experience with deformation induced fatigue cracking in bridge structures and measurements of web gap out-of-plane bending stresses and distortion.

Fatigue Behavior Of Web Gusset Plates

The study confirmed that the fatigue classification (Category E) assigned to the ends of gusset plates connected to the girder web by welds is satisfactory. Stress cycles in the web gap gusset weld toe generally were less than the fatigue limit of 4.5 ksi (31.1 MPa). No cracking developed at these locations after 10 to 20 million cycles of loading. The laboratory studies suggest that the fatigue resistance of the gusset plate detail is greater than would be expected from the direct addition of in-plane and out-of-plane bending. No cracks formed at the outside ends of any of the gusset plates, even when this combined stress was well above 4.5 ksi (31.1 MPa)

Fitting gusset plates around a transverse connection plate without a direct attachment as was done with Detail C does not appear to be desirable. Relatively high cyclic stresses developed in the web gap at small out-of-plane deformations (0.0015 in. (0.04 mm)). This resulted in weld toe stress range levels that exceeded the fatigue limit and resulted in cracks at relatively short fatigue lives. A positive attachment with welds or bolted connections is needed between the transverse stiffener and gusset plate. Even with a positive welded attachment, the web gap between the weld toes should be at least four times the web thickness.

The fatigue resistance of the transverse connection plate weld toes in the web gap at the gusset plate is equal or greater than Category C. The experimental data fell near the upper bound of other Category C data developed from transverse stiffeners and from T-specimens subjected to web-plate bending. The web gap distortion of the laboratory specimens was found to develop reversal of stresses in the web gap similar to the stresses observed in bridges. The maximum stress range was found to occur at the transverse connection plate with the stress range at the gusset plate end often below the fatigue limit. Hence, the laboratory experimental results were similar to experience with actual bridges where most cracking in the gusset plate web gap developed at the transverse connection plate weld toe.

Fatigue Behavior of Transverse Connection Plates

This study has shown that the fatigue resistance of transverse connection plate web gaps subjected to distortion is Category C for both weld toe sites at the end of the transverse connection plate. The connection plate end was observed to develop cracks below the Category C resistance curve but exceeded the resistance curve before they were through thickness and required retrofitting.

The web-flange welds with their smoother transition only developed cracks at cycle lives well above the Category C resistance curves.

Cracks developing from distortion induced cyclic stresses that were less than 15 ksi (105 MPa) at the weld toe could be arrested by drilling holes at the crack tips. This was only true for the 6 ksi (41.2 MPa) in-plane bending stress range tests which is most characteristic of actual bridges.

Successful arrest of cracking at details with higher distortion induced cyclic stresses (> 15 ksi (105 MPa)) requires a positive attachment between the connection plate and the girder flange in order to bridge the web gap and reduce the magnitude of the out-of-plane web bending stress.

Removing part of the transverse connection plate to soften the web gap region reduces the cyclic stress and reduces significantly the crack growth rate. The increased gap size must be at least $20t$ to be fully effective where t is the web plate thickness *(17)*.

Recommended Specification Changes and Commentary

The results of this study and the review do field experience suggest that changes to the AASHTO Specification *(8)* are desirable to minimize cracking in web gaps and end connection angles.

It is recommended that Clause 10.19.2.3 of the AASHTO Specifications be revised as follows:

> **10.19.2.3** End connections of stringers and floorbeams preferably shall be bolted with high strength bolts. ~~However, they may be riveted or welded. In the case of welded end connections, they shall be designed for the vertical loads and the end bending moment resulting from the deflection of the members.~~ *When angles are used to provide these connections, the gage of the outstanding legs shall equal or exceed* $\sqrt{Lt/12}$ *where L is the span length of the stringer or floor beam in inches and t is the angle thickness (in.) for the upper and lower 20% of the connection length. When the stringer or floorbeam is bolted to vertical connection plates, which are welded to the girder webs, the plate shall be rigidly connected to both top and bottom flanges by welded or bolted connections.*

Commentary for Clause 10.19.2.3:

This experimental study and field experience has demonstrated that web

gaps are susceptible to fatigue cracking unless they are effectively bridged. Clause 10.19.2.3 has been modified in two ways, both related to the fatigue cracking observed in web gaps and to minimize cracking in other components such as the end connection angles. One change is to soften the end restraint which has a beneficial effect on the connection angles as well as the forces imposed on the web plate. To accomplish this softening, an increased gage is provided for the upper and lower 20% of the connection length. The relationship suggested was recommended in NCHRP Report 302 *(21)*. It is developed from a model relating end rotation of the stringer or girder to the stress range introduced in the connection angle as a result of this deformation.

The second change is the mandatory requirement to provide a rigid connection between the vertical connection plate for stringers or floor beams and the top and bottom flanges. Although this requirement is cited in Clause 10.20.1 for diaphragm and cross frames, it is needed for other cases as well. The end restraint at stringers and floor beams has resulted in extensive cracking in web gaps. This condition must be avoided in future construction.

The use of a riveted or welded shear connection was eliminated from the clause. Riveted connections are no longer used in new construction. Welded shear connections between the web of stringers or floor beams and the transverse connection plate are very low in fatigue resistance and should not be used. The magnitude of end restraint is not well defined and experience shows such connections to be undesirable.

It is recommended that Clauses 10.21.3 and 10.21.4 be revised as follows:

10.21.3 When required, lateral bracing shall be placed in the exterior bays between diaphragms or crossframes. All required lateral bracing shall be placed in or near the plane of the flange being braced. *Preferably the lateral gusset plates will be bolted to the girder flanges.*

10.21.4 Where beams or girders comprise the main members of through spans, such members shall be stiffened against lateral deformation by means of gusset plates or knee braces with solid webs which shall be connected to the stiffeners on the main members and the floor beams. If the unsupported length of the edge of the gusset plate (or solid web) exceeds 60 times its thickness, the plate or web shall have a stiffening plate or angles connected along its unsupported edge. *When the gusset plate is attached to the girder webs, a positive connection shall be provided between the gusset plate and intersecting vertical connection plates or stiffeners. When welded joints are used between the gusset plate and vertical connection plates, a gap length of 4 times the web thickness or 2 in., whichever is greater should be used. When bolted connections are used, at least 4 preloaded high strength bolts should be provided for each shear plane and the web gap made 6 times the web thickness or 3 in. whichever is greater.*

Commentary for Clauses 10.21.3 and 10.21.4:

This experimental study, the review of existing field measurements, and field experience with fatigue cracking have demonstrated that the lateral bracing gusset plates provide low fatigue resistance (Category E or E'). They are also susceptible to distortion when welded to girder webs and not attached to the transverse connection plates. A preferable connection with significantly higher fatigue strength is the gusset plate bolted to the girder flange with high strength bolts. This provides at least a Category B fatigue resistance based on net section and may be higher depending on the number of bolts and faying surface conditions

When gusset plates are attached to the girder web, it is necessary to provide a positive attachment to intersected vertical connection plates. Otherwise, web gap distortion under live load, produces excessive web gap stress range excursions and eventual cracking in the web gaps. Even when positive attachment of the intersecting components is provided, some web gap distortion occurs. In order to minimize the possibility of cracking, minimum web gap sizes are provided for welded and bolted connections.

Recommended Design Guidelines For Preventing Cracks In Small Gap Regions

During the last twenty years, fatigue and fracture studies of welded details have demonstrated that welded attachments on the tension flange are not any more severe than similar welded attachments to the web. Both of these detail locations provide the same fatigue strength for design. Stiffeners and transverse connection plates used at diaphragms locations provide a Category C detail whether welded to the web alone or to the web and flange. Lateral gusset connection plates provide a Category E detail. Proper design and recognition of the detail severity accounts for the strength of the welded detail regardless of its placement on the flange or web. In addition, mandatory notch toughness requirements have eliminated steels which are susceptible to premature brittle fracture originating from small defects and high weld toe stress concentrations. Therefore, it is recommended that floorbeam and diaphragm connection plates be positively attached to both top and bottom flanges of the girder. The available results from this laboratory study and field measurements from several bridges has indicated that welded joints between connection plates and the girder flanges and between the transverse connection plate and lateral gusset plate are more rigid and therefore are more effective when the gap length is 4 times the web plate thickness or 2 in. (51 mm), whichever is greater. When bolted connections are used, they should incorporate relatively rigid splice components such as 3/4 in. (19 mm) thick angles or built-up components. At least 4 preloaded high strength bolts should be provided for each shear plane. In addition, it is desirable to increase the web gap to 6 times the web thickness or 3 in. (76 mm) whichever is greater when a bolted connection is used to connect gusset plates to transverse connection plates. These recommendations result from field measurements on a variety of structures with web gap cracking where various reinforcements have been

examined *(7, 9)*.

Experimental and theoretical studies on the behavior and response of web gaps at diaphragm connection plates of multigirder bridges indicated that undesirable out-of-plane web bending stresses developed in the negative moment regions for both K-type and X-type diaphragms *(9)*. The study indicated that providing a positive attachment was the most effective way to prevent undesirable cyclic stresses and web gap cracking.

Parametric studies indicate that K-type bracing was more favorable for the web gap response than is X-type bracing. In addition, three- girder bridges were found to be more favorable for the web gap than 4- and 5-girder bridges. Out-of-plane deformation was reduced for the three- girder bridge for all loading positions of the truck *(9)*.

Recommended Guidelines For Retrofitting Multigirder And Floorbeam-Girder Bridges

Available experimental field studies on multigirder bridges with diaphragms and this laboratory study suggest that cracking can be arrested with drilled holes at the crack tip. Cracks along the web-flange connection can be expected to move into low stress regions so that drilled holes can effectively stop further growth. Cracks forming at the end of the transverse connection plates often form from the weld root and propagate through the weld and eventually into the web plate. This requires that the retrofit holes be installed after the cracks have moved into the web plate. The laboratory experimental results indicate that the web gap cracks can be arrested with drilled holes providing the distortion induced cyclic stress is less than 15 ksi (105 MPa) and the in-plane bending stress is 6 ksi (42 MPa) or less. Field measurements on existing structures likely to experience web gap cracking at diaphragms have demonstrated that the in-plane bending stress range seldom exceeds 6 ksi (42 MPa) *(7, 9)*.

Floorbeam-girder bridges without positive attachment of the floorbeam connection plates to the girder flange can be expected to develop web gap cracks primarily in the negative moment regions where the slab restrains the girder flange. Cracks may also form adjacent to the bottom flange but this will depend in large measure on the lateral resistance of the bottom flange and the geometric placement of the bottom lateral system. Lateral connection plates bolted or welded directly to the bottom flange provide more restraint and are likely to enhance cracking in positive moment regions if the floorbeam connection plate is not attached to the bottom flange. Retrofitting can be carried out by making a positive attachment between the connection plate and the flange or by cutting short the floor-beam connection plate so that a very large web gap (12 in. (305 mm)) is provided (see reference (17)). In either case holes need to be drilled at the crack tips.

In the negative moment regions adjacent to the piers, experimental studies on bridges indicated that cutting short the floorbeam connection plates provides a significant decrease in the out-of-plane bending stress . At least 12 in. of the connection plate must be removed, in order to insure that cracks do not reinitiate from the holes drilled at the crack tips *(17)*. The advantage of this scheme is that it can be carried out while the structure remains in service.

Direct attachment of the connection plate to the top flanges of girders was found to be the most effective way to minimize out-of-plane displacement stresses. Welding is difficult because of the overhead position and the dirt accumulated between the end of the connection plate and the girder flange surface. If the work is carried out while the bridge is in service, traffic should be stopped so that movement is minimized while the weld is made. Careful cleaning and preheat will be needed to insure quality welds. When direct attachment is provided by bolted attachments such as angles, channels or fabricated components, these elements should be at least ¾ in. (19 mm) thick and four or more preloaded high strength bolts should be used for every shear plane. Often, a positive attachment to the top flange is made when the slab is replaced as this improves access and ease of carrying out the retrofit.

The drilled holes installed at the tips of cracks that have turned transverse to the in-plane bending stress in the girder web should satisfy the relationship *(14)*

$$\frac{\Delta K}{\sqrt{\rho}} < 4\sqrt{\sigma_y} \quad (\text{for } \sigma_y \text{ in ksi})$$

$$\frac{\Delta K}{\sqrt{\rho}} < 10.5\sqrt{\sigma_y} \quad (\text{for } \sigma_y \text{ in MPa})$$

where ΔK is the stress intensity range for the in-plane bending stresses. The stress intensity range can be approximated by $\Delta K = S_r\sqrt{\pi a_r}$, where S_r is the in-plane bending stress range and a_r the crack size as illustrated in Figures 39 and 60. The radius of the hole, ρ, used to satisfy this relationship can be estimated from these known factors.

CHAPTER FOUR
CONCLUSIONS AND SUGGESTED RESEARCH

The conclusions in this chapter are based on an analysis and evaluation of the test data acquired during this laboratory study, on the results of other experimental work in the laboratory and field, and on theoretical studies.

FATIGUE BEHAVIOR OF WEB GUSSET PLATES

1. Strain measurements at all gusset plate outer ends verified the development of a secondary bending gradient through the web's thickness. The nominal, in-plane bending stress of 6 ksi (41.4 MPa) was maintained. However, the driving forces produced an overall lateral translation of the gusset plates. Such translations were sufficient to elevate the secondary stress ranges at the outer weld terminations by 3 to 4 ksi (20.7 to 27.6 MPa). This resulted in combined stresses that substantially exceeded the fatigue limit for Category E. No cracks were detected at any of these end terminations after 10 to 20 million stress cycles. The test results suggest that out-of-plane distortion stress range is not as adverse as the in-plane stress range.

The laboratory observations are generally supported by the experience with actual bridges. Measurements have indicated similar combinations of in-plane and out-of-plane bending stress but no significant cracking even when the fatigue limit is exceeded.

2. Crack development in the web gaps between transverse connection plate and lateral gusset plates were found to be compatible with the fatigue strength provided by Category C.

3. The study indicated that it was undesirable to provide intersecting vertical connection plates or stiffeners and lateral gusset plates without a positive attachment between these elements by welding or bolting. Substantial increases in the relative out-of-plane displacement occurred when no direct connection was provided. This increased the probability of fatigue cracking at gusset plate web gaps.

4. The stress-time response of the web gaps of lateral gusset plates in bridge structures is a complex interaction of the girder flanges, the floorbeams, and the laterals. Current design procedures do not provide a means of adequately evaluating these stress conditions.

The inability to accurately predict stresses require providing adequate web gaps and a positive attachment between transverse stiffeners (or vertical connection plates) and lateral gusset plates that intersect if cracking is to be minimized. The horizontal gaps between these intersecting elements should be at least 2 in. (51 mm) when welded connections are used and 3 in. (76 mm) when bolted connections are used.

FATIGUE BEHAVIOR OF TRANSVERSE CONNECTION PLATES AT WEB GAPS

1. Cracks forming at the ends of transverse connection plates in the web gap were found to provide a fatigue strength compatible with Category C.

2. The end of the transverse connection plate was observed to provide a higher stress concentration than the web-flange weld toe. This resulted in most of the fatigue cracks initially forming at the end of the transverse connection plate (13 of 15), even though the stress range was often greater at the web-flange weld.

3. Only one of the girders developed a crack that propagated into the girder flange. This occurred when the in-plane bending stress range was 12 ksi (82.8 MPa). The crack initiated from the web-flange crack surface which was irregular and produced a notch effect.

RETROFITTING PROCEDURES

1. The placement of holes through the girder web at the tip of the cracks that formed in the horizontal and vertical web gaps were capable of arresting crack growth and preventing cracks from reinitiating when the relationship

$$\frac{\Delta K}{\sqrt{\rho}} < 4\sqrt{\sigma_y} \quad (\text{for } \sigma_y \text{ in ksi})$$

$$\frac{\Delta K}{\sqrt{\rho}} < 10.5\sqrt{\sigma_y} \quad (\text{for } \sigma_y \text{ in MPa})$$

is satisfied.

For gusset plate-stiffener intersections it is also necessary to provide a positive attachment between the gusset plate and the transverse stiffener in order to minimize the distortion induced stress component.

2. At transverse connection plate web gaps, placement of holes at the crack tip will prevent further crack growth for out-of-plane distortion stress range levels less than 15 ksi (105 MPa). When high levels of distortion induced stress range exist, a positive connection must be provided between the transverse connection plate and the girder flange in order to minimize the distortion induced stress.

3. A few details were retrofitted by partial removal of the transverse connection plate to increase the web gap. The data are insufficient to provide a recommended procedure. Field tests on floor beam end connection web gaps *(17)* have demonstrated that this technique is feasible. Care must be excersized to ensure that web gap distortion does not increase substantially when this procedure is used.

TRANSVERSE CONNECTION PLATES FOR MULTIGIRDER BRIDGES

Based on field observations and measurements, and available analytical studies on multigirder bridges the following observations can be made on the behavior of small gaps at the ends of diaphragm transverse connection plates.

1. Out-of-plane displacement induced web gap stresses are highly localized in the vicinity of the gap regions. the vertical (transverse) stresses reduce rapidly in the horizontal direction away from the centerline of the transverse connection plate, and in the vertical direction away from the end of the transverse connection plate.

2. Web gap stresses at a diaphragm transverse connection plate are dependent upon the lateral position of a truck load. The stresses in gaps at exterior girders are higher when the load is over or near the top of the girder. At interior girders, loads in the traffic lane away from the girder cause higher web stresses in the connection plate gap *(7, 9, 18, 19)*.

3. The web gap stresses at diaphragm transverse connection plates in the positive moment regions (i.e. at gap adjacent to the bottom flange) of continuous girders are much smaller than those in negative moment regions of girders. Cracks were only detected at end of connection plates adjacent to the top flange in highway bridges unless staggered diaphragms were used in skewed or curved structures. Cracks have also been detected in gaps adjacent to the bottom flange in simply supported railroad and mass transit bridges. Measurements on these types of structures have indicated that the web gap stresses are about the same magnitude as those observed in highway bridges adjacent to the top flange *(7)*.

4. Under normal traffic loading, K-type truss diaphragms were found to exert less force on the girder webs than the X-type truss diaphragms. Other conditions being the same, the web stresses in the gaps of connection plates for K-type diaphragms are lower and not as likely to exhibit cracking as early *(9, 18)*.

5. For the same distance between the flange and the connection of diaphragm components, deeper girders have lower forces in the components of the diaphragm. This results in lower web stresses at the diaphragm connection plate gap.

6. For two lane, multigirder highway bridges under normal traffic loads, the out-of-plane plate bending stresses in the web gaps at diaphragm connection plates are substantially lower for 3-girder bridges than for 4- or 5-girder bridges *(9, 18)*.

TRANSVERSE CONNECTION PLATES AND GUSSET PLATES FOR FLOORBEAM- GIRDER BRIDGES

1. Studies on floorbeam-girder bridges have indicated that displacement induced web gap cyclic stresses cause cracking in three general locations. The most prominent was the top end of the vertical connection plate of floorbeams adjacent to bridge piers. Next were the horizontal gaps between the lateral bracing gusset plates and the floorbeam connection plates, (and outside the facia girder along the exterior stiffeners opposite the gaps). Structures without a positive attachment between the gusset plate and the transverse connection plate

were the most susceptible to cracking. When a positive attachment was provided, only a limited number of cracks have formed generally when bolted connections were used with small web gaps. The third condition is at the bottom end of the floorbeam connection plate and the bottom flange. Flange gusset plates connected to the bottom lateral system have resulted in cracks in the bottom web gap when no positive attachment was provided between the transverse connection plate and the bottom flange.

2. The out-of-plane displacement induced web stresses at the gaps are highly localized in the vicinity of the gap regions. This condition is similar to the conditions that develop at diaphragm connection plates of multigirder bridges. The magnitude of the deformation is greater at floorbeams.

3. The web plate of the main girders at the ends of floorbeam connection plates is subject to out-of-plane bending because of the end rotation of the floorbeam. The web plate at the gusset plate gap is subject to out-of-plane plate bending primarily because of the out-of-plane forces developed in the laterals and the end rotation. These forces introduce twisting into the lateral gusset plate region.

4. A number of retrofit procedures have been applied to the floorbeam connection plate and lateral gusset plate regions. Drilled holes alone at ends of cracks at the top end of floorbeam connection plates were not effective in arresting the cracks. Measured strains in these cracked regions indicated that the web stresses were still high and that cracking would continue to develop without a positive attachment between the connection plate and beam flange.

The horizontal gaps between the gusset end and the transverse connection plate should be about 2 in. (51 mm) when welded connections are used. When bolted connections are provided to bridge the web gap, the gap should be increased to at least 3 in. (76 mm).

RECOMMENDATIONS FOR FURTHER RESEARCH

The laboratory fatigue tests provided in this report and the review of web gap cracking in actual bridge structures indicated that further work is needed in order to better understand and provide rational design criteria for new bridges and more reliable way of retrofitting existing structures.

Transverse Stiffener-Gusset Plate Web Gaps

The experimental work reported in *NCHRP Report 227 (14)* and in this study have demonstrated that positive welded connections between the gusset and transverse stiffener reduces the web gap distortion to levels that are below the fatigue limit. However, further work is needed on mechanical connections to better establish the relationship between web gap geometry, distortion of the web gap, and characteristics of the connections to resist web gap distortion.

Lateral Gusset Plates On Girder Webs

The ends of lateral gusset plates have a demonstrated fatigue resistance corresponding to Categories E or E' for in-plane bending. This study has indicated that out-of-plane web bending stress is not as adverse as the in-plane bending stress. The twelve details in this program had a combined cyclic stress at the ends of the gusset plate between 9 and 10 ksi (62 and 69 MPa). No cracks formed after 10 to 20 million stress cycles. Actual bridge structures have indicated that the gusset plate is twisted from the out-of-phase loading in the laterals. Further laboratory studies are needed to establish the fatigue strength of lateral connection plates in existing structures. It appears desirable to develop experimental results which simulate the out-of-plane twist. This would permit an assessment of the necessity to retrofit these details.

Cyclic Loads In Diaphragms And Girder Spacing

A recent development in design practice is the increased spacing of girders. This results in cyclic forces in the diaphragms that are transmitted to the transverse connection plates. The cyclic forces acting on the diaphragm connection plates have resulted in fatigue cracks forming in the welded connection between the transverse connection plate and the top flange. Measurements on one of the structures experiencing cracking suggested that the floorbeam and slab was twisting the top flange. A second structure had intermediate cross frames and exhibited similar cracking at the welded connection. This type of cracking has been extensive in Japan where much smaller stiffeners (6 mm × 50 mm) have been used. There is a need to examine the geometric conditions and develop rational design criteria for the transverse connection plate welds used in bridge structures, particularly as the girder spacing is increased. Both laboratory experimental and field measurements are needed.

Secondary Vibrations In Web Gaps

High frequency vibration has been observed at the bottom gap of floorbeam connection plates in positive moment region at Canoe Creek Bridge and at similar location of a railroad bridge. The frequency of the vibration appears to be close to the natural frequency of the plate panel. The stress range caused by this vibration is about as large as the stress range caused by loads for the distorted web gaps. This high frequency vibration was also observed at the edges of the drilled holes at the top gap of the floorbeam connection plate, and may account for the re-initiation and development of cracks in such short time intervals as was the case for the Canoe Creek Bridge. Studies are needed to determine the geometric conditions and characteristics of lateral systems and bridges that are susceptible to this type of response.

REFERENCES

1. Fisher, J. W., *Bridge Fatigue Guide - Design and Details,* American Institute of Steel Construction, (1977) .
2. Fisher, J. W., "Fatigue Cracking in Bridges from Out-of-Plane Displacements", *The Canadian Journal of Civil Engineering*, Vol. 5, No. 4, (1978).
3. Fisher, J. W., *Fatigue and Fracture of Steel Highway Bridges, Case Studies,* Wiley-Interscience, (1984) .
4. Fisher, J. W. and Keating, P. B., "Fatigue Cracking in Box Girders from Web Gap Distortion", *Steel Structures: Recent Research Advances,* Elsevier Applied Science Publisher, (1986).
5. Fisher, J. W., Yen, B. T., and Wagner, D. C., "Review of Field Measurements for Distortion Induced Fatigue Cracking in Steel Bridges", *Transportation Research Record 1118*, Transportation Research Board, (1987).
6. Fisher, J. W. and Keating, P. B., "Distortion-Induced Fatigue Cracking at Bridge Details with Web Gaps", *Journal of Constructional Steel Research*, Vol. 12, (1989), pp. 215-228.
7. Demers, C. and Fisher, J. W., "A Survey of Localized Cracking in Steel Bridges: 1981 to 1988, Volume 1, Final Report", *Center for Advanced Technology for Large Structural Systems, FHWA-RD-89-166*, (April 1989).
8. AASHTO, *Standard Specifications for Highway Bridges, 14th Edition,* AASHTO, (1989) .
9. Fisher, J. W., Kaufmann, E. J., Kostem, C. N., Lee, J. J., Moser, D., Papavizas, P. G., and Yen, B. T., "Deformation Induced Cracking in Steel-Girder Bridges and Retrofit Guidelines", *Fritz Engineering Laboratory Report 500-3(87), Lehigh University,* (July 1987).
10. Fisher, J. W., Hausammann, H., Sullivan, M.,D., and Pense, A. W., "Detection and Repair of Fatigue Damage in Welded Highway Bridges", *NCHRP Report 206,*

Transportation Research Board, (June 1979).

11. Goerg, P., *Uber die Aussagefahigkeit von Dauer versuchen mit Prufkorpern aus Baushahl ST37 and ST52*, Der Stahlban, No 2, 1963 .
12. Mueller, J. A. and Yen, B. T., *Girder Web Boundary Stresses and Fatigue*, Welding Research Council Bulletin 127, (1968) .
13. Fisher, J. W., Menzemer, C. A., Lee, J. J., Yen, B. T., and Kostem, C. N., "Distortion Induced Stresses in a Floorbeam-Girder Bridge: Canoe Creek", *Fritz Engineering Laboratory Report 500-2(86), Lehigh University*, (April 1986).
14. Fisher, J. W., Barthelemy, B. M., Mertz, D. R., and Edinger, J. A., "Fatigue Behavior of Full-Scale Welded Bridge Attachments", *NCHRP Report 227, Transportation Research Board*, (November 1980).
15. Fisher, J. W., "Report on Strain Measurements on Woodrow Wilson Bridge", *FHWA Turner Fairbank Highway Research Center*, (1983).
16. Mertz, D. R., "Displacement-Induced Fatigue Cracking in Welded Steel Bridges", PhD dissertation, Lehigh University, Bethlehem, PA, (April 1984).
17. Koob, M. J., Frey, P. D., and Hanson, J.M., "Evaluation of Web Cracking at Floor Beam to Stiffener Connections of the Poplar Street Bridge Approaches, FAI Route 70, East St. Louis, St. Clair County, Illinois", *Wiss, Janney, Elstner Associates for the Illinois Department of Transportation*, (September 1985)Summarized in Transportation Research Record 1118 (1987)
18. Lee, J. J., Castiglioni, C., Fisher, J. W., Kostem, C. N., and Yen, B. T., "Displacement Induced Stresses in Multigirder Steel Bridges", *Fritz Engineering Laboratory Report 500-1(86), Lehigh University*, (February 1986).
19. Fisher, J. W., Kardara, A., Kaufmann, E. J., Lee, J. J., Pense, A. W., and Yen B. T., "Final Report on Cracking of I-79 Bridges 2680 and 2682", *Fritz Engineering Laboratory Report 501-1(85), Lehigh University*, (May 1985).
20. Fisher, J. W., Pense, A. W., Menzemer, C. C., and Kaufmann, E., J., "Final Report on I-79 Tied Arch Cracking - Neville Island Bridge", *Fritz Engineering Laboratory Report*

494-1(84), Lehigh University, (December 1984).

21. Fisher, J. W., Yen, B. T., Wang, D., and Mann, J. E., "Fatigue Evaluation of Riveted Bridge Structures", *NCHRP Report 302, Transportation Research Board*, (December 1987).

Table 1: Results of measurements at bearing stiffener, Poplar Street Bridge

MAXIMUM OUT-OF-PLANE DISPLACEMENT (IN.)		WEB GAP STRESSES (KSI)	
TYPICAL TRUCKS	MAXIMUM	TYPICAL TRUCKS	MAXIMUM
< 0.001	> 0.001	9.8 - 13.0	14.0
< 0.001	0.001	5.6 - 8.2	10.5
< 0.0005	0.0005	4.2 - 5.1	6.5
< 0.001	0.001	2.6 - 4.2	4.9
< 0.0005	> 0.0005	1.0	1.4

Table 2: Results of measurements at floor beam connections, Poplar Street Bridge

CRACK LENGTH (IN.)	MAXIMUM OUT-OF-PLANE DISPLACEMENT (IN.)
7.0	0.043
6.0	0.030
4.5	0.025
3.5	0.020
3.25	0.021
3.0	0.021
2.75	0.025
2.5	0.008
1.875	0.024
1.75	0.022
1.5	0.028
Uncracked	0.001
Uncracked	> 0.001
Uncracked	0.000

Table 3: Summary of lateral gusset plate details

Detail	Gap Size	In-Plane Stress Range	Out-of-Plane Stress Range	Extrapolated at	Cycles to Crack	Cycles to Retrofit
T5-1 (Type A)	1.45 in[c] (2.0 in)[a]	6.0 ksi	15.0 ksi	Transverse Weld Toe	No Cracking Detected	20,000,000[b]
T5-2 (Type A)	1.5 in[c] (2.0 in)[a]	6.0 ksi	11.5 ksi	Transverse Weld Toe	No Cracking Detected	20,000,000[b]
T5-3 (Type B)	0.8 in[c] (1.5 in)[a]	6.0 ksi	13.0 ksi	Transversen Weld Toe	No Cracking Detected	10,000,000[b]
T5-4 (Type B)	0.9 in[c] (1.5 in)[a]	6.0 ksi	15.0 ksi	Transverse Weld Toe	No Cracking Detected	10,000,000[b]
T5-6 (Type B)	2.2 in[c] (3.0 in)[a]	6.0 ksi	10.0 ksi	Transverse Weld Toe	No Cracking Detected	10,000,000[b]
T5-7 (Type B)	2.2 in[c] (3.0 in)[a]	6.0 ksi	11.0 ksi	Transverse Weld Toe	No Cracking Detected	10,000,000[b]
T5-8 (Type B)	2.45 in[c] (3.0 in)[a]	6.0 ksi	15.5 ksi	Transverse Weld Toe	No Cracking Detected	20,000,000[b]
T5-5 (Type B)	0.9 in[c] (1.5 in)[a]	6.0 ksi	19.5 ksi	Transverse Weld Toe	5,000,000	9,400,000
T5-9 (Type C)	0.2 in[c] (1.0 in)[a]	6.0 ksi	23.0 ksi	Transverse Weld Toe	1,280,000	3,800,000
T5-10 (Type C)	0.3 in[c] (1.0 in)[a]	6.0 ksi	26.3 ksi	Transverse Weld Toe	1,280,000	2,900,000
T5-11 (Type C)	2.4 in[c] (3.0 in)[a]	6.0 ksi	28.3 ksi	Transverse Weld Toe	1,150,000	3,300,000
T5-12 (Type C)	2.3 in[c] (3.0 in)[a]	6.0 ksi	31.5 ksi	Transverse Weld Toe	1,100,000	3,300,000

[a] Nominal gusset plate web gap, see Figure 4
[b] Cycles at which the test was terminated
[c] The actual gap size between the weld toes

Table 4: Summary of retrofit history of gusset plate details: (a) First retrofit; (b) Final retrofit

(a)

DETAIL	CRACK LENGTH (IN.)	CYCLES ($\times 10^6$)	HOLE DIAMETER (IN.)	$\Delta K/\sqrt{\rho}$ (KSI)
T5-5	6.2	5.0	1 1/4	23.7
T5-9	3.3	3.8	1	19.3
T5-10	3.1	2.9	3/4	20.9
T5-11	2.2	3.3	1 1/4	17.3
T5-12	2.35	3.3	1 1/4	17.3

(b)

DETAIL	CRACK LENGTH (IN.)	CYCLES ($\times 10^6$)	RETROFIT PROCEDURES	$\Delta K/\sqrt{\rho}$ (KSI)	TEST TERMINATED ($\times 10^6$)
T5-5	9.8	12.0	2 in. hole	26.0	20
T5-9	4.5	5.3	Bolted attachment	24.5	10
T5-10	6.3	3.8	1 1/4 in. holes and bolted attachment	18.5	10
T5-11	2.2	3.3	1 1/4 in. holes and bolted attachment	17.3	10
T5-12	2.35	3.3	1 1/4 in. holes and bolted attchment	17.3	10

Table 5: Summary of transverse connection plate details

Detail	Gap Size	In-Plane Stress Range	Out-of-Plane Stress Range	Extrapolated at	Cycles to Crack	Cycles to Retrofit
T1-L1 G1	0.44 in (1.5 in)[a]	6.0 ksi	12.6 ksi	Web-Flange Weld	No Cracking Detected	22,600,000[b]
T1-L1 G2	0.39 in (1.5 in)[a]	6.0 ksi	13.5 ksi	Web-Flange Weld	No Cracking Detected	22,600,000[b]
T2-L1 G1	2.01 in (3.0 in)[a]	6.0 ksi	7.3 ksi	Web-Flange Weld	No Cracking Detected	22,600,000[b]
T2-L1 G2	1.81 in (3.0 in)[a]	6.0 ksi	8.9 ksi	Connection Plate End	4,503,000	22,600,000[b]
T1-L2 G3	0.24 in (1.5 in)[a]	6.0 ksi	32.5 ksi	Connection Plate End	1,799,000	17,000,000[b]
T1-L2 G4	0.34 in (1.5 in)[a]	6.0 ksi	9.4 ksi	Web-Flange Weld	No Cracking Detected	17,000,000[b]
T2-L2 G3	1.99 in (3.0 in)[a]	6.0 ksi	14.5 ksi	Web-Flange Weld	No Cracking Detected	17,000,000[b]
T2-L2 G4	2.75 in (3.0 in)[a]	6.0 ksi	7.7 ksi	Connection Plate Weld	17,000,000[c]	17,000,000[b]
T1-I G5	0.65 in (1.5 in)[a]	6.0 ksi	7.5 ksi	Connection Plate End	10,690,000	20,000,000[b]
T1-I G6	0.84 in (1.5 in)[a]	6.0 ksi	11.2 ksi	Web-Flange Weld	No Cracking Detected	20,000,000[b]
T2-I G5	1.93 in (3.0 in)[a]	6.0 ksi	8.8 ksi	Connection Plate End	8,700,000	20,000,000[b]
T2-I G6	1.95 in (3.0 in)[a]	6.0 ksi	19.2 ksi	Connection Plate End	1,105,000	3,023,000
T1-H G7	0.50 in (1.5 in)[a]	6.0 ksi	20.2 ksi	Connection Plate End	714,000	5,017,000
T1-H G8	0.53 in (1.5 in)[a]	6.0 ksi	6.2 ksi	Web-Flange Weld	No Cracking Detected	11,400,000[b]
T2-H G7	1.98 in (3.0 in)[a]	6.0 ksi	12.7 ksi	Web-Flange Weld	No Cracking Detected	11,400,000[b]
T2-H G8	2.01 in (3.0 in)[a]	6.0 ksi	23.3 ksi	Connection Plate End	522,000	2,846,000
T3-L G9	1.13 in (1.5 in)[a]	12.0 ksi	16.4 ksi	Connection Plate Weld	3,332,000	6,000,000[b]
T3-L G10	0.40 in (1.5 in)[a]	12.0 ksi	10.2 ksi	Connection Plate End	3,332,000	6,000,000[b]

[a] Nominal web gap
[b] Cycles at which the test was terminated
[c] Crack found after completion of test

Detail	Gap Size	In-Plane Stress Range	Out-of-Plane Stress Range	Extrapolated at	Cycles to Crack	Cycles to Retrofit
T4-L G9	1.95 in (3.0 in)[a]	12.0 ksi	8.4 ksi	Connection Plate End	No Cracking Detected	6,000,000[b]
T4-L G10	2.02 in (3.0 in)[a]	12.0 ksi	14.8 ksi	Connection Plate End	855,000	3,332,000
T3-H G11	0.44 in (1.5 in)[a]	12.0 ksi	27.5 ksi	Web-Flange Weld	499,000	1,981,000
T3-H G12	0.41 in (1.5 in)[a]	12.0 ksi	15.3 ksi	Web-Flange Weld	1,130,000	1,981,000
T4-H G11	2.11 in (3.0 in)[a]	12.0 ksi	24.7 ksi	Connection Plate End	208,300	1,246,000
T4-H G12	1.90 in (3.0 in)[a]	12.0 ksi	27.1 ksi	Connection Plate End	141,500	1,246,000

[a] Nominal web gap
[b] Cycles at which the test was terminated
[c] Crack found after completion of test

Table 6: Summary of retrofit history of transverse connection plate details: (a) First retrofit; (b) Final retrofit

(a)

DETAIL	CRACK LOCATION	CYCLES ($\times 10^6$)	CRACK SIZE (IN.)	RETROFIT PROCEDURE	$\Delta K/\sqrt{\rho}$ (KSI)
T2-I G6	Connection plate end	3.02	1.2	One 3/4 in. hole	11.2
T1-H G7	Connection Plate End	5.02	1.8	Removed 5 1/2 in. connection plate	
T2-H G8	Connection plate end	2.85	2.0	One 1 in. hole	12.5
T4-L G10	Connection plate end	3.33	2.4	Bolted attachment	
T3-H G11	Web-flange weld	1.98	5.8	Bolted attachment	
T3-H G12	Web-flange weld	1.98	2.6	Bolted attachment	
T4-H G11	Connection plate end	1.25	1.2	1 in. hole	22.4
T4-H G12	Connection plate end	1.25	3.5	1 1/4 in. hole	29.7

(b)

DETAIL	CYCLES ($\times 10^6$)	CRACK SIZE (IN.)	RETROFIT PROCEDURE	TEST TERMINATED ($\times 10^6$)
T2-I G6	8.75	1.4	One 3/4 in. hole	20.0
T1-H G7	6.96	2.1	Removed 5 1/2 in. of connection plate	11.4
T2-H G8		2.0		11.4
T4-L G10				6.0
T3-H G11				3.04
T3-H G12				3.04
T4-H G11				3.04
T4-H G12	1.98	4.0	Removed 4 in. of connection plate and drilled hole	3.04

Table 7: Summary of transverse connection plate details with cracks but no retrofit

DETAIL	CRACK LOCATION	INITIAL CRACK LENGTH (IN.)	CYCLES TO CRACK ($\times 10^6$)	FINAL CRACK LENGTH (IN.)	TOTAL CYCLES ($\times 10^6$)
T2-L1 G2	Connection plate end	0.9	4.5	3.8	22.6
T1-L2 G3	Connection plate end	0.6	1.8	3.1	17.0
T2-L2 G4	Connection plate end	0.25	17.0	0.25	17.0
T1-I G5	Connection plate end	0.6	10.7	2.5	20.0
T2-I G5	Connection plate end	0.6	8.7	1.9	20.0
T3-L G9	Connection plate weld	0.45	3.33	0.9	6.0
T3-L G10	Connection plate end	0.4	2.5	1.1	6.0

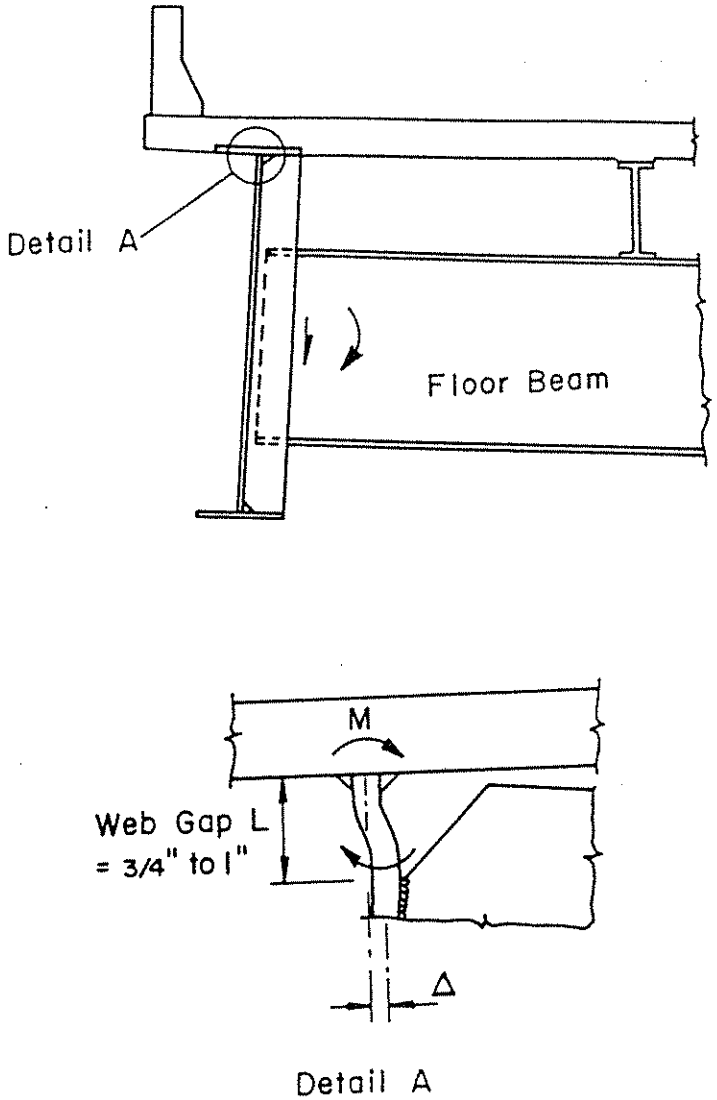

Figure 1: Schematic of distortion in web gap at end of floorbeam transverse connection plate

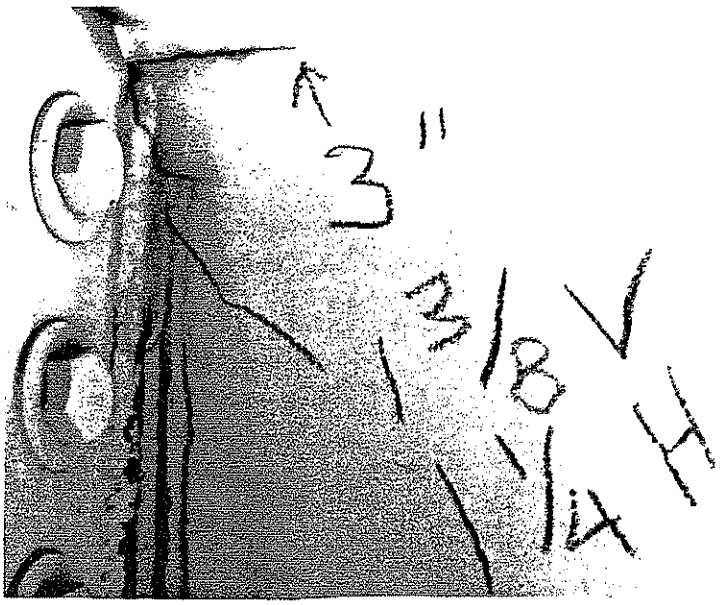

(a)

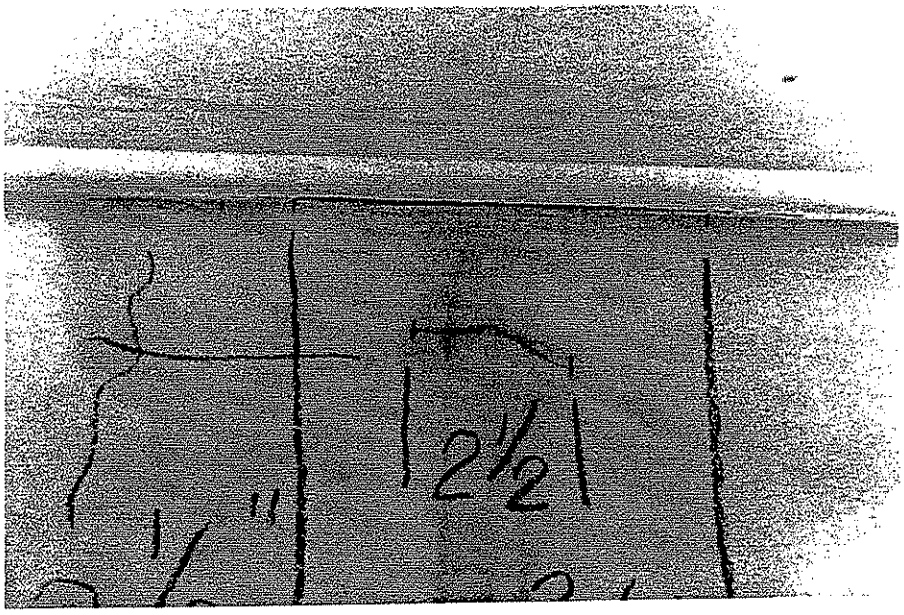

(b)

Figure 2: (a) Web gap fatigue cracking at the transverse connection plate for a floorbeam; (b) Web gap cracking on the exterior girder web face

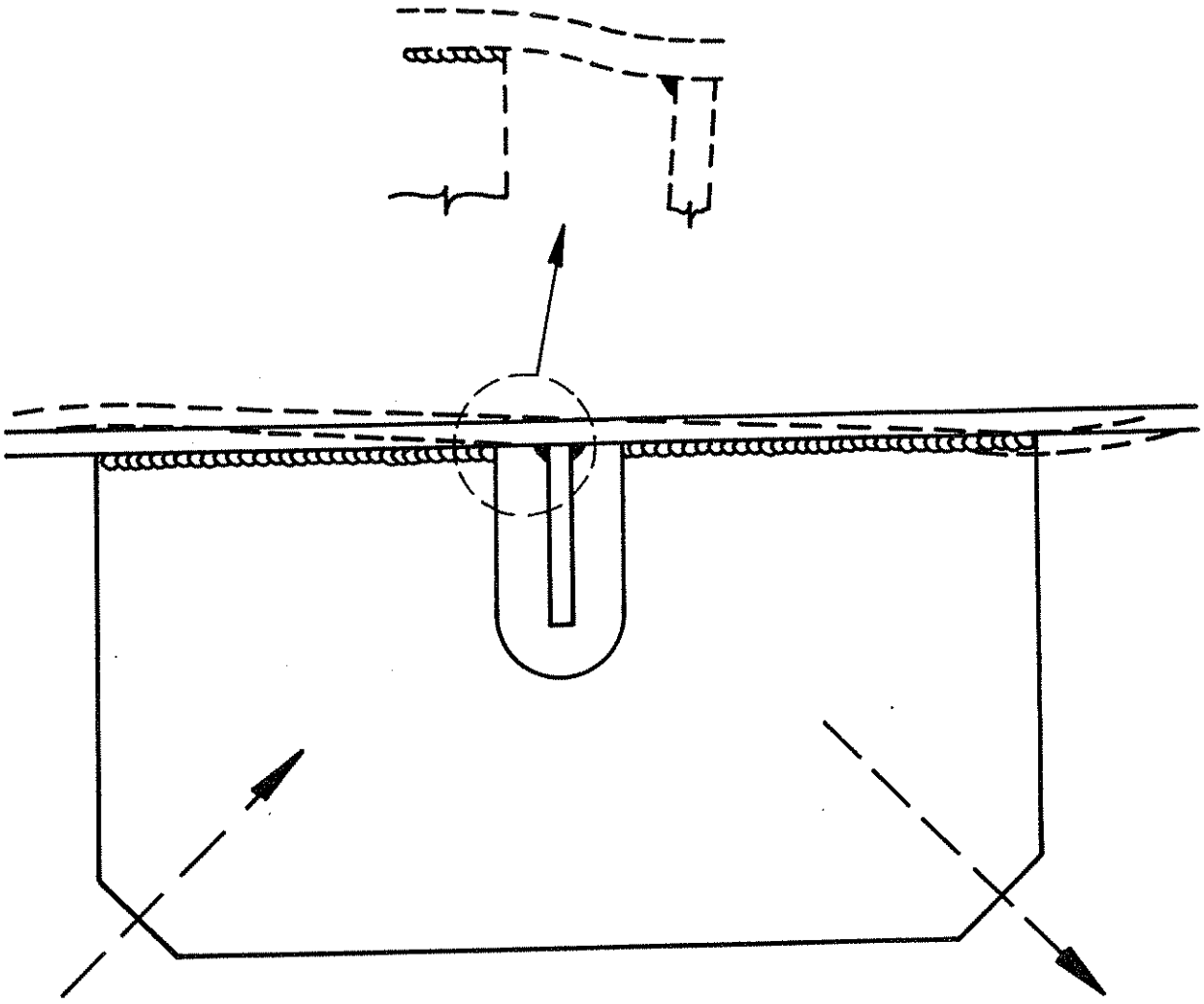

Figure 3: Schematic of distortion in web gap at lateral gusset plate

- All Holes To Be 1"dia. For 7/8"dia. Bolts
- All Gusset PL To Be 1/2" Thick
- All Gusset To Web Welds To Be 5/16"
- All 1/2" PL Welds To Be 5/16"

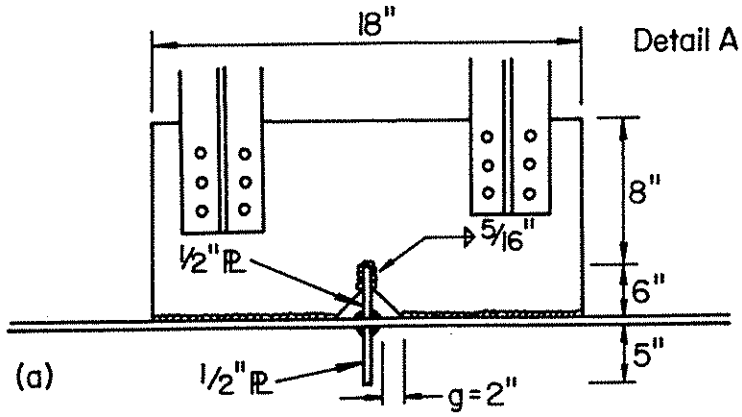

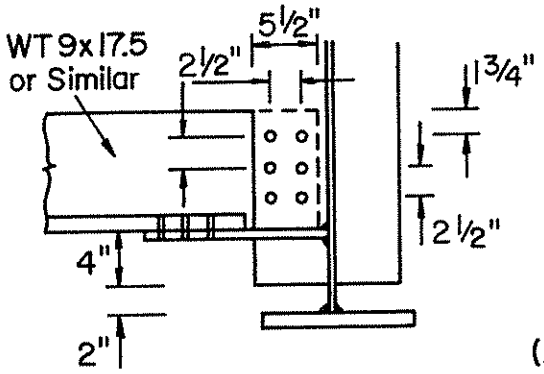

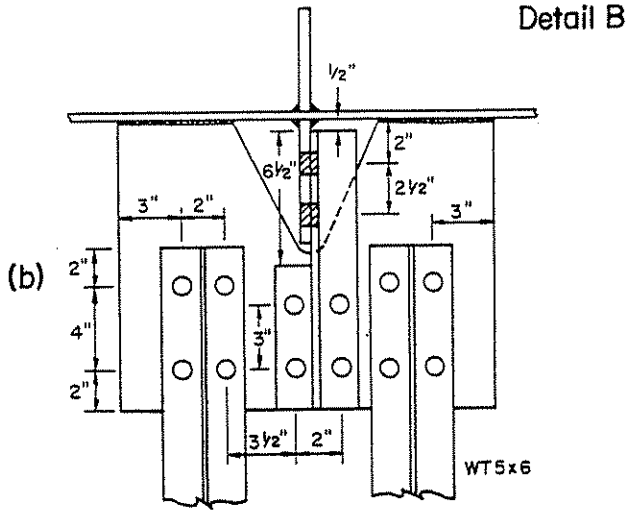

- All Holes Are 1" dia. For 7/8" dia. A325 Bolts

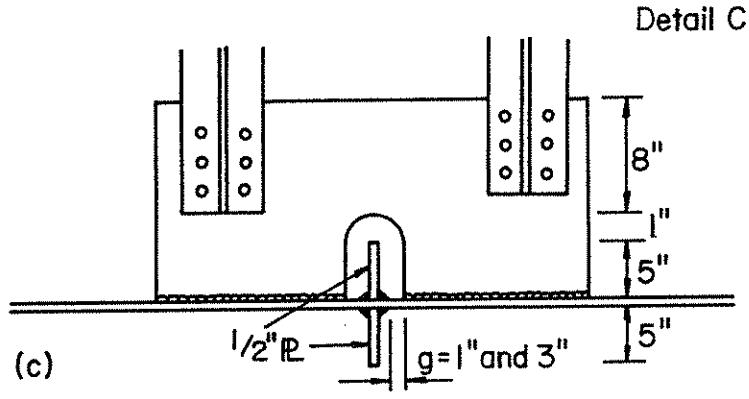

Figure 4: Gusset plate connection details

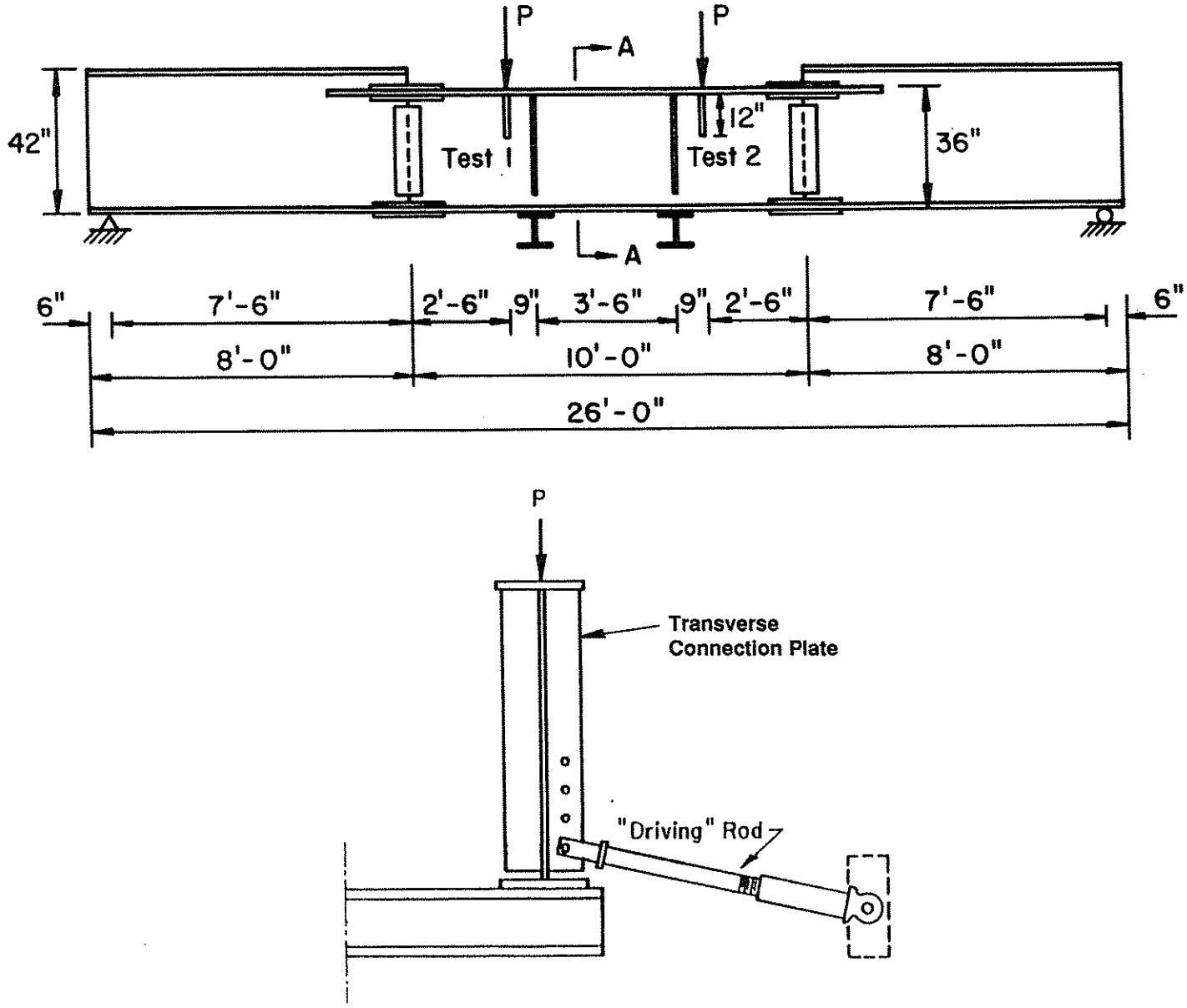

Figure 5: Test setup for transverse connection plates

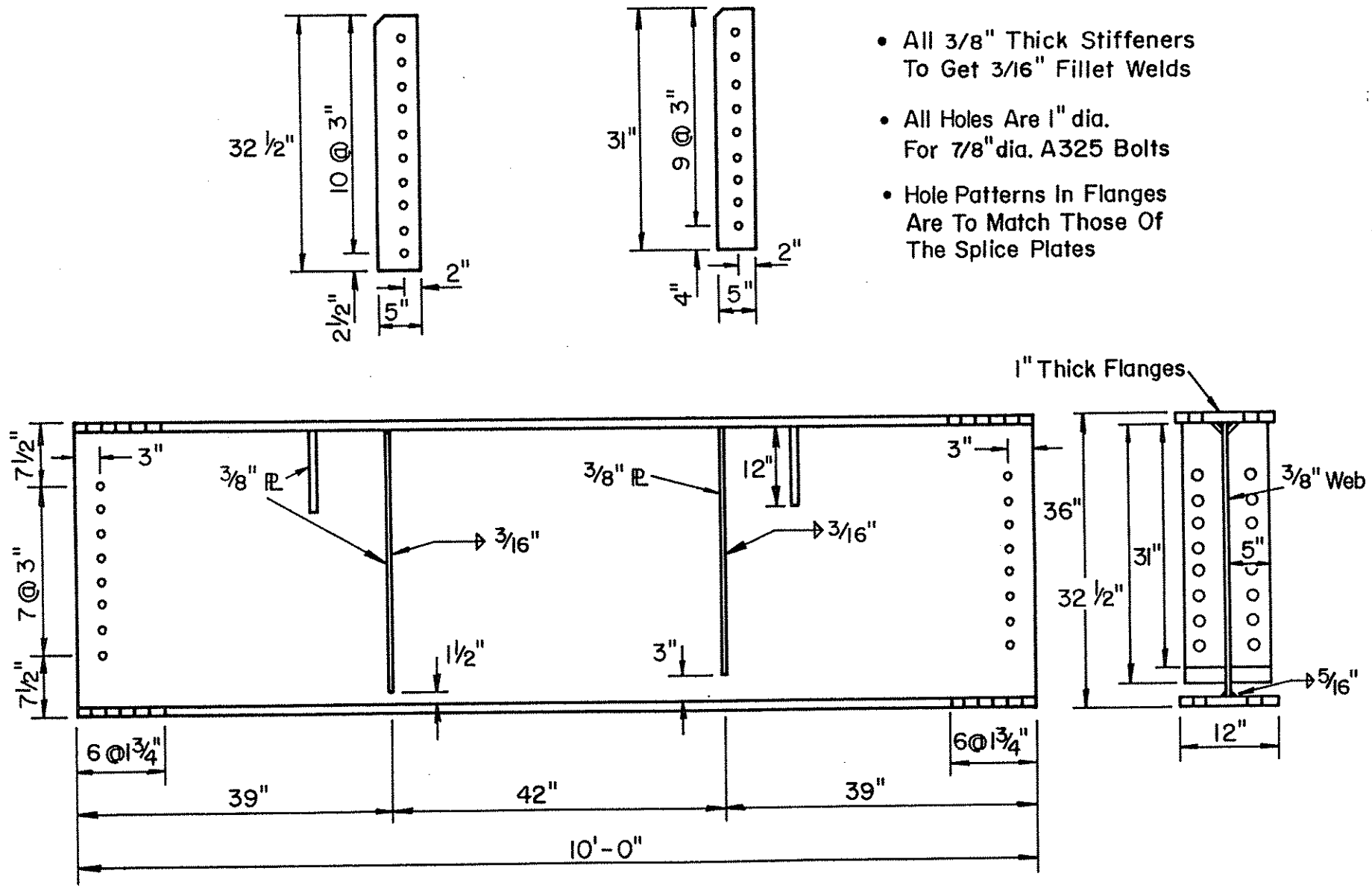

Figure 6: Test specimen for transverse connection plate web gaps

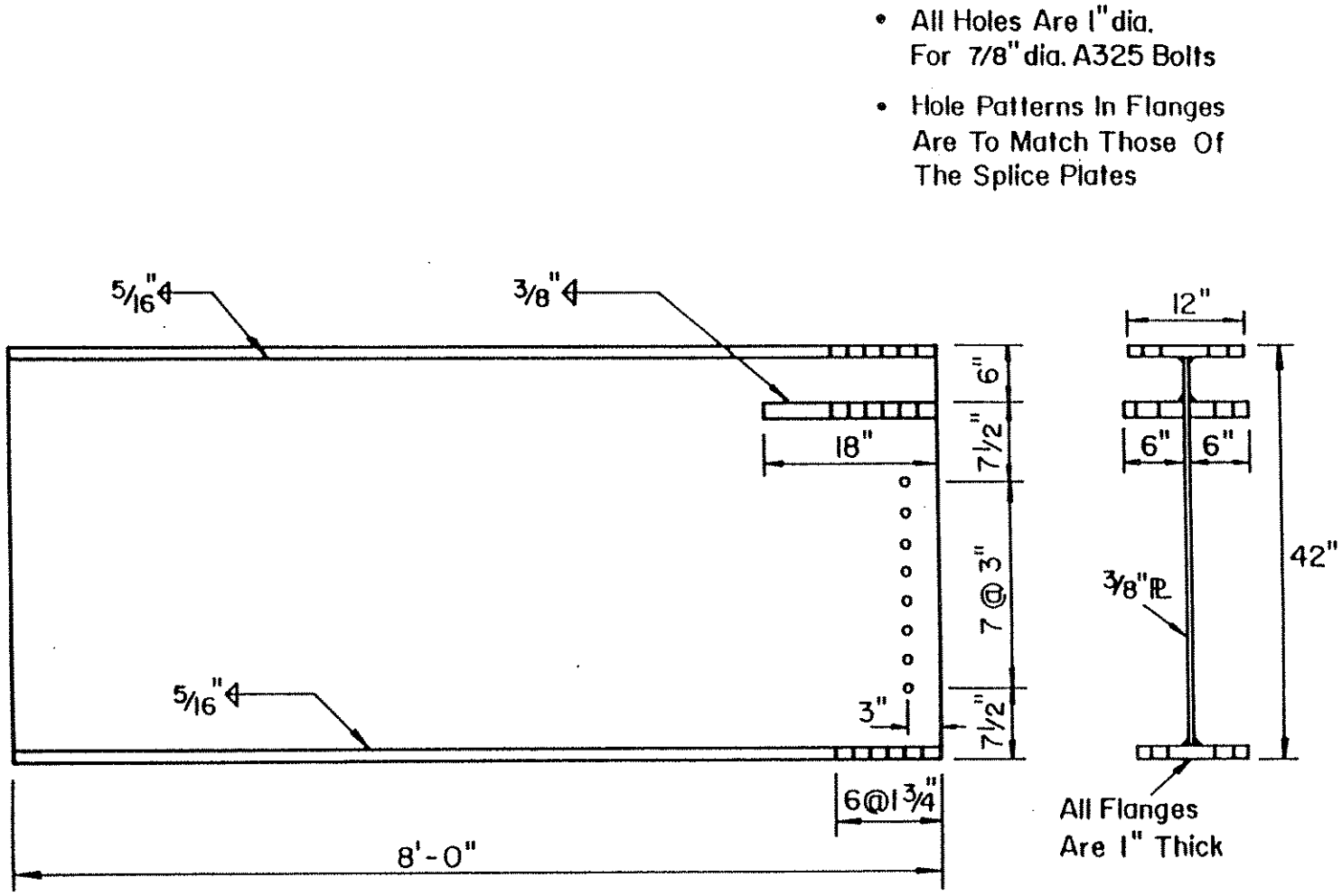

Figure 7: Reusable end members for the test sections

- All 3/8" Thick Connection PL To Get 3/16" Fillet Welds
- All 1/2" Thick Connection PL To Get 5/16" Fillet Welds
- All Holes To 1" dia. For 7/8" dia. A325 Bolts
- Outer Connection PL To Be 38"x 5"x 3/8"
- Inner Connection PL To Be 38"x5"x 3/8"
- Or 38"x 6"x 1/2" Based On Detail Type
- Outer PL To Be Perforated As Shown

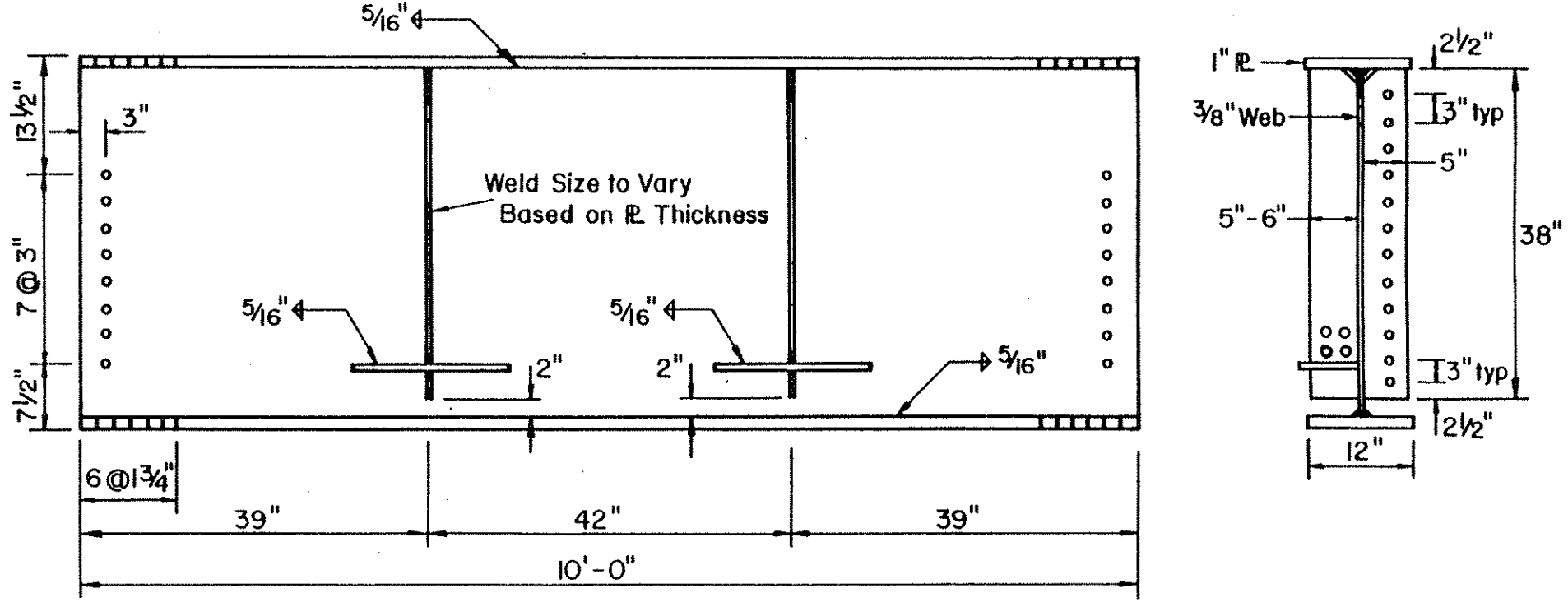

Figure 8: Test specimen for gusset plates framing around transverse connection plates

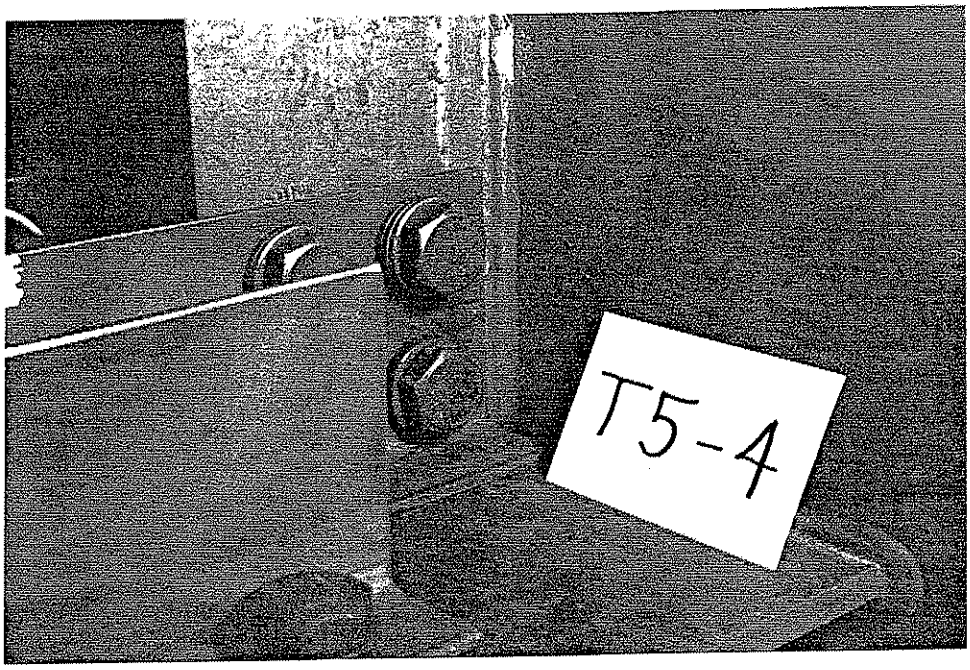

Figure 9: Gusset plate bolt pattern

Primary S_r	6 ksi		12 ksi	
Web Gap / Level of Distortion	1 - 1/2 in.	3 in.	1 - 1/2 in.	3 in.
Low	T1 - L1 T1 - L2	T2 - L1 T2 - L2	T3 - L	T4 - L
Intermediate	T1 - I	T2 - I	T3 - I	T4 - I
High	T1 - H	T2 - H		

Figure 10: Factorial experiment arrangement for web gap distortion of transverse stiffenters

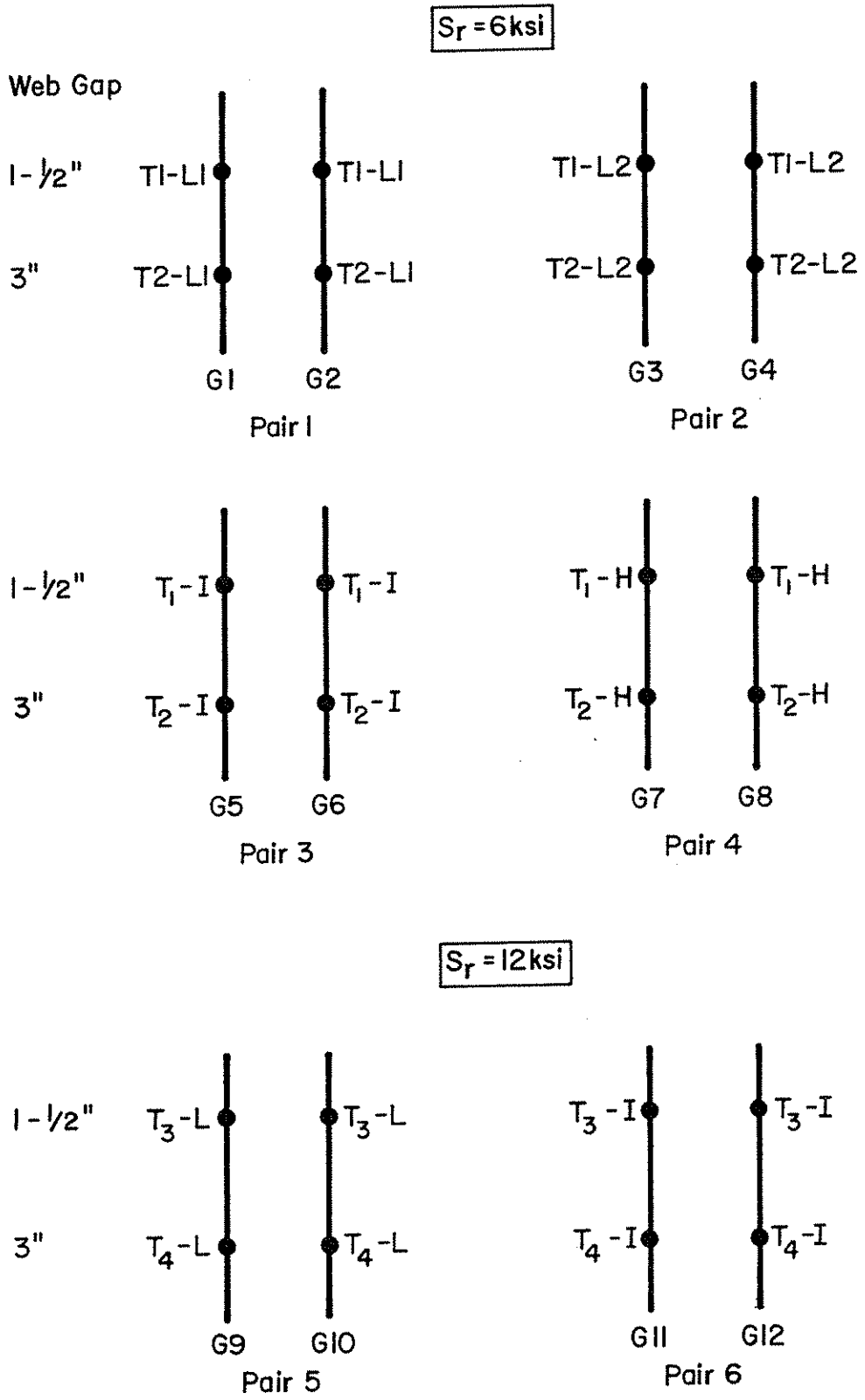

Figure 11: Girder-detail relationship for distortion at transverse stiffener web gaps

National Web Gap Length (in.)	Detail Type A	Detail Type B	Detail Type C
1.0			T5 - 9 T5 - 10
1.5		T5 - 3 T5 - 4 T5 - 5	
2.0	T5 - 1 T5 - 2		
3.0		T5 - 6 T5 - 7 T5 - 8	T5 - 11 T5 - 12

a

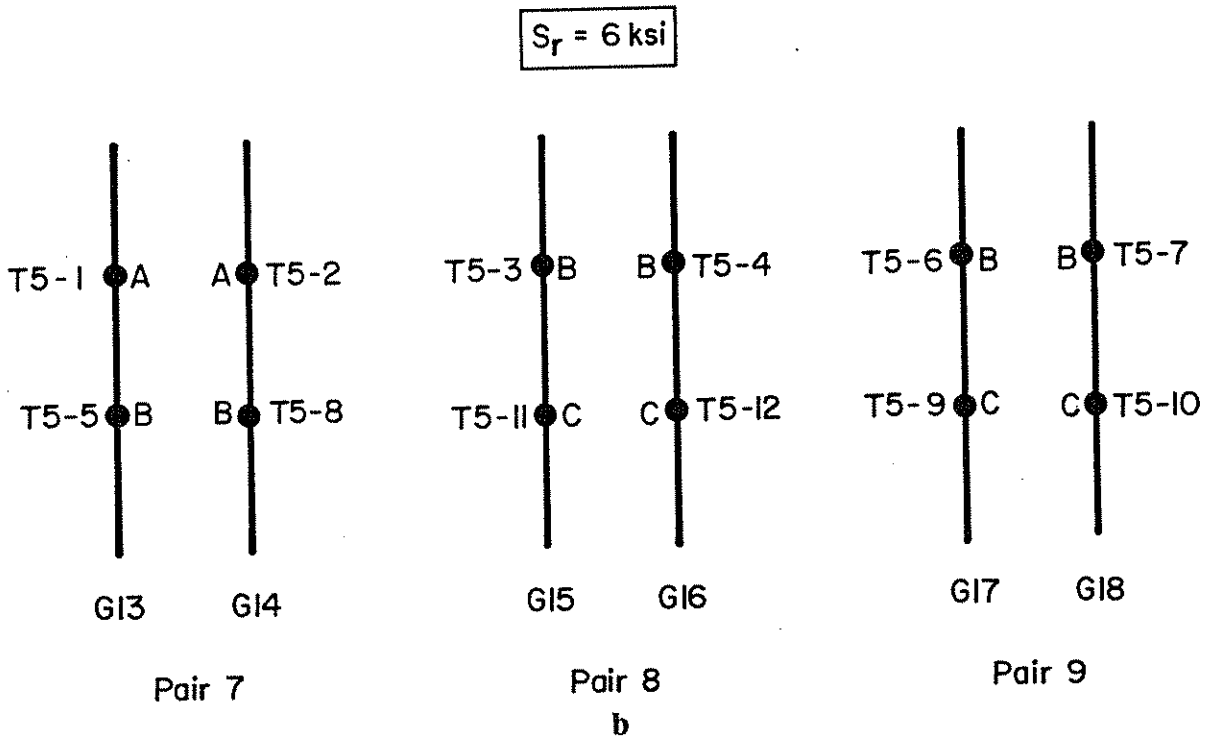

b

Figure 12: (a) Girder-detail relationship for lateral gusset plates; (b) Girder-detail arrangement for the three pairs of test girders with lateral gusset plates.

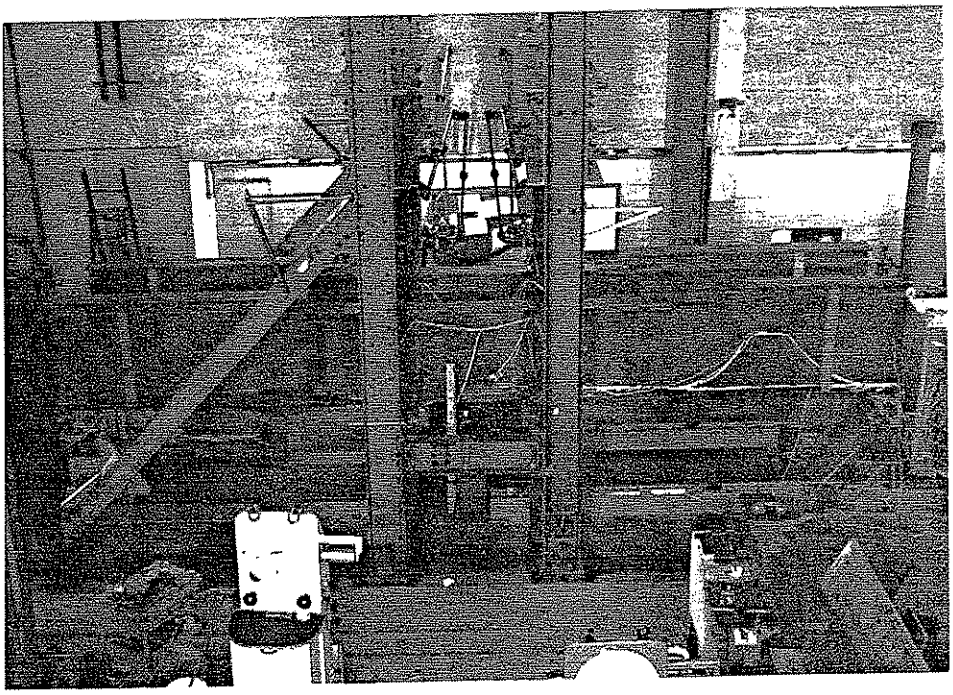

Figure 13: Test girders in place on the test bed

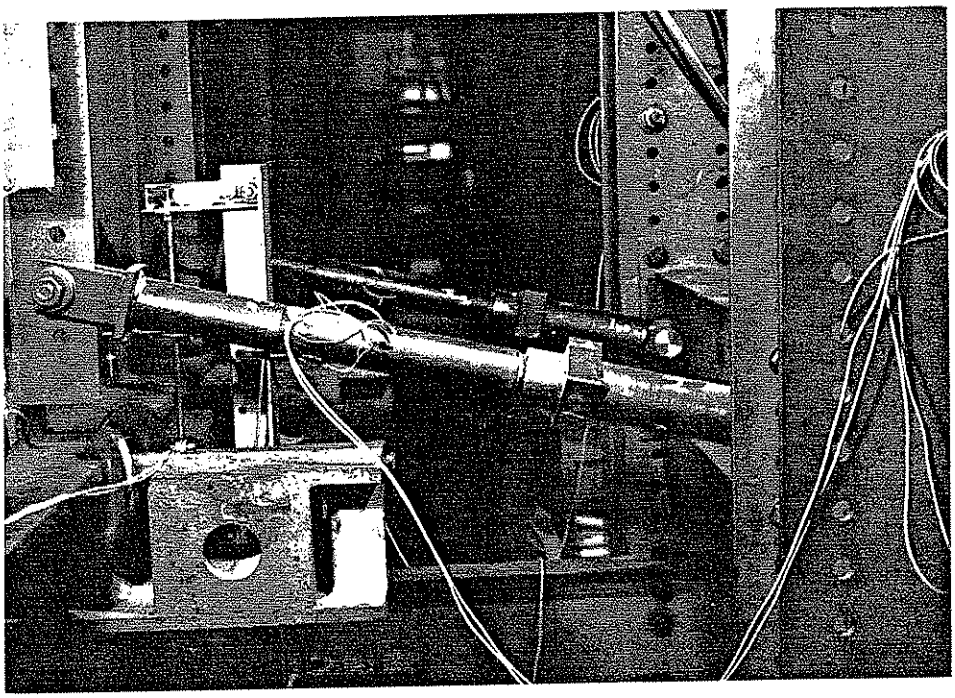

Figure 14: Sections clamped to bottom flange and rods used to induce distortion

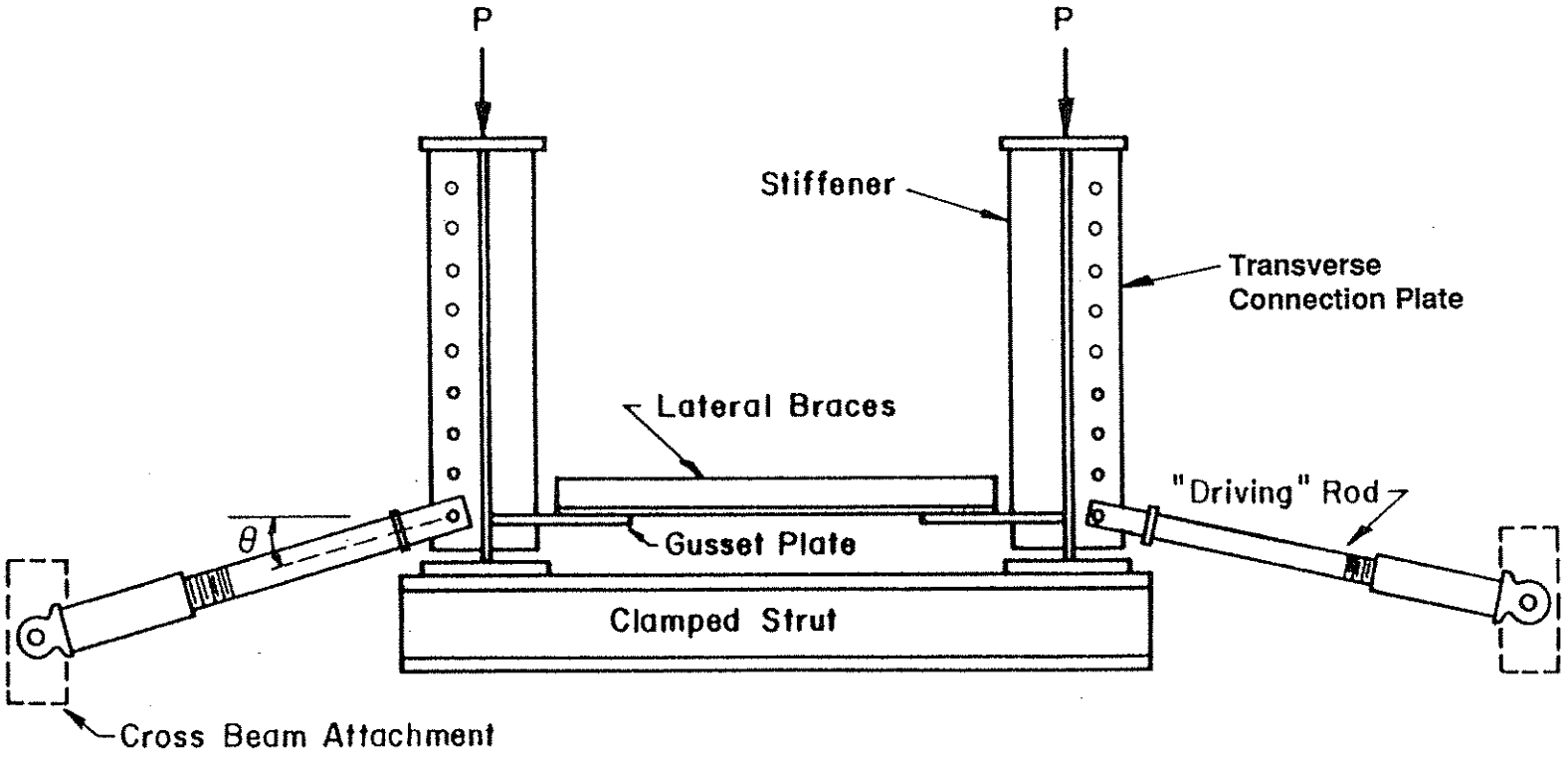

Figure 15: System of loading and restraint

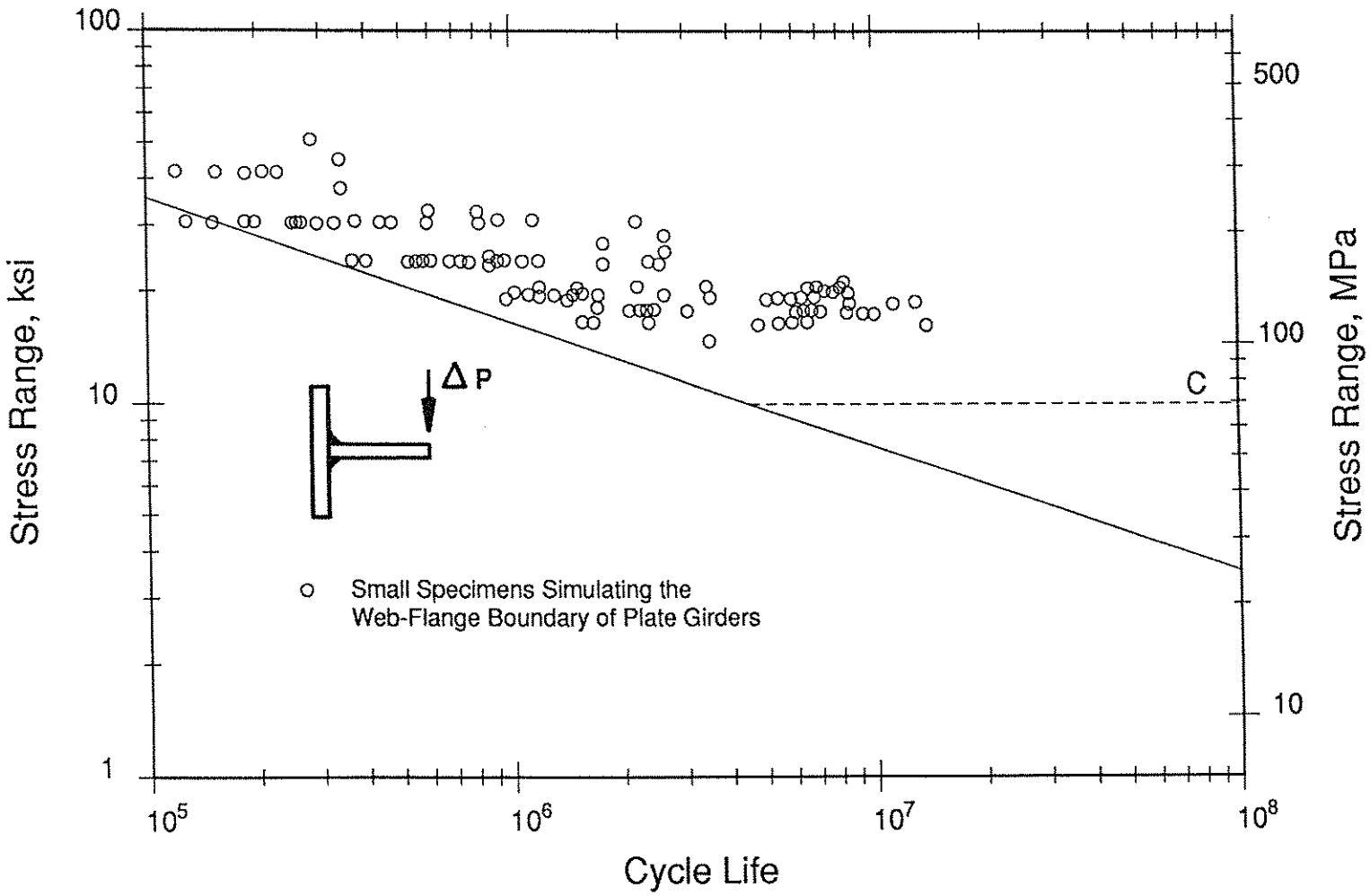

Figure 16: Fatigue test results from small simulated plate bending tests

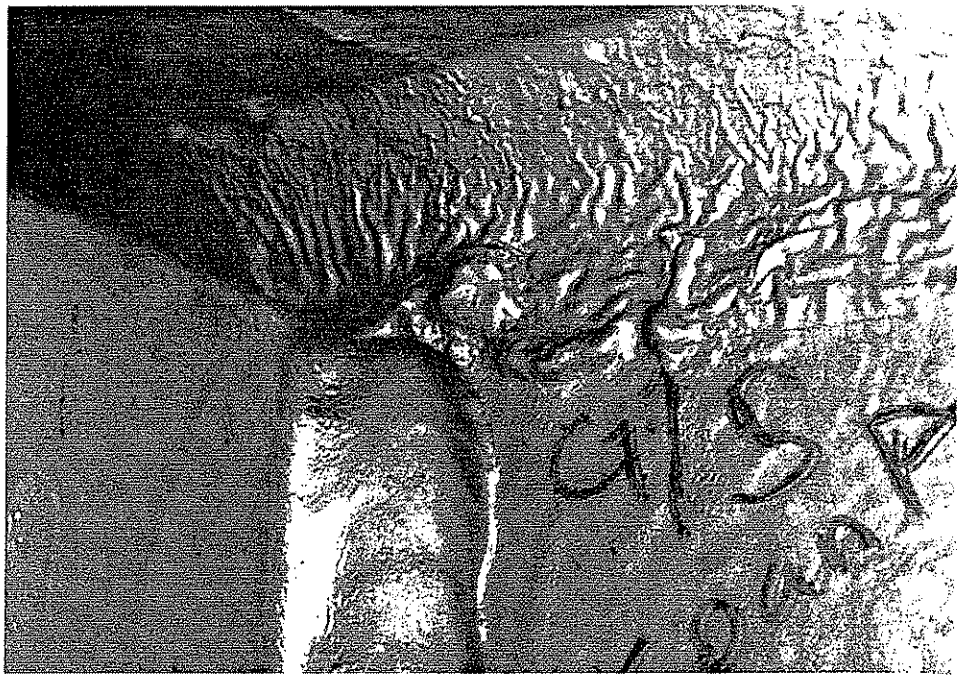

Figure 17: Cracks at connection plates, Beaver Creek Bridge, Reference 18

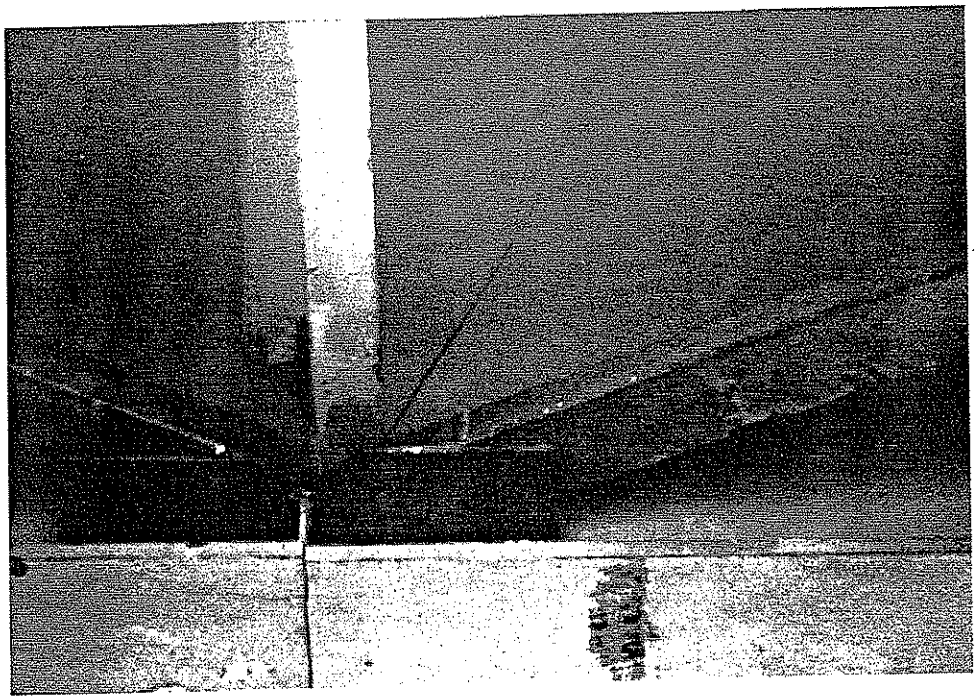

Figure 18: Two Gusset plates welded to the web

Figure 19: Lateral gusset plate detail, I-79 Bridge #2682, Reference 19

Figure 20: Lateral gusset plate detail, Canoe Creek Bridge, Reference 13

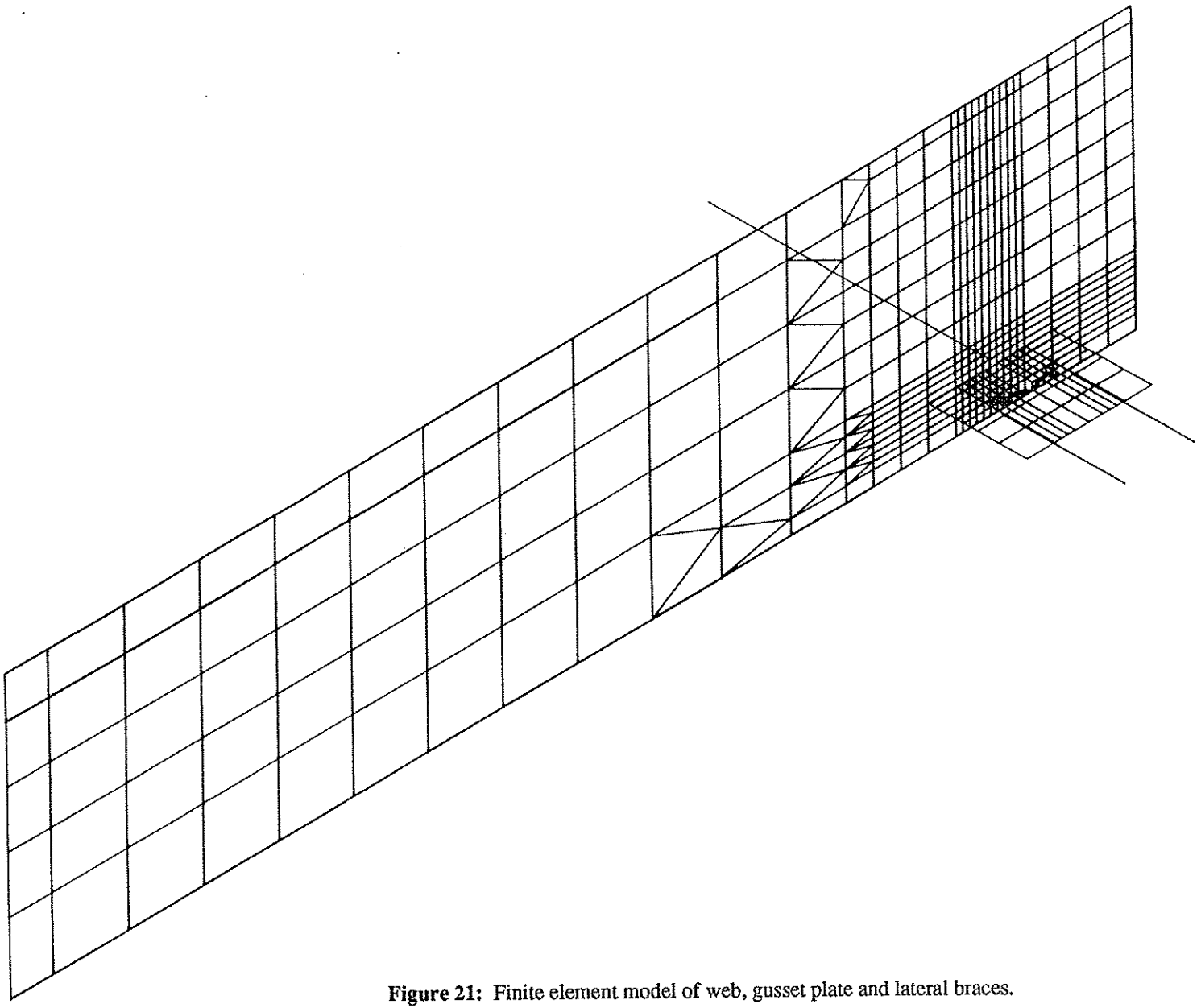

Figure 21: Finite element model of web, gusset plate and lateral braces.

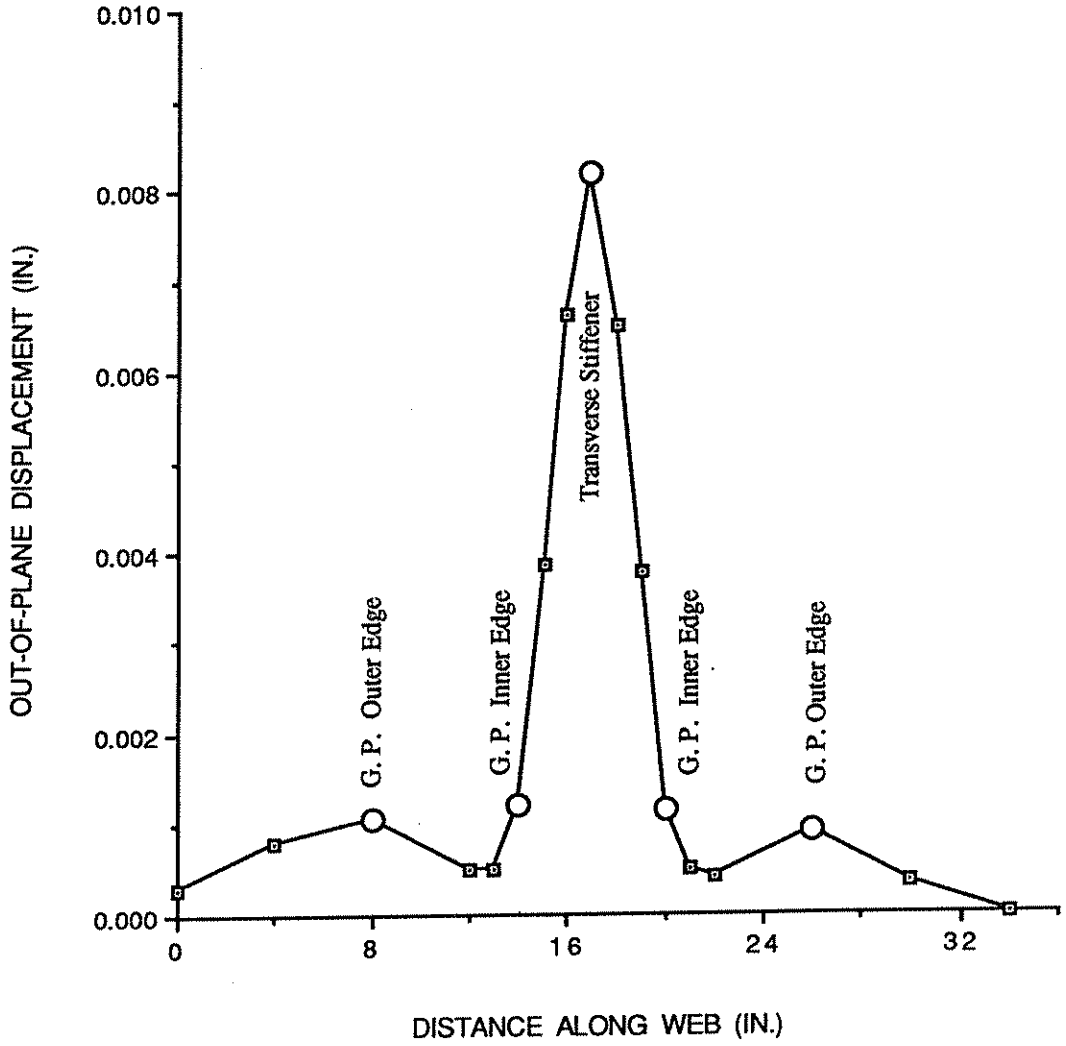

Figure 22: Lateral displacement along Detail C; Θ=–20°, 3 in. gap

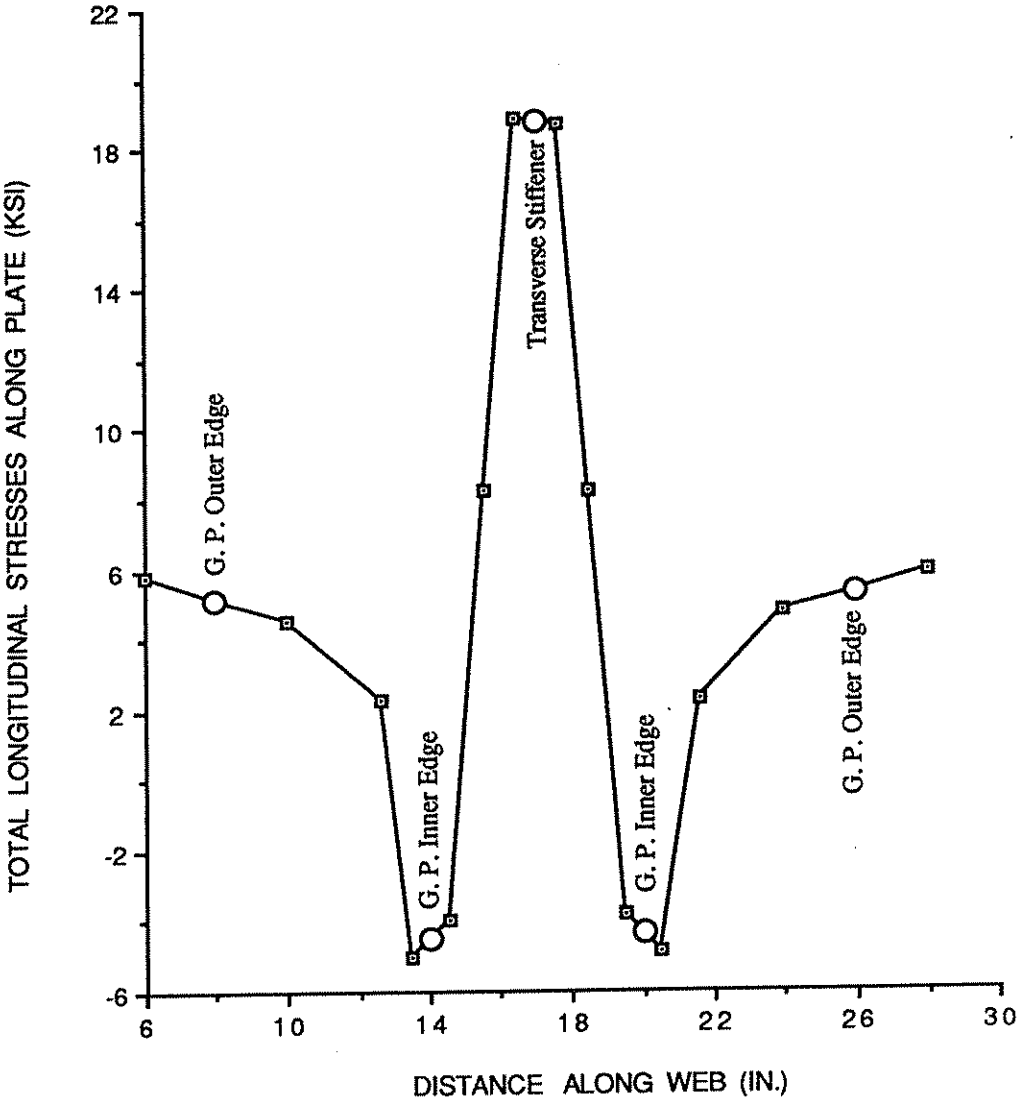

Figure 23: Combined stress distribution, Detail C; Θ=–20°, 3 in. gap

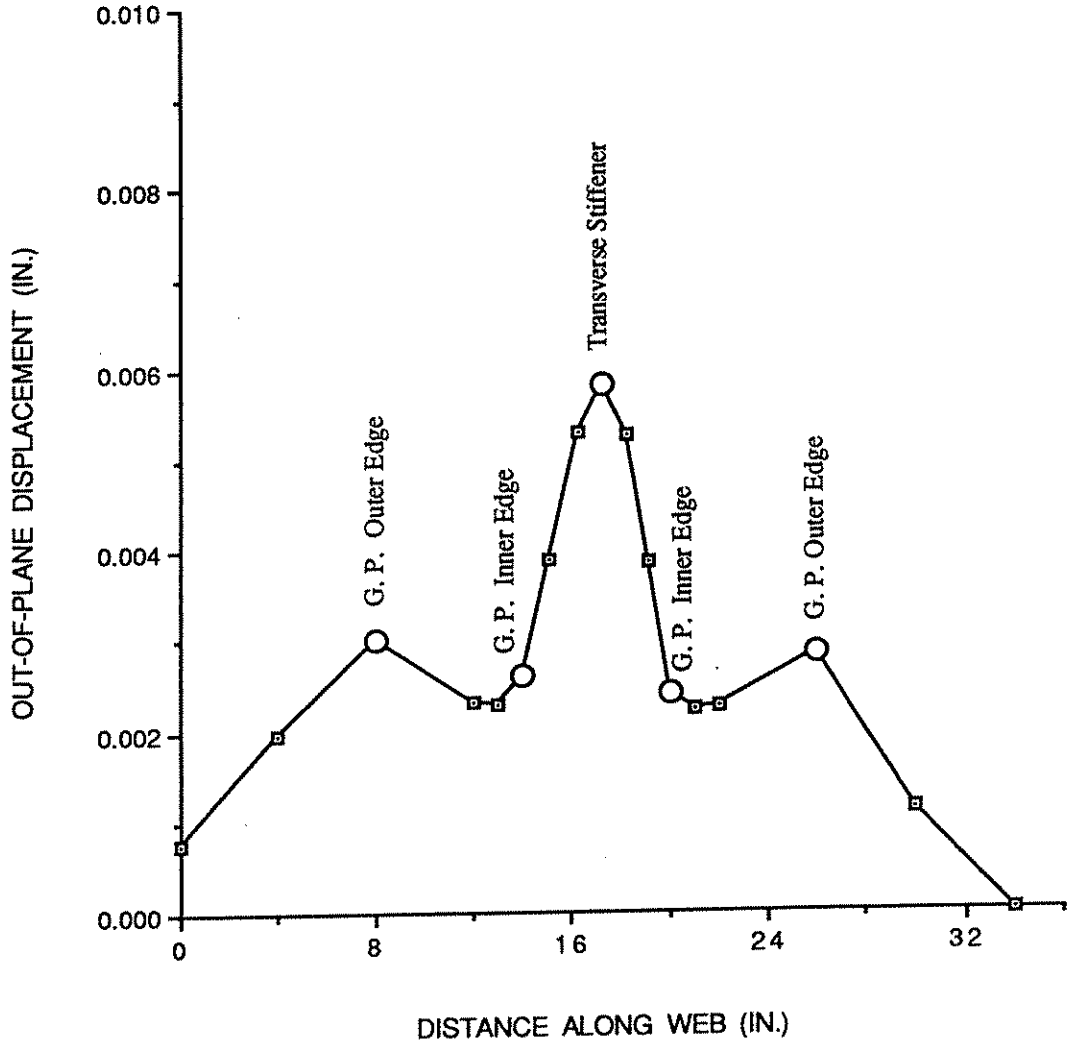

Figure 24: Lateral displacement along Detail B; Θ=–20°, 3 in. gap

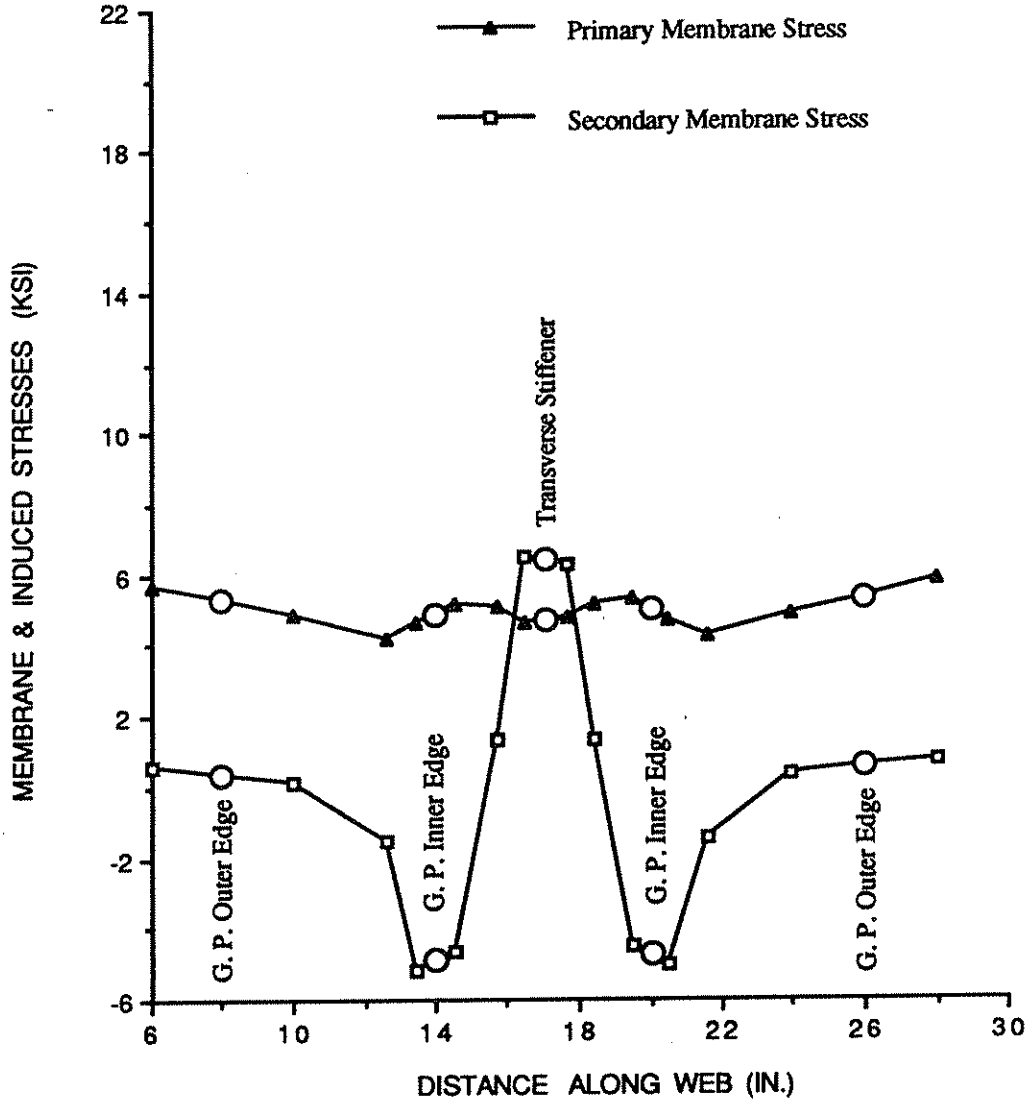

Figure 25: Stress distribution, Detail B; Θ=–20°, 3 in. gap

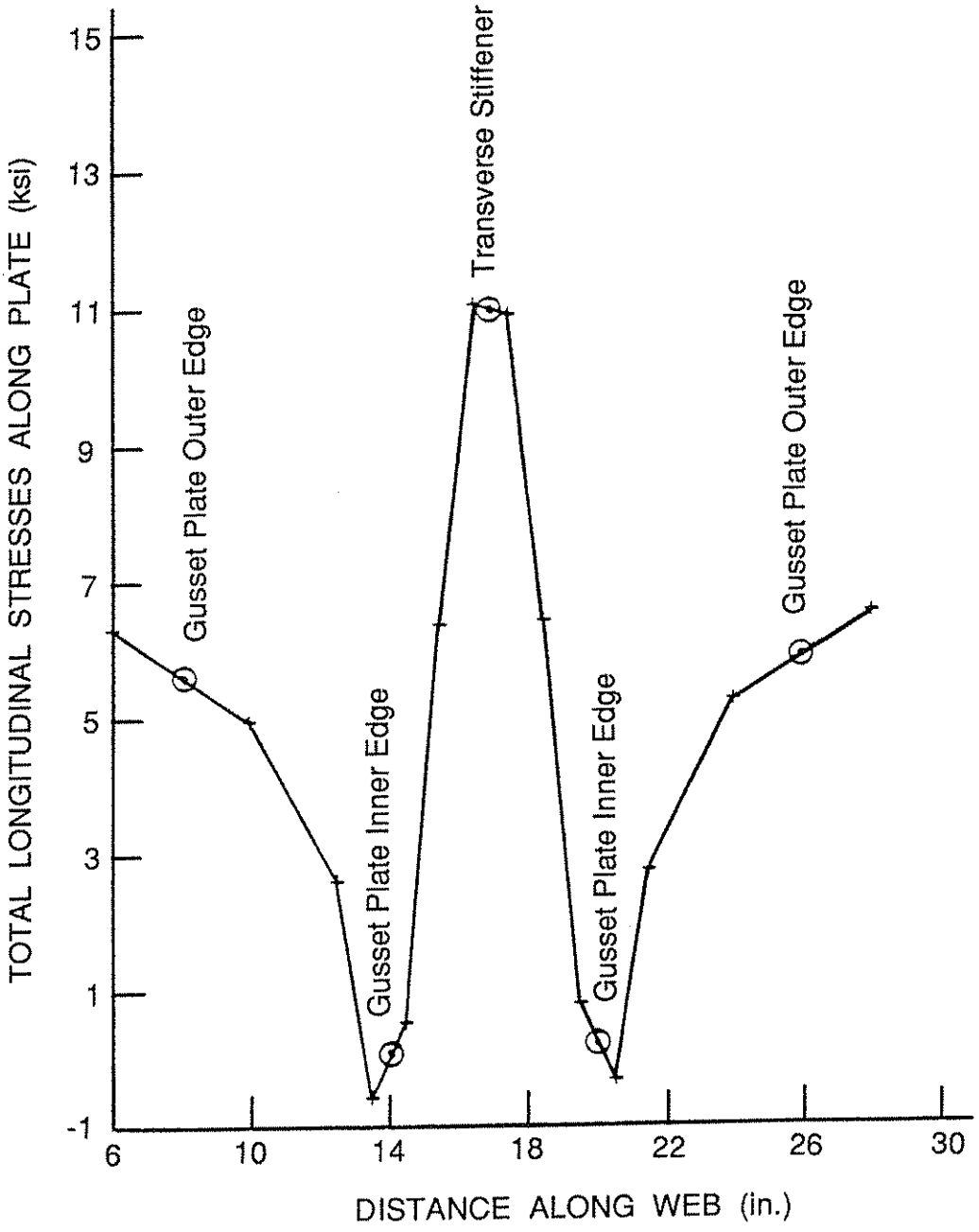

Figure 26: Combined stress distribution, Detail B; Θ=20°, 3 in. gap

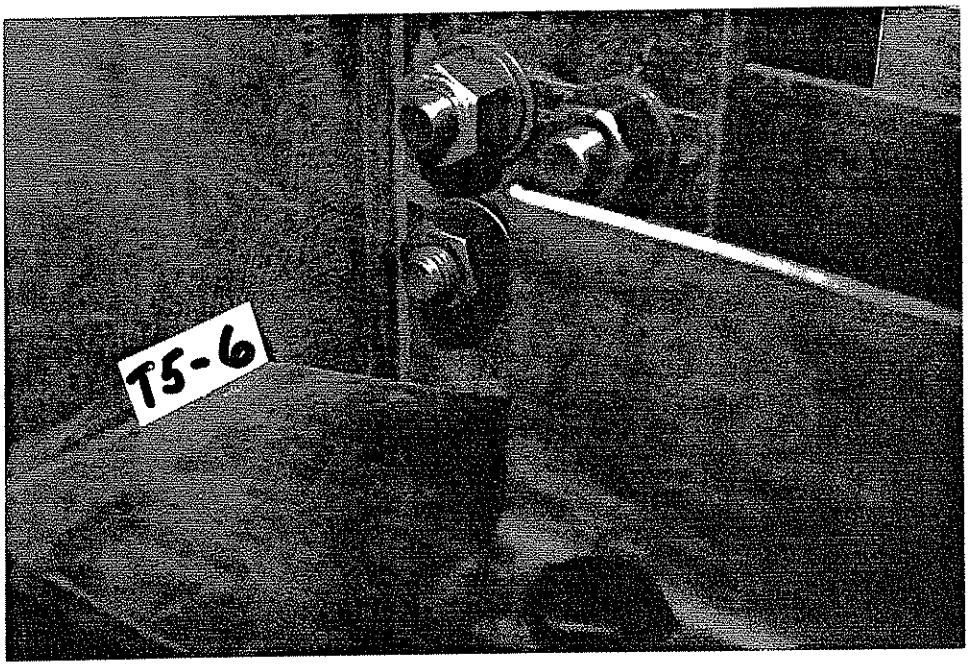

(a)

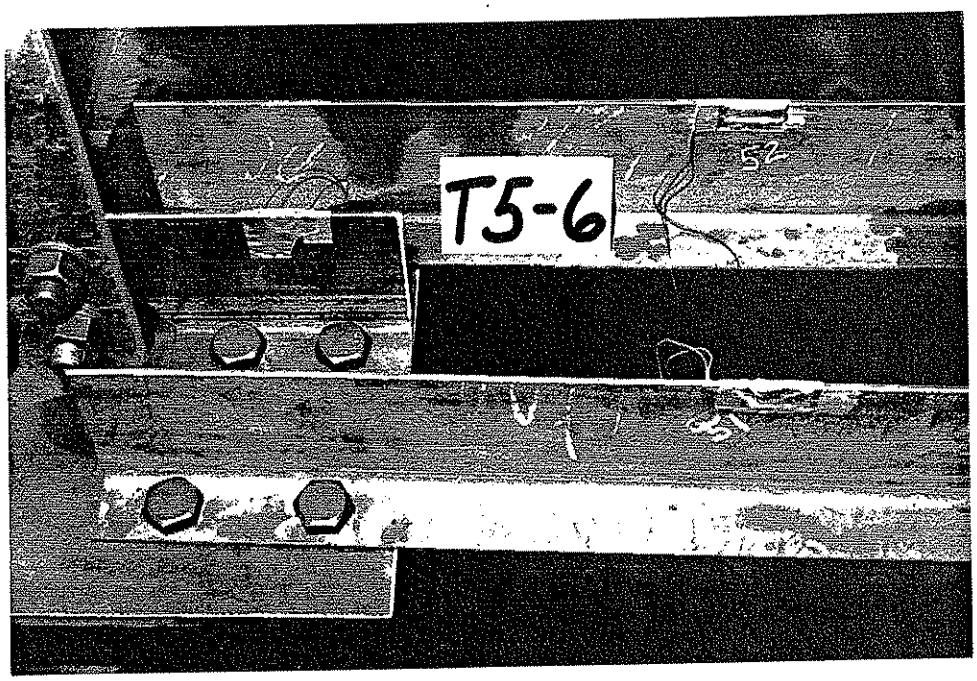

(b)

Figure 27: (a) View of web gap detail for T5-6 (Type B) with 3 in. (76 mm) gap; (b) Overview of Detail T5-6

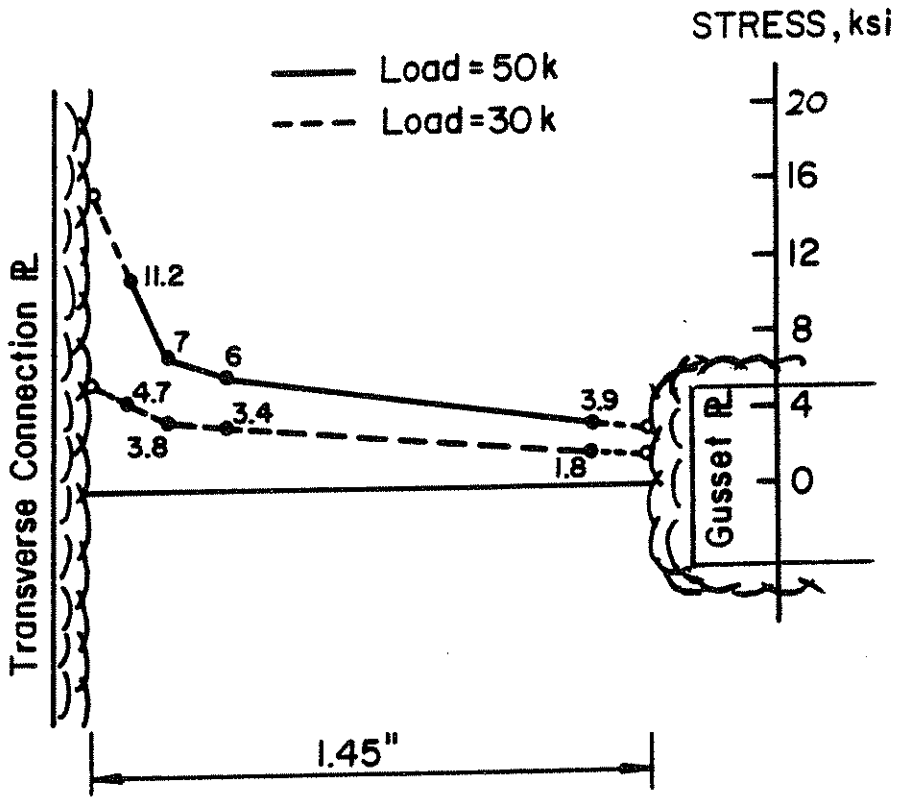

Figure 28: Stress gradient for Detail T5-1 (Type A), east web gap

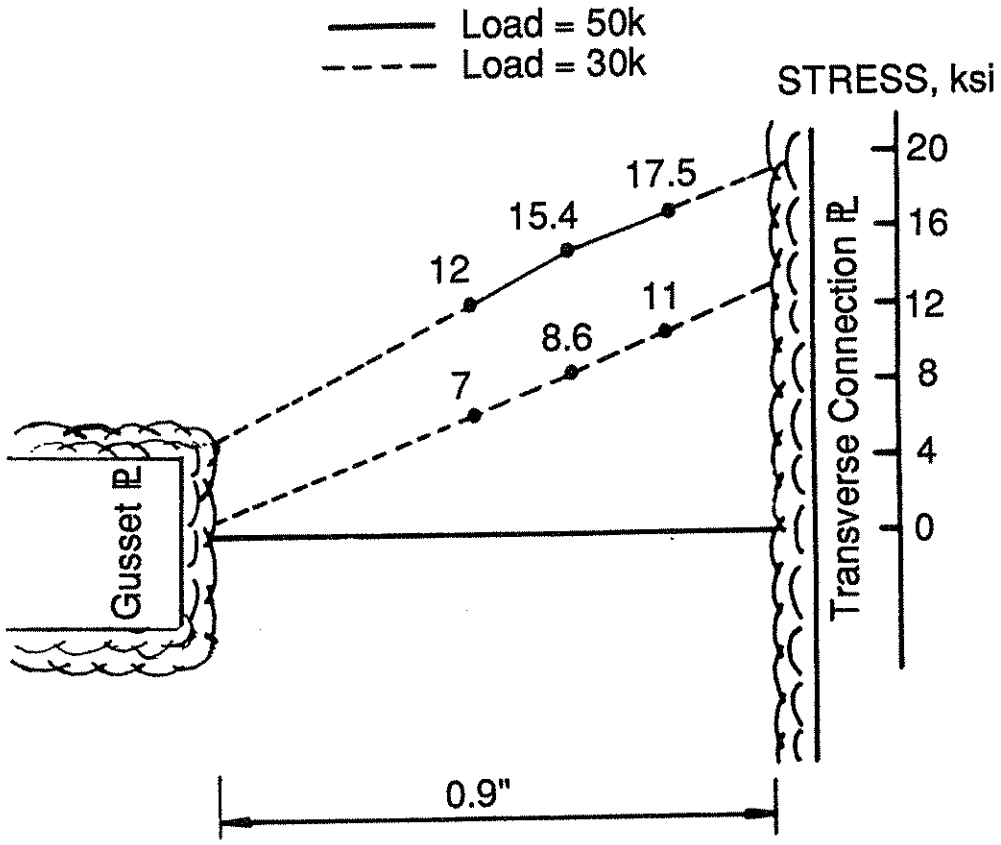

Figure 29: Stress gradient for Detail T5-5 (Type B), west web gap

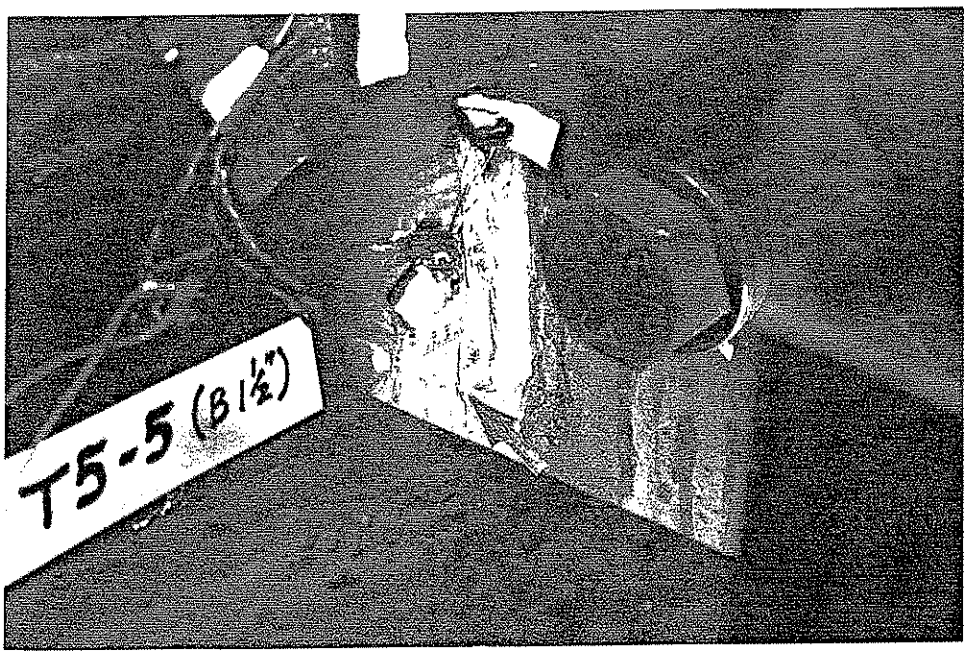

Figure 30: Fatigue cracking at Detail T5-5 (Type B), west web gap

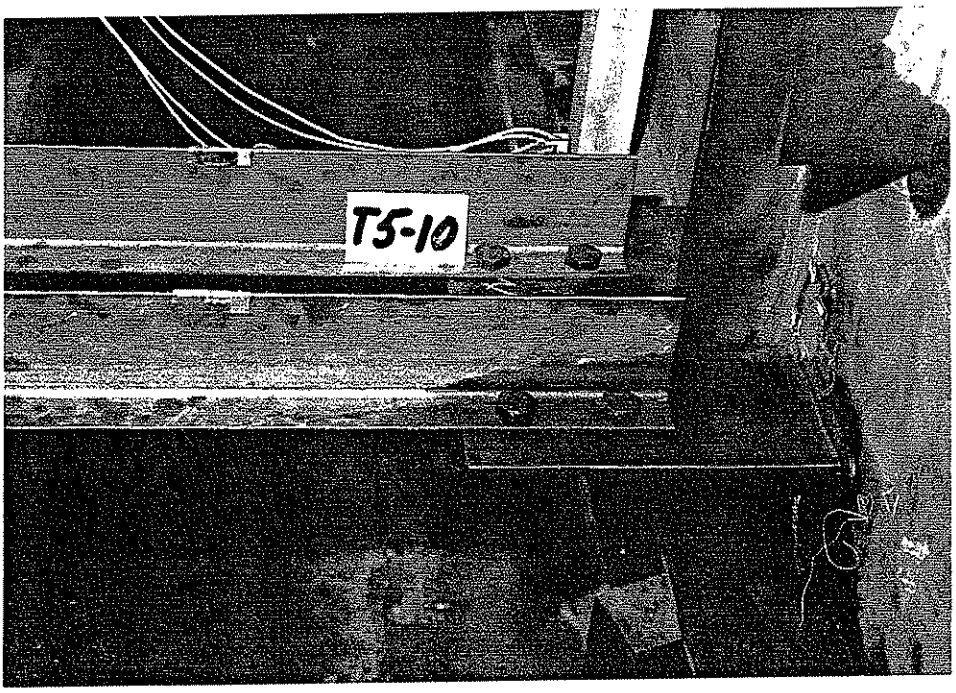

Figure 31: Detail C gusset plate with attached laterals

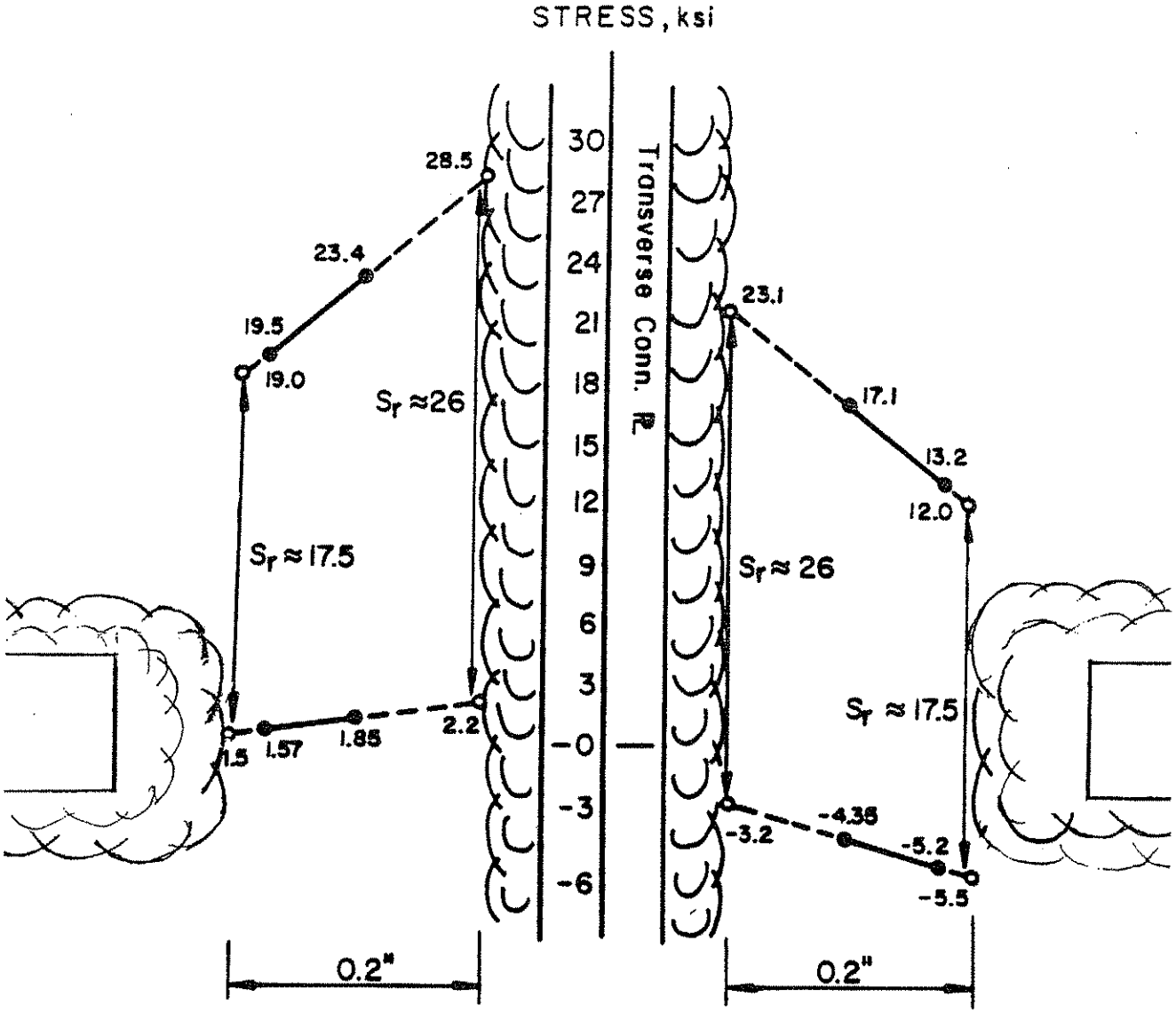

Figure 32: Stress gradients for Detail T5-10 (Type C)

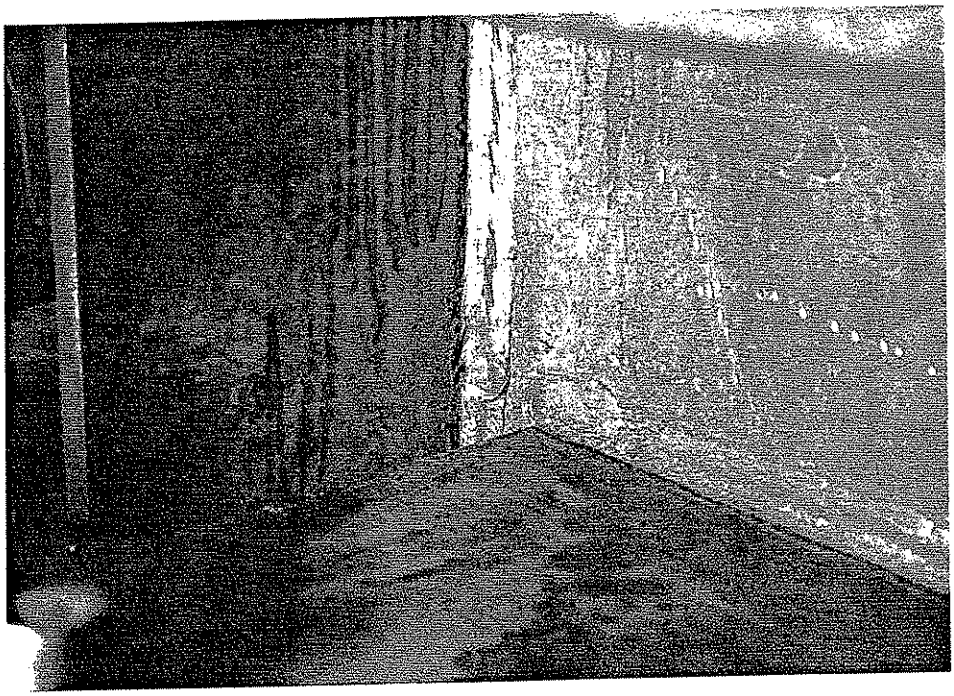

Figure 33: Cracking along vertical weld toe in the horizontal web gap

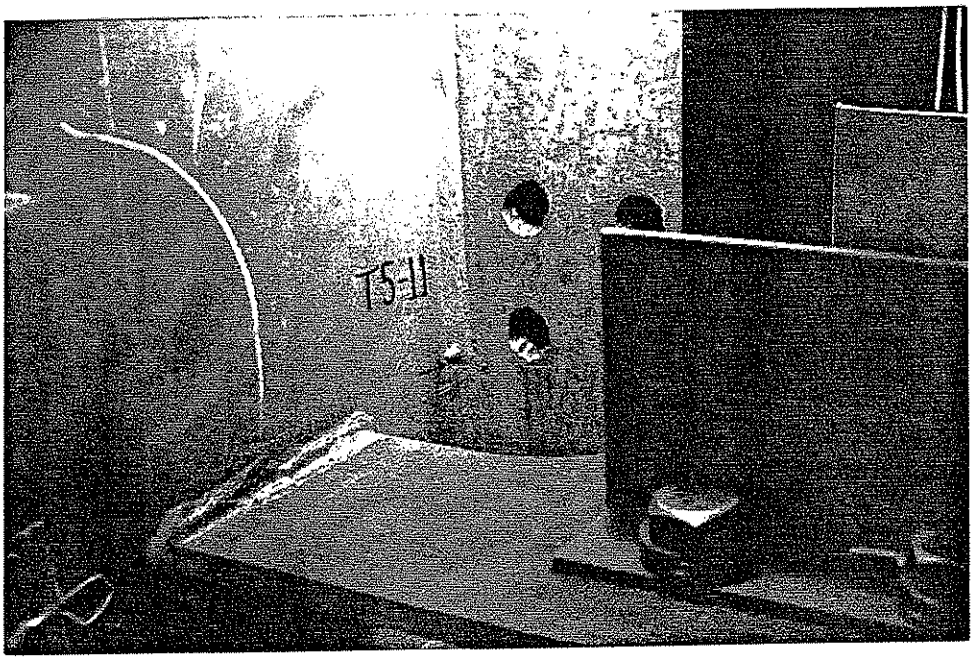

Figure 34: Detail T5-11 (Type C) with 3 in. web gap

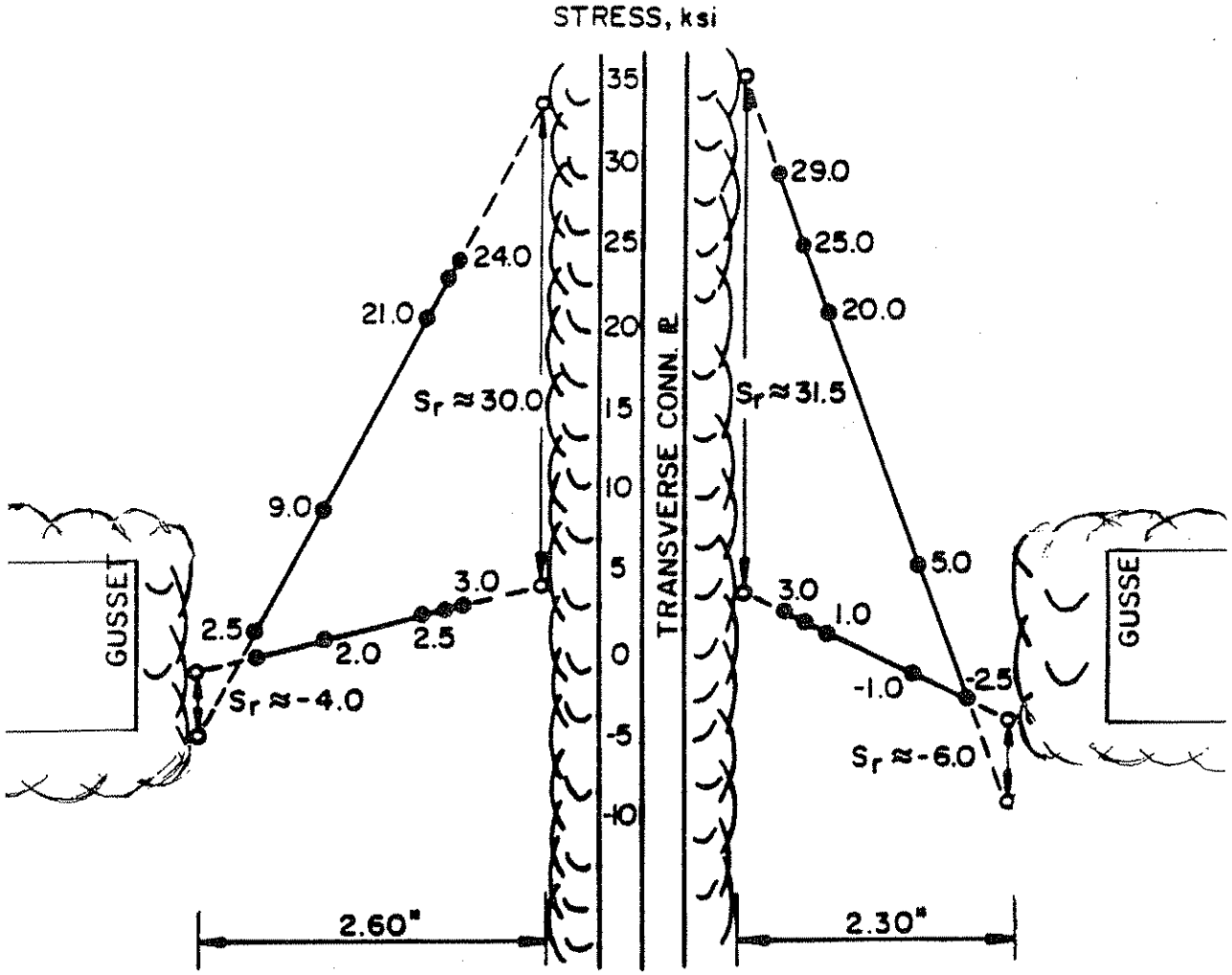

Figure 35: Stress gradients for Detail T5-12 (Type C)

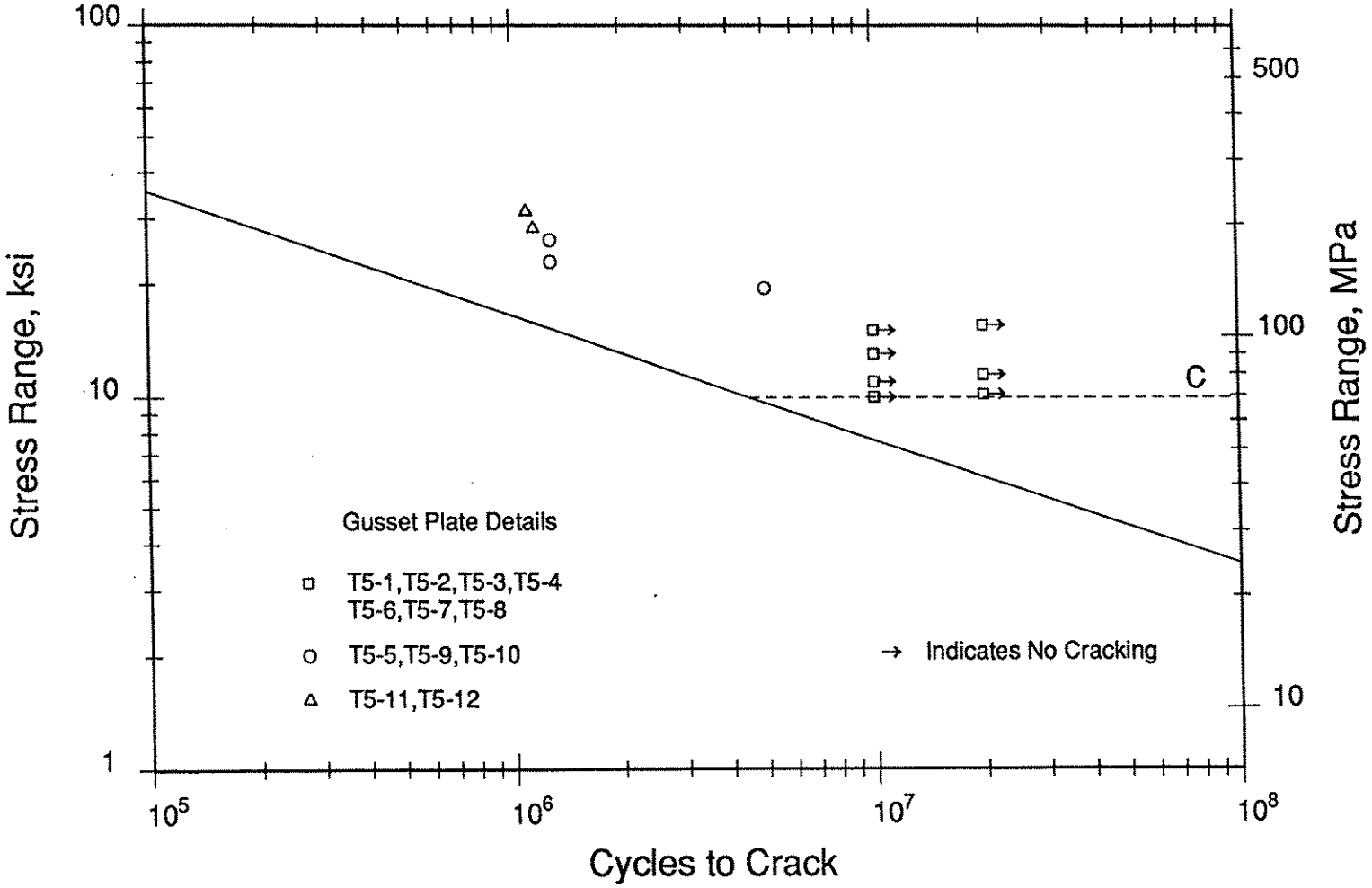

Figure 36: Comparison of test results for gusset plate details with Category C Fatigue Resistance Curve

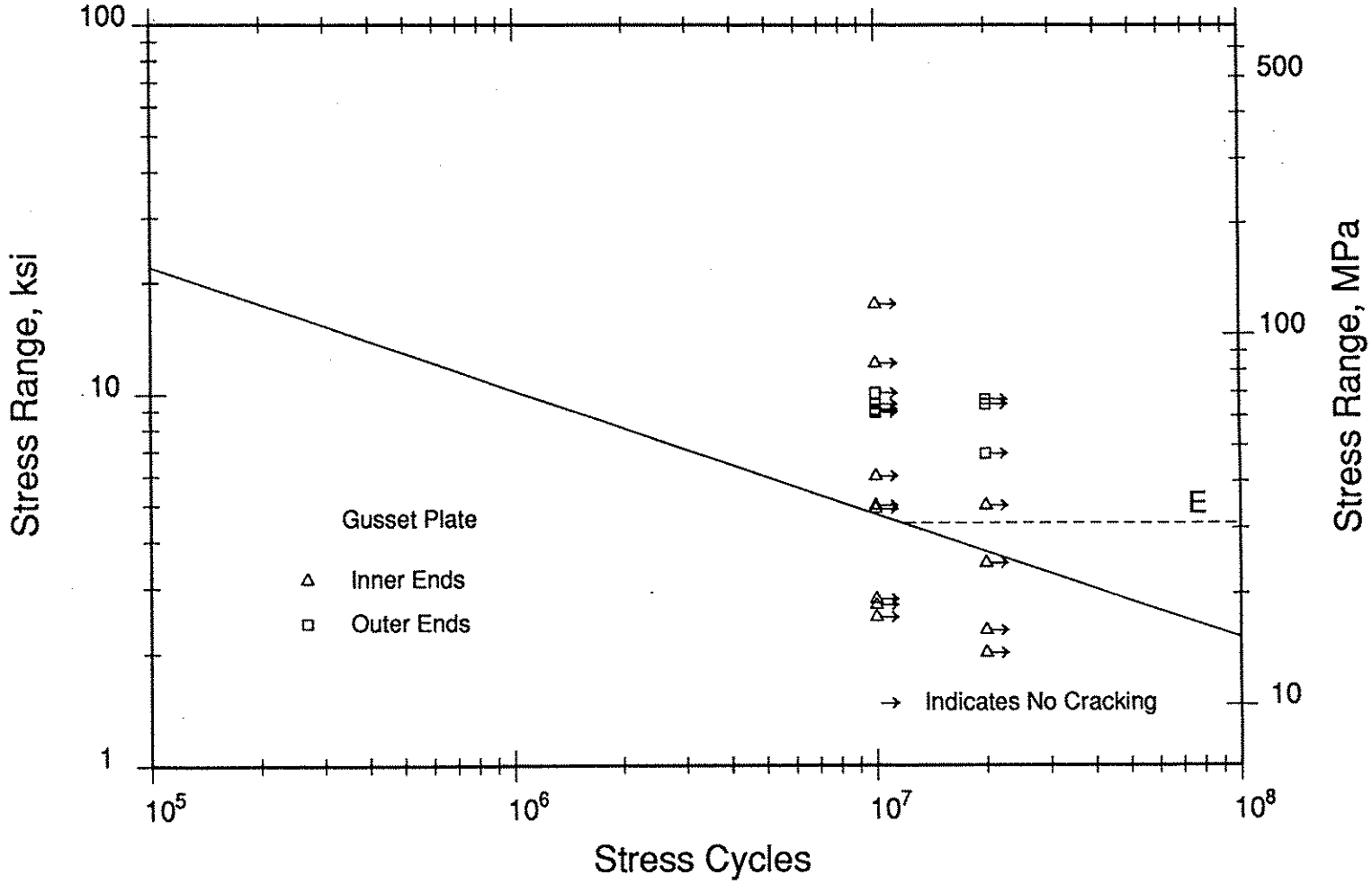

Figure 37: Comparison of test results for gusset plate details with Category E Fatigue Resistance Curve

Figure 38: Retrofit holes installed

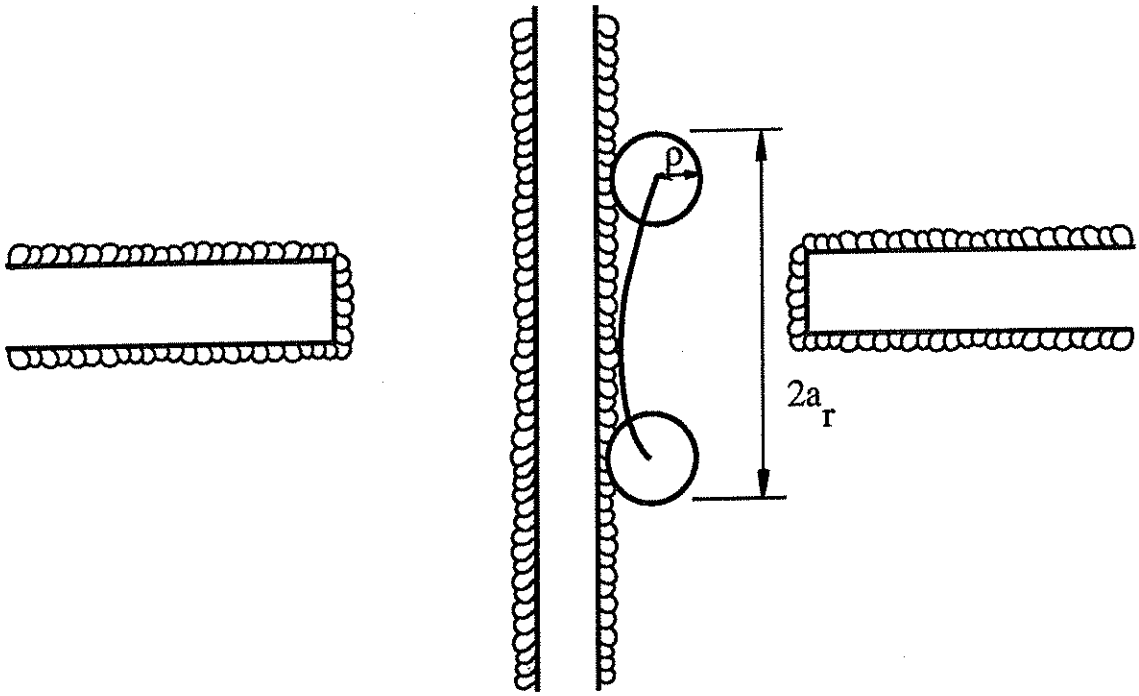

Figure 39: Retrofit holes at lateral gusset plate web gaps

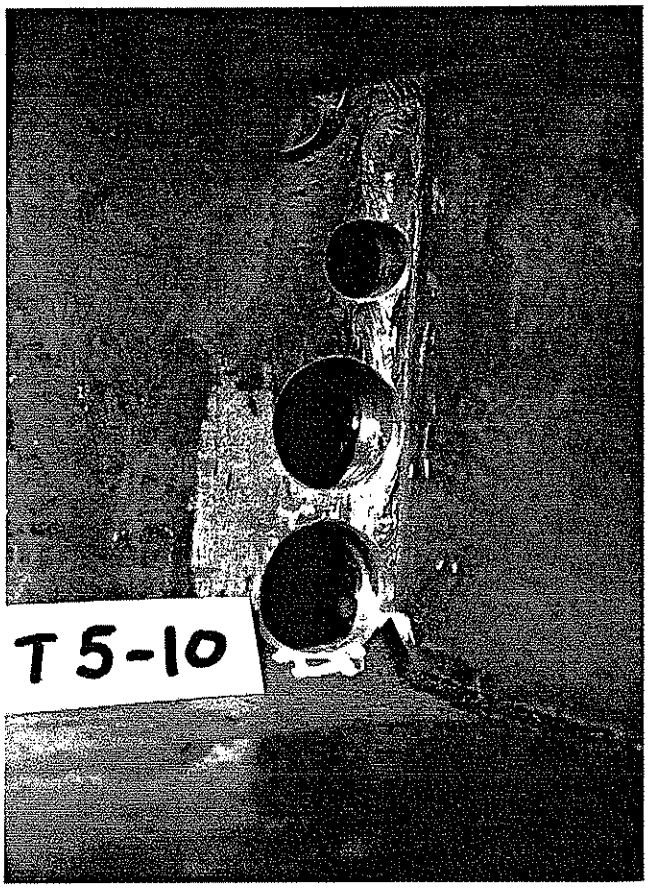

Figure 40: Additional crack arrest holes installed at crack tip

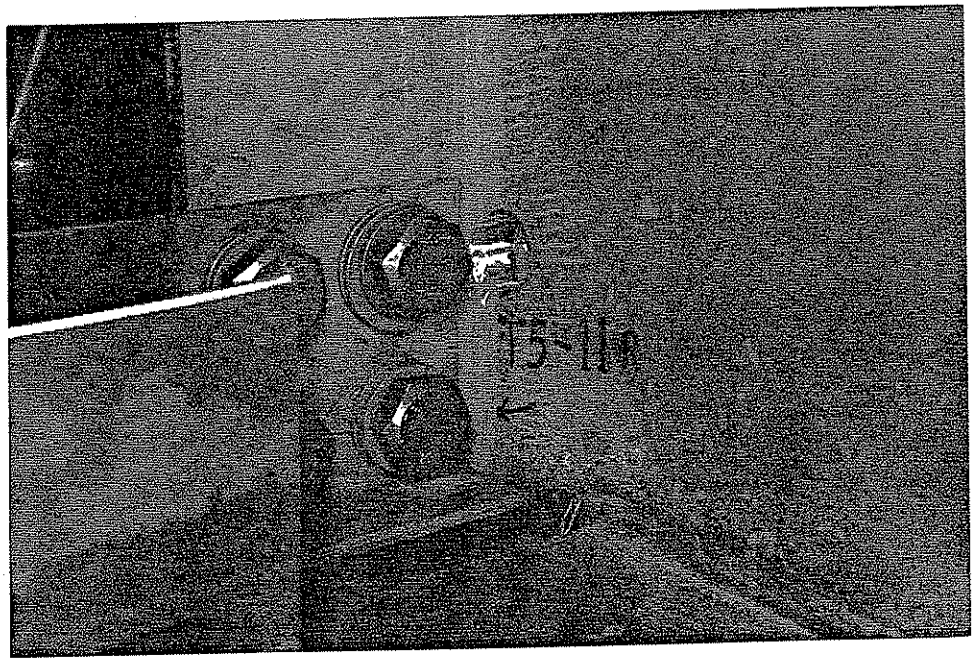

Figure 41: Retrofit hole and bolted attachment provided

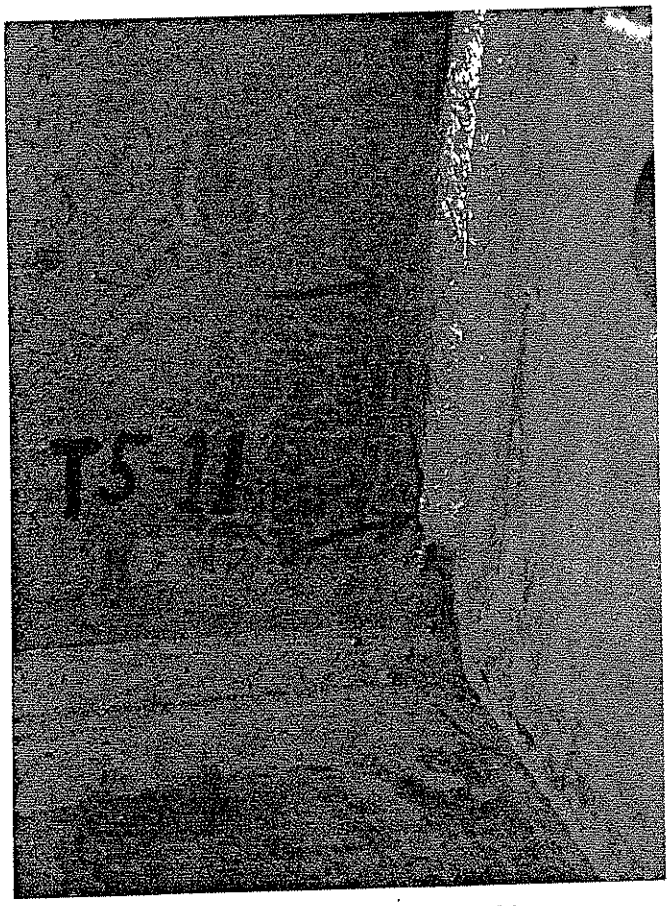

Figure 42: Crack along vertical connection plate weld

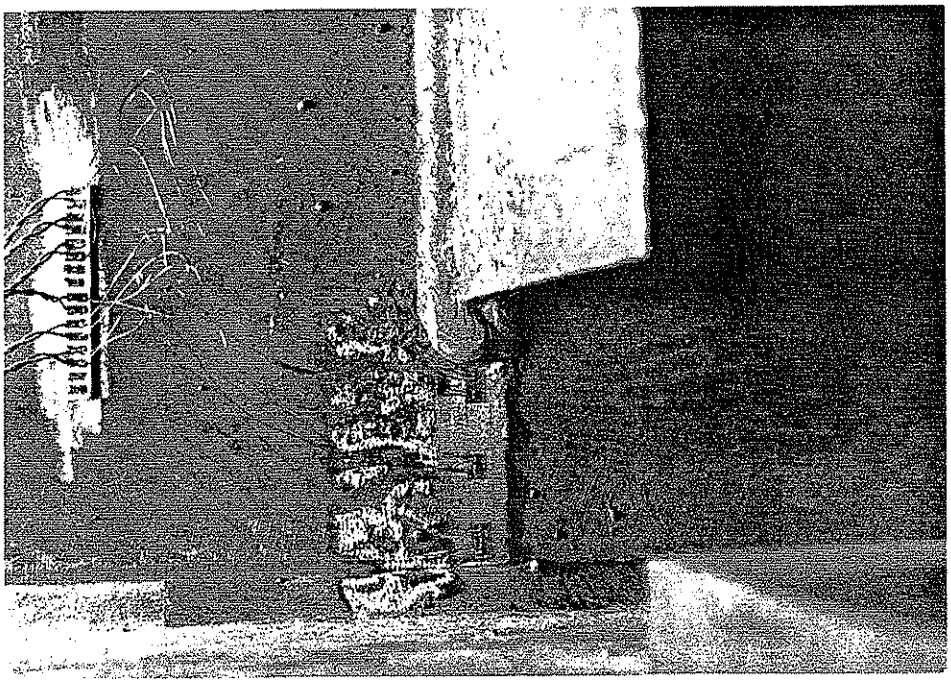

Figure 43: Strain gages installed in web gap between transverse connection plate and web-flange weld

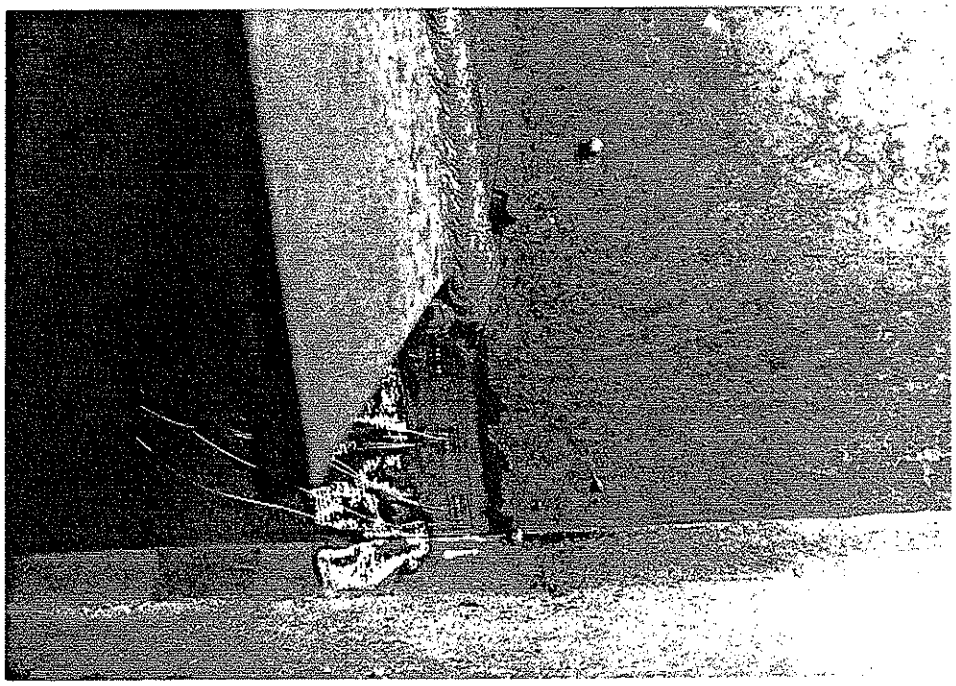

Figure 44: Crack forming at end of connection plate weld and extending up the transverse weld in (T2-L1) 3 in. gap

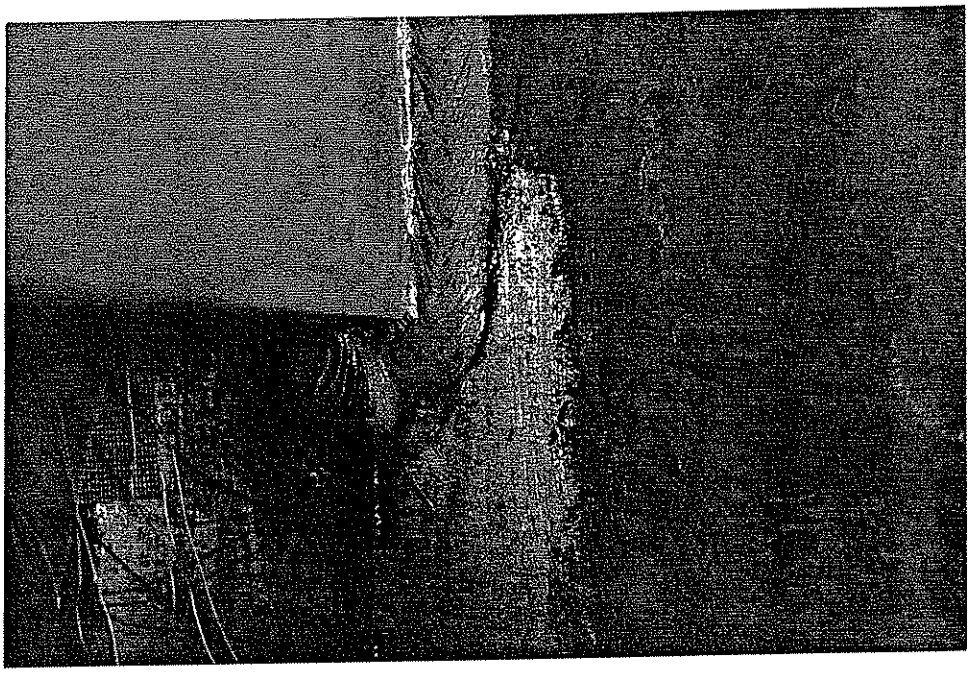

Figure 45: Closeup view of crack at end of transverse connection plate welds (3 in. detail)

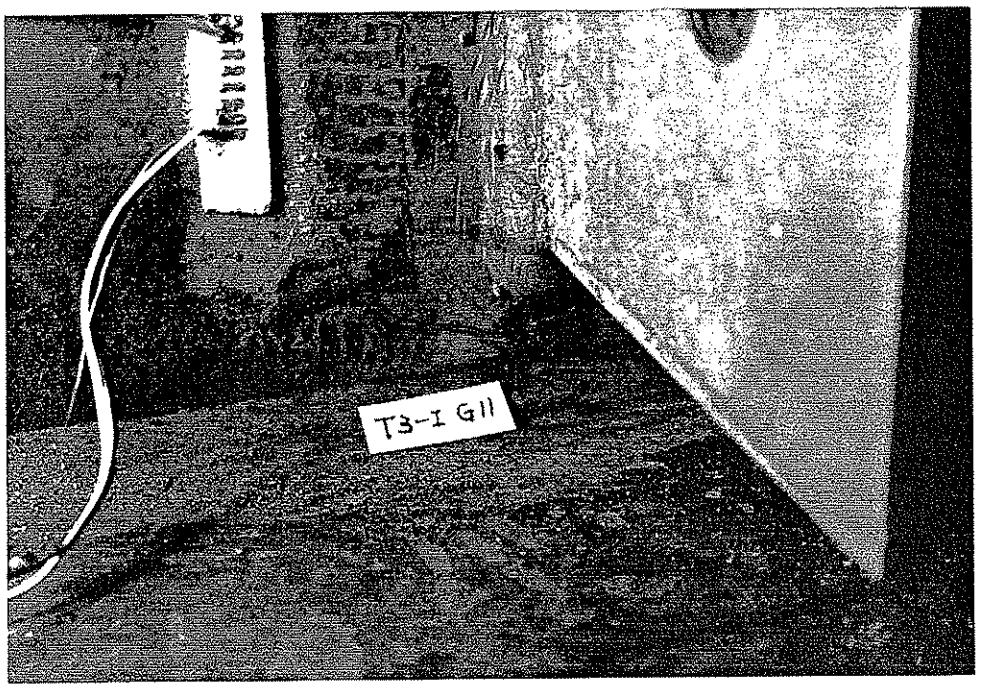

(a)

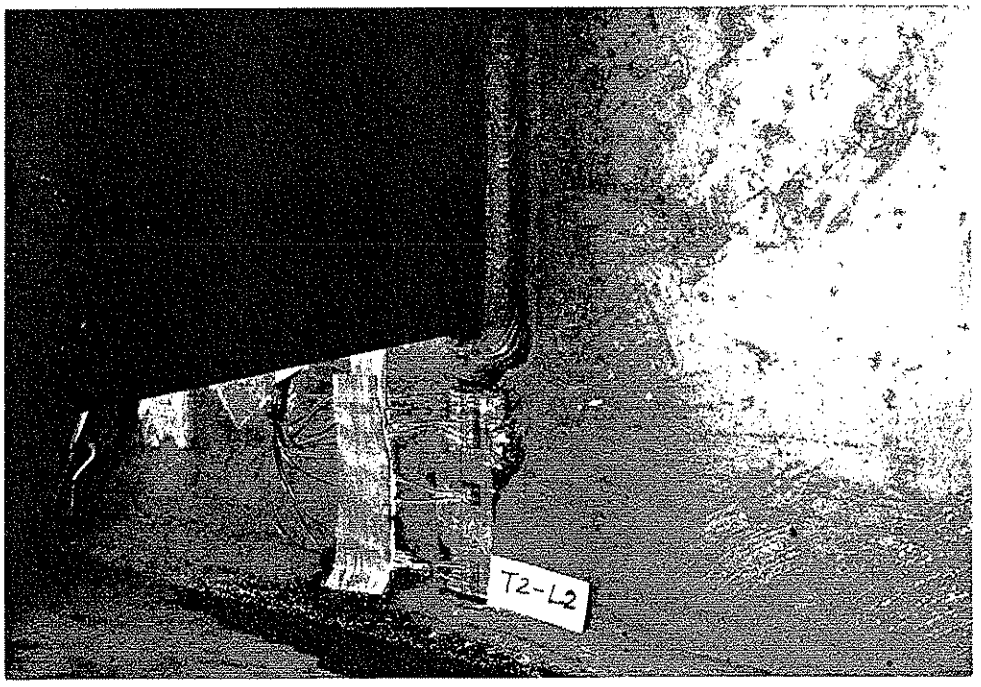

(b)

Figure 46: Cracks forming at ends of connection plates: (a) Branching crack at end of connection plate with 1½ in. web gap; (b) Small crack in weld after completion of test at a 3 in. web gap

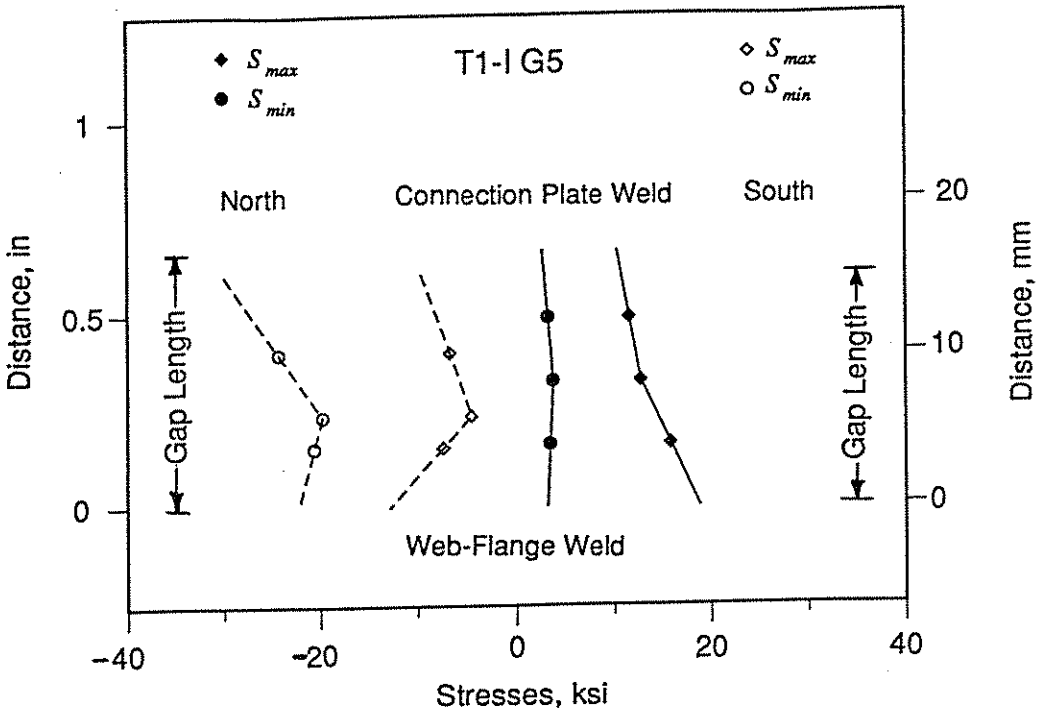

(a)

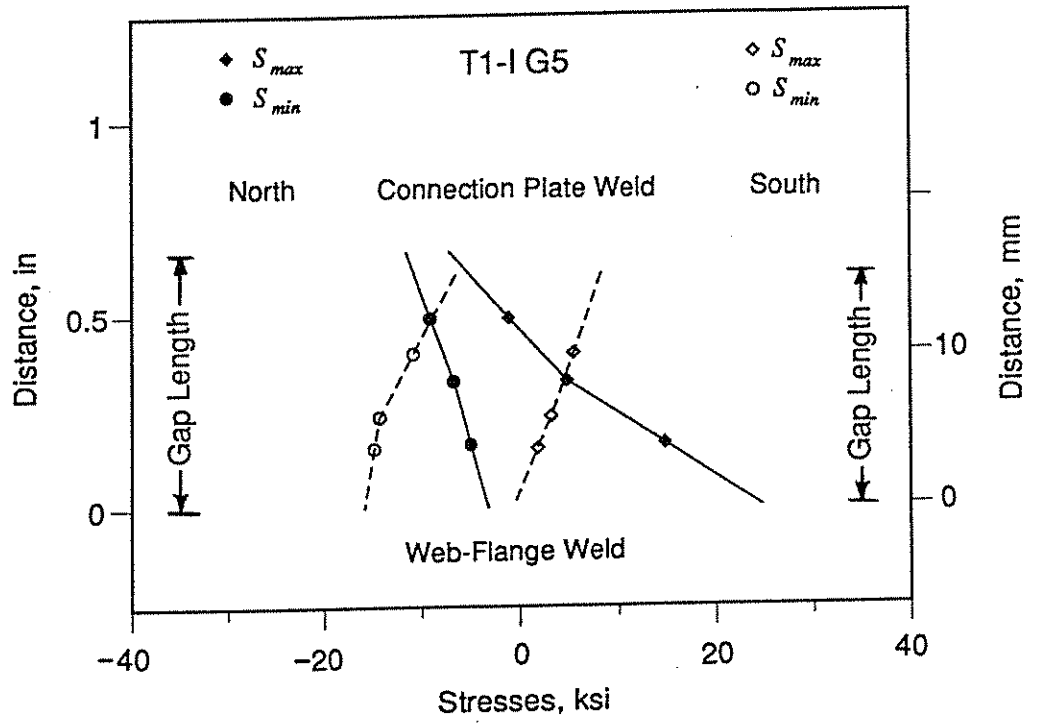

(b)

Figure 47: Stress gradients at Transverse Connection Plate Detail T1-I G5 (1 1/2 in. gap) before and after cracking at end of connection plate: (a) Prior to cracking, (b) After 10.7×10^6 cycles and visible cracking

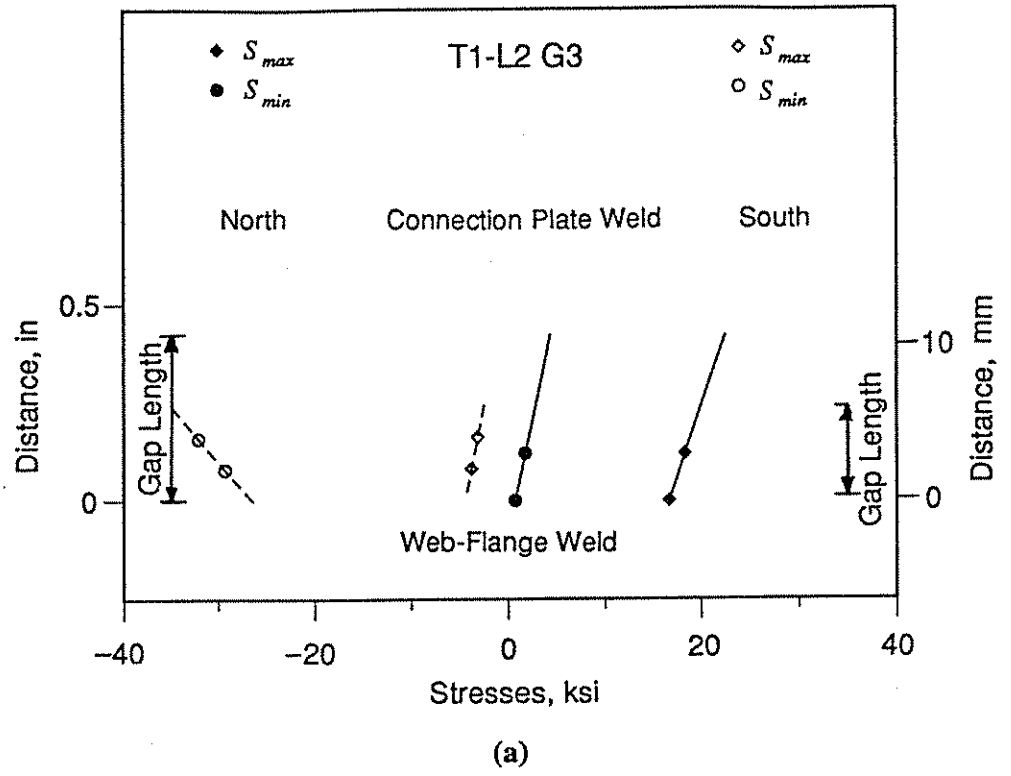

(a)

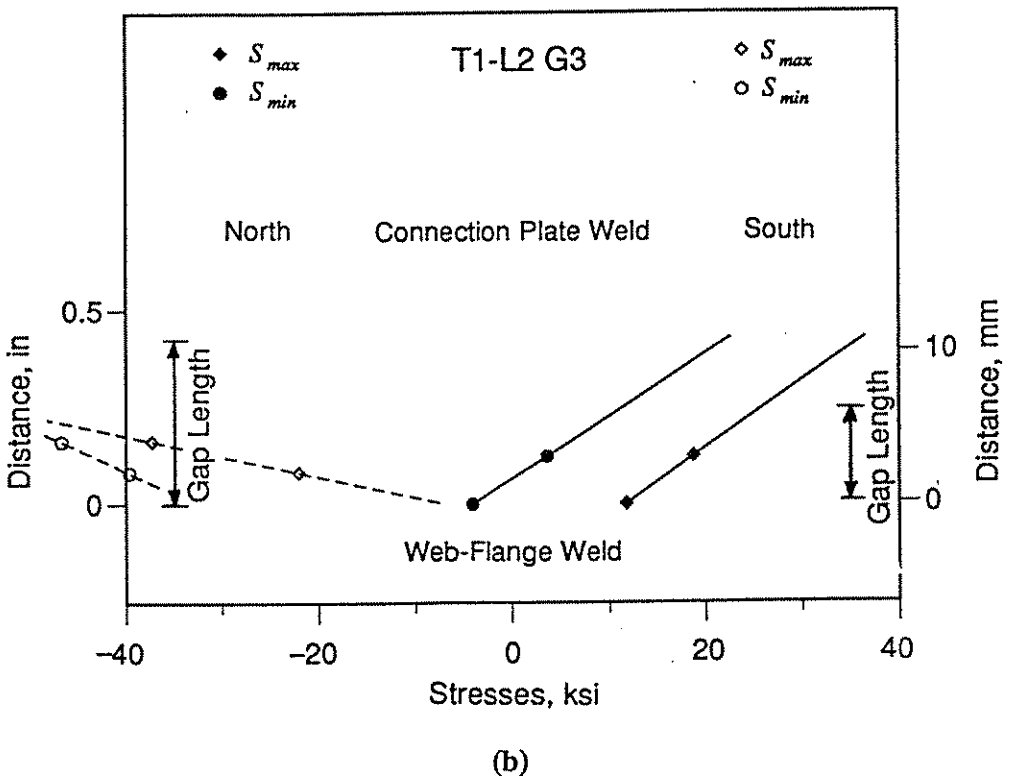

(b)

Figure 48: Stress gradients at Transverse Connection Plate Detail T1-L2 G3 (1 1/2 in. gap) before and after cracking at end of connection plate: (a) At start of test; (b) After cracking and 1.8×10^6 cycles

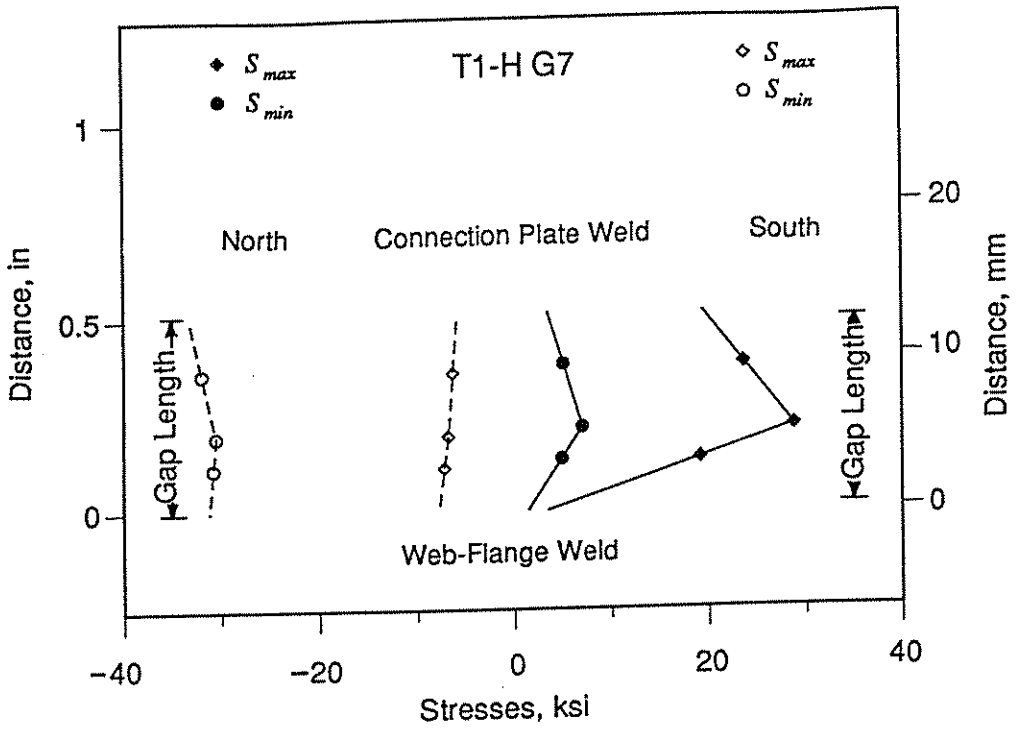

(a)

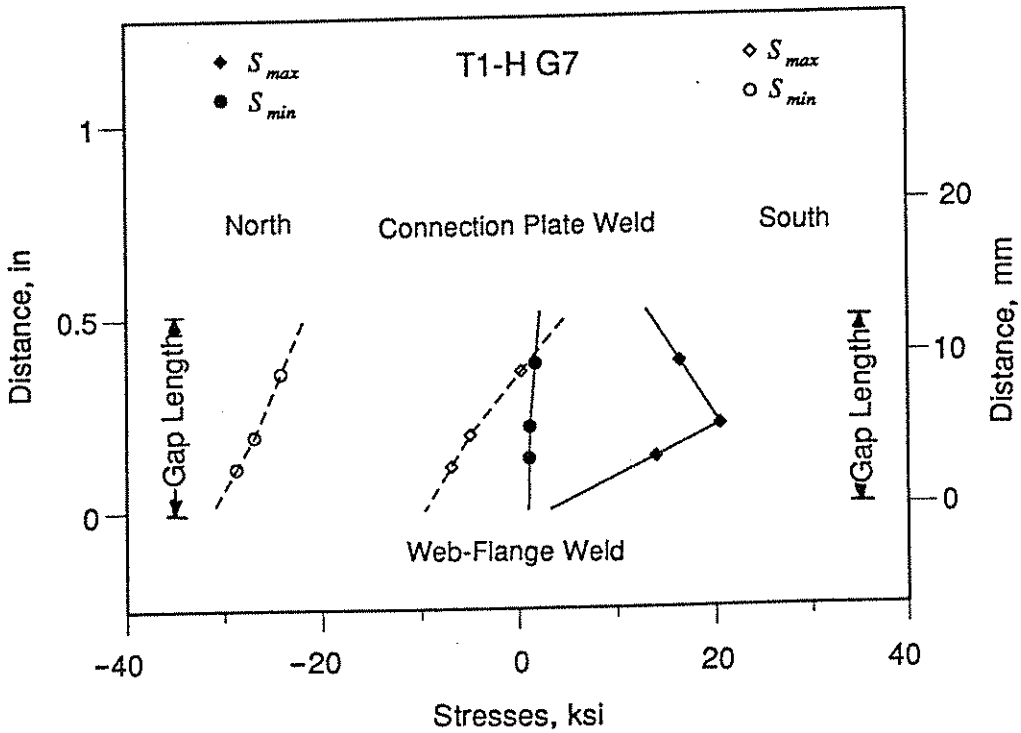

(b)

Figure 49: Stress gradients at Transverse Connection Plate Detail T1-H G7 (1 1/2 in. gap) before and after cracking at end of connection plate: (a) At start of test; (b) After cracking at 0.71×10^6 cycles

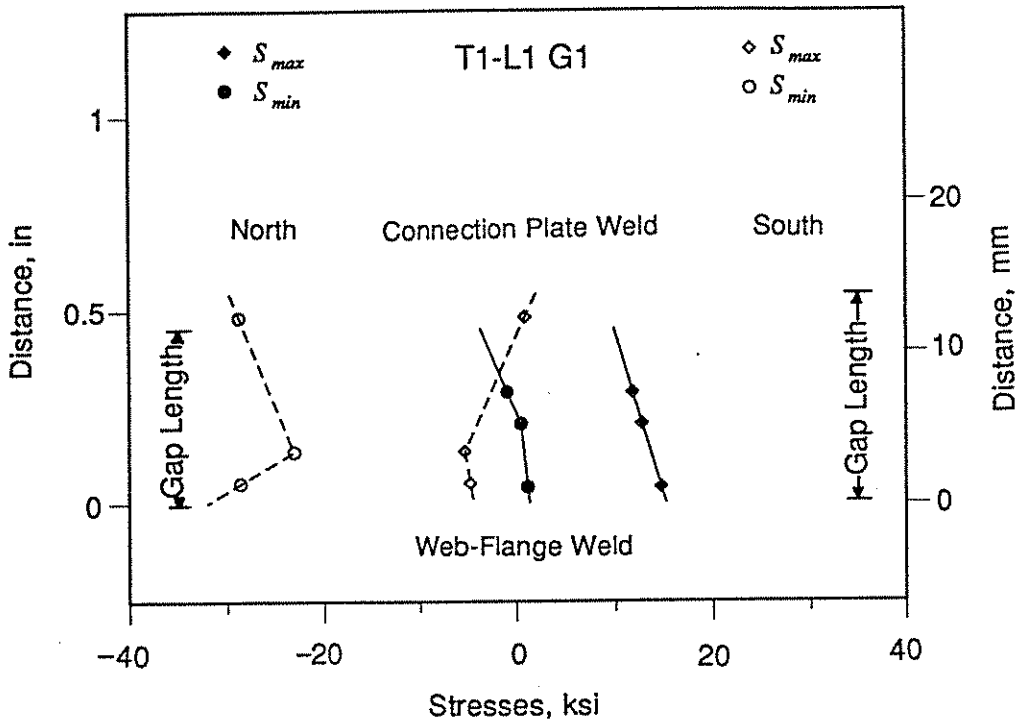

Figure 50: Distortion stresses at Transverse Connection Plate Detail T1-L1 G1 (1 1/2 in. gap) which had no detectable crack growth in web gap

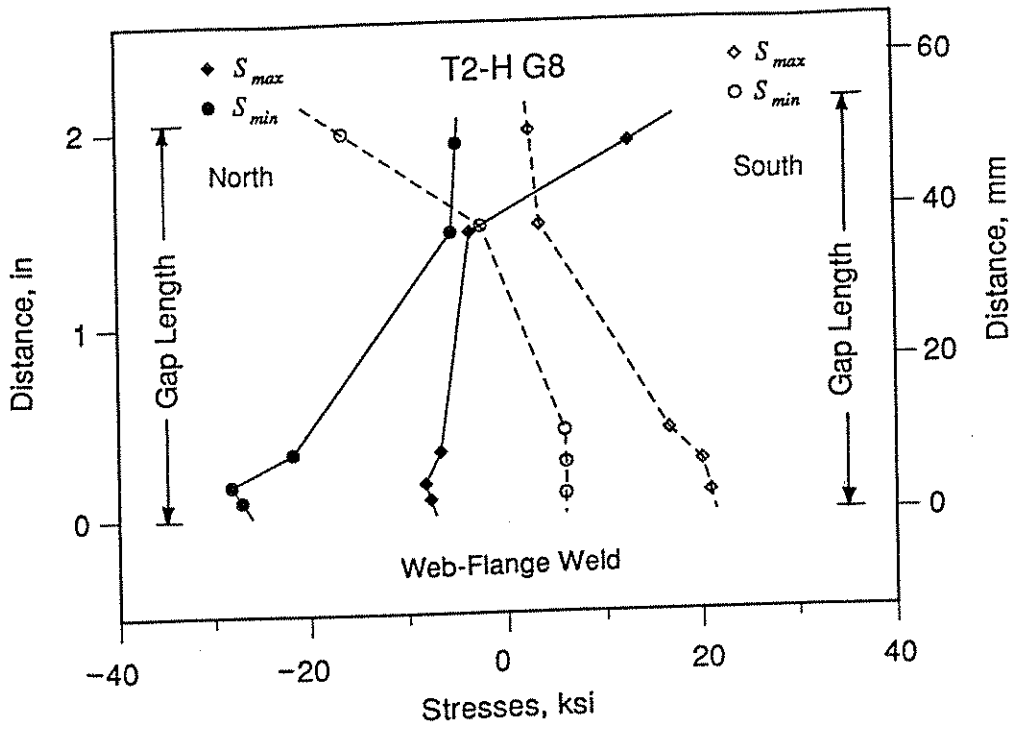

(a)

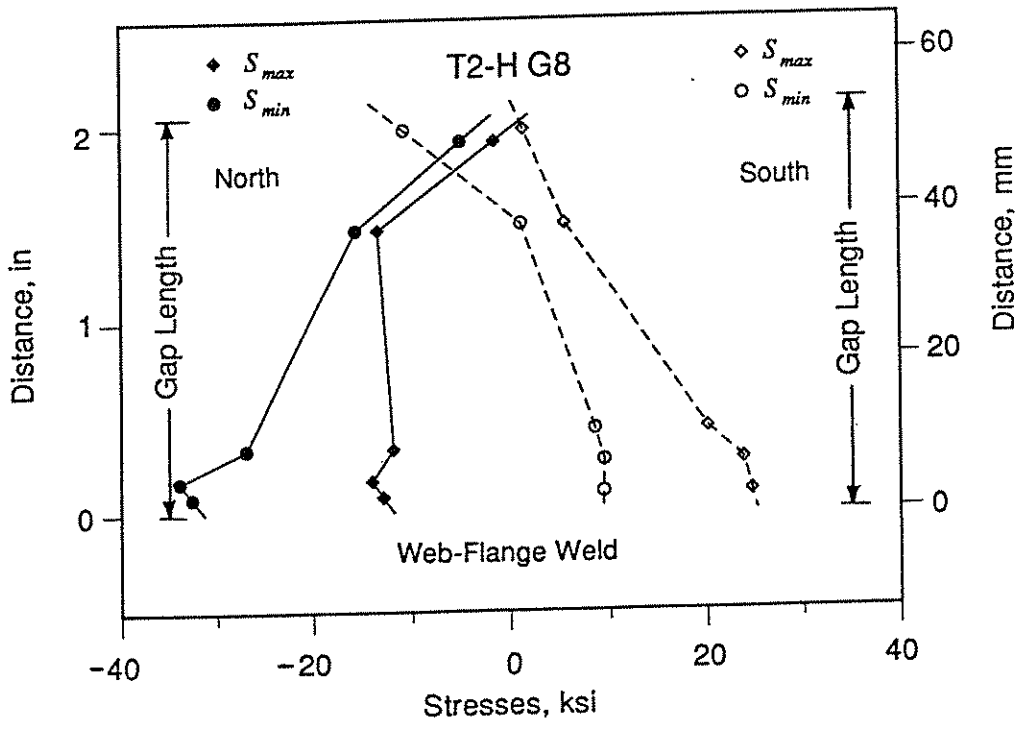

(b)

Figure 51: Stress gradients at Transverse Connection Plate Detail T2-H G8 (3 in. gap) before and after cracking at end of connection plate: (a) prior to cracking; (b) after 0.52×10^6 cycles and visible cracking

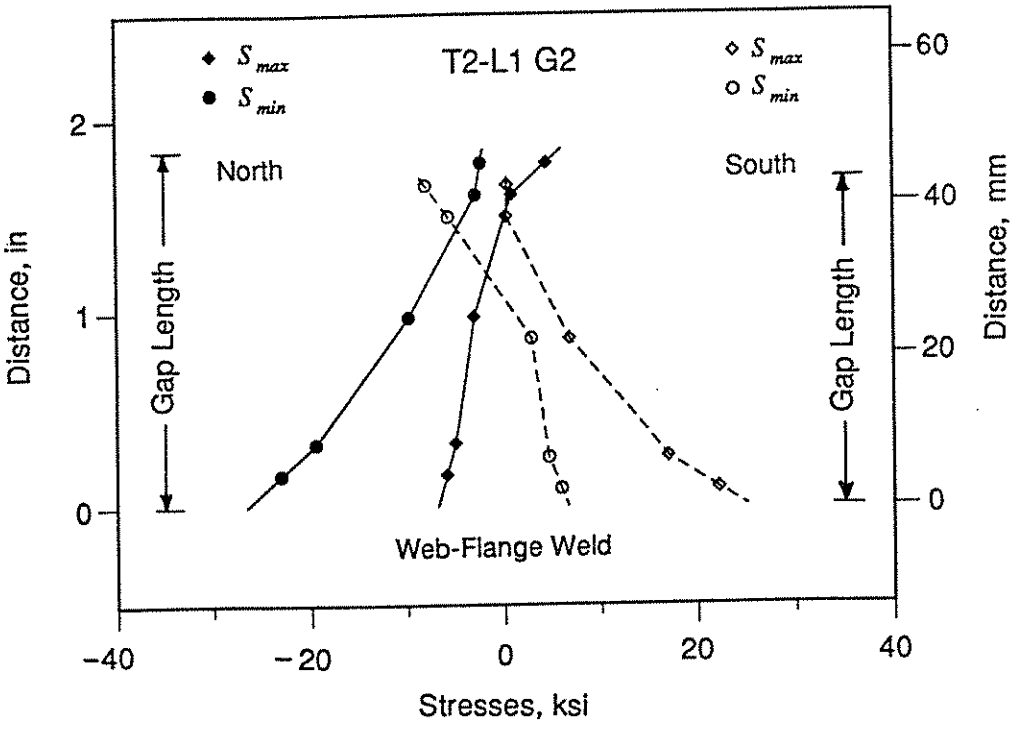

Figure 52: Stress gradients at Transverse Connection plate Detail T2-L1 G2 (3 in. gap) before and after cracking at end of connection plate: (a) At start of test; (b) After cracking at 4.5×10^6 cycles

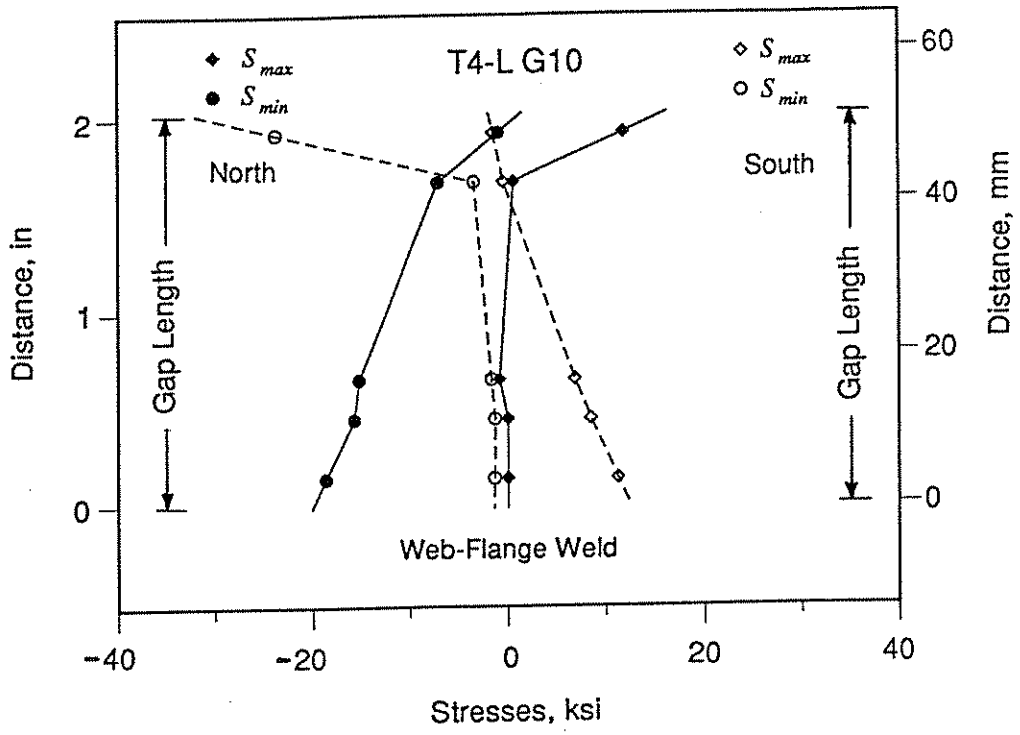

Figure 53: Stress gradients at Transverse Connection Plate Detail T4-L G10 (3 in. gap) before and after cracking at end of connection plate: (a) At start of test; (b) After 3.3×10^6 cycles and visible cracking

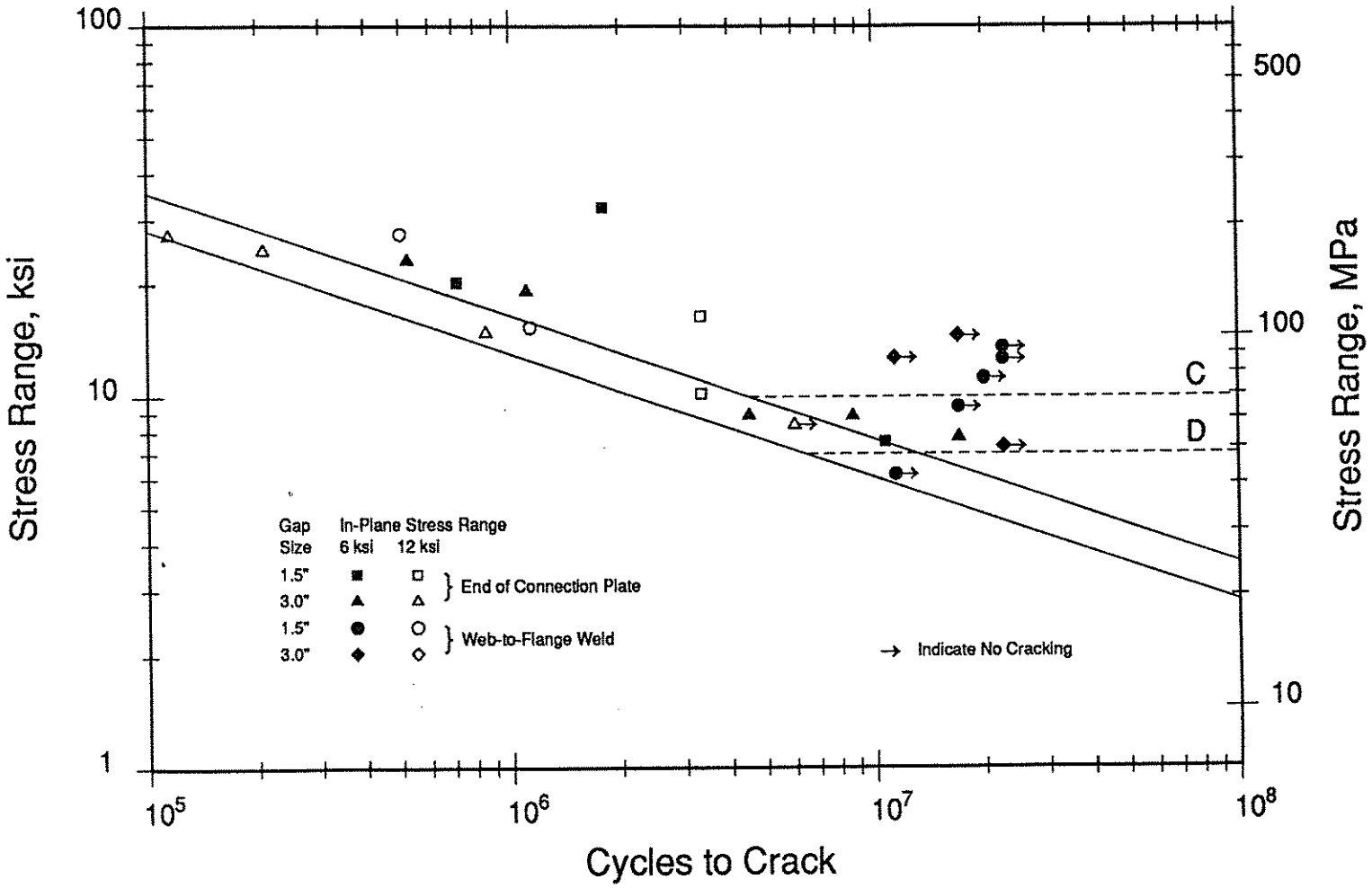

Figure 54: Cycles at which cracks were first detected at transverse connection plate details

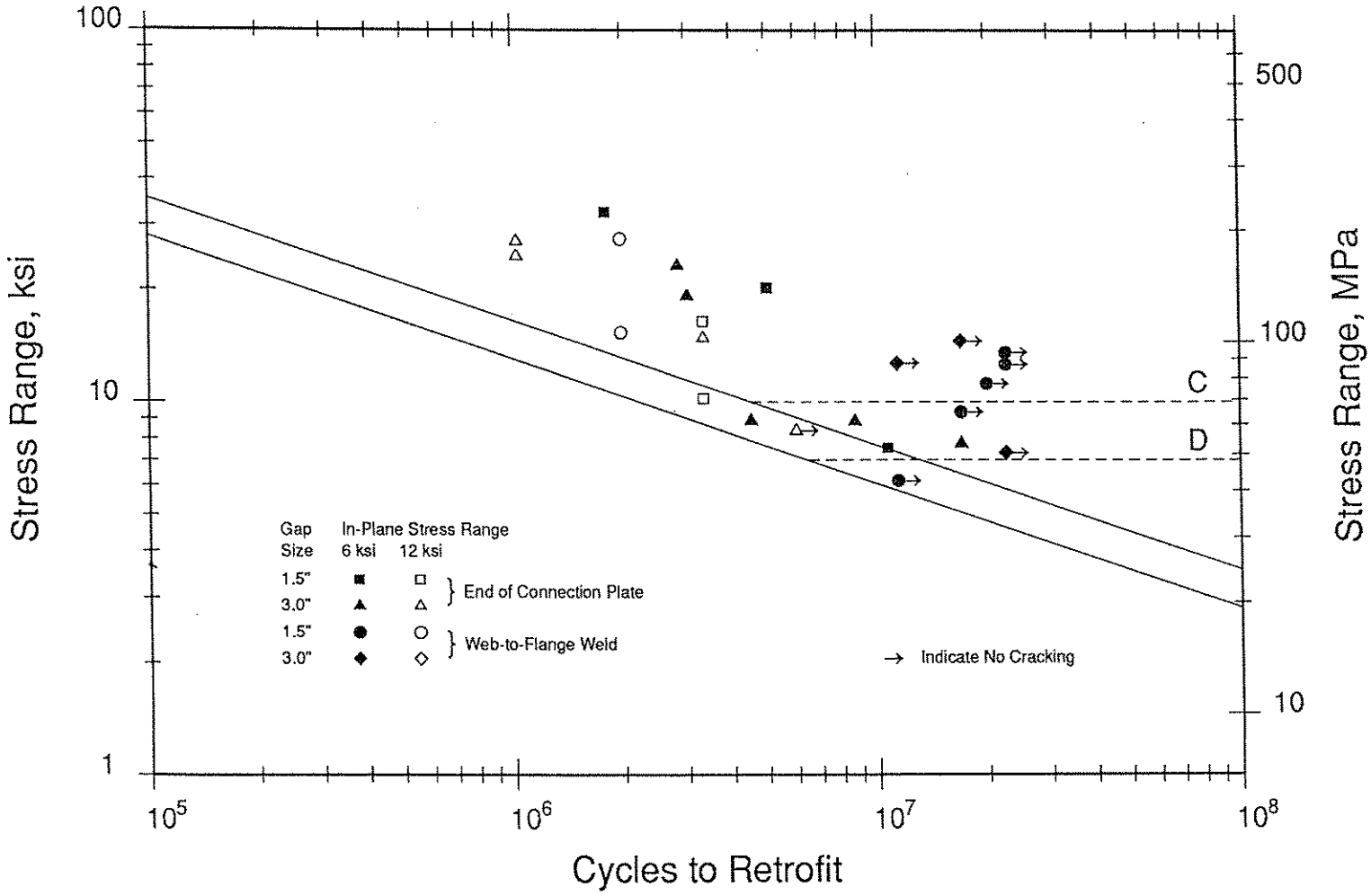

Figure 55: Comparison of cycle life at time details were retrofitted at transverse connection plate details

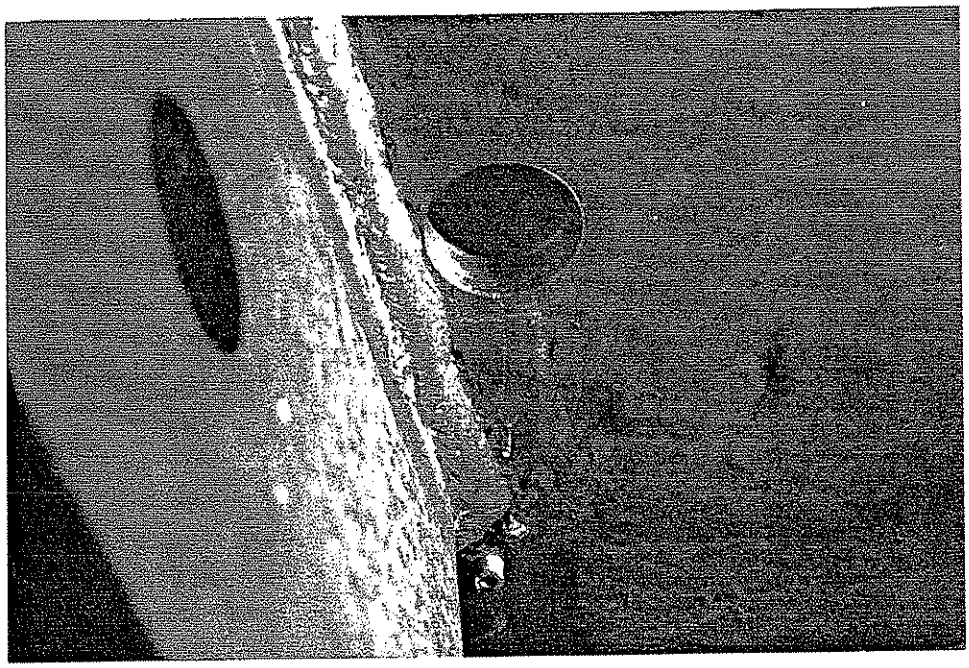

Figure 56: Retrofit hole(7/8 in.) at crack tip T2-H G8

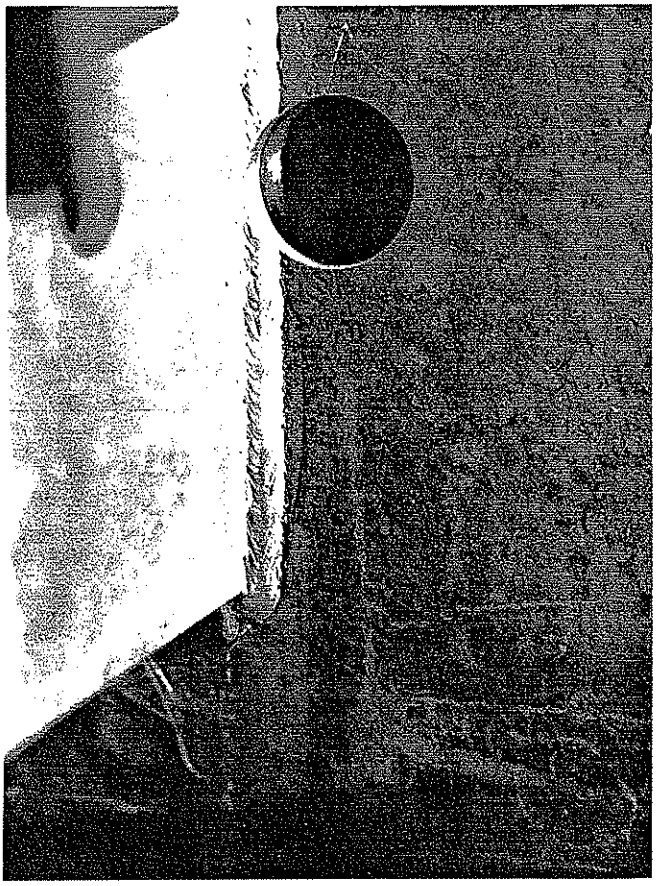

Figure 57: Retrofit hole (1 1/4 in.) at crack tip T4-I G12

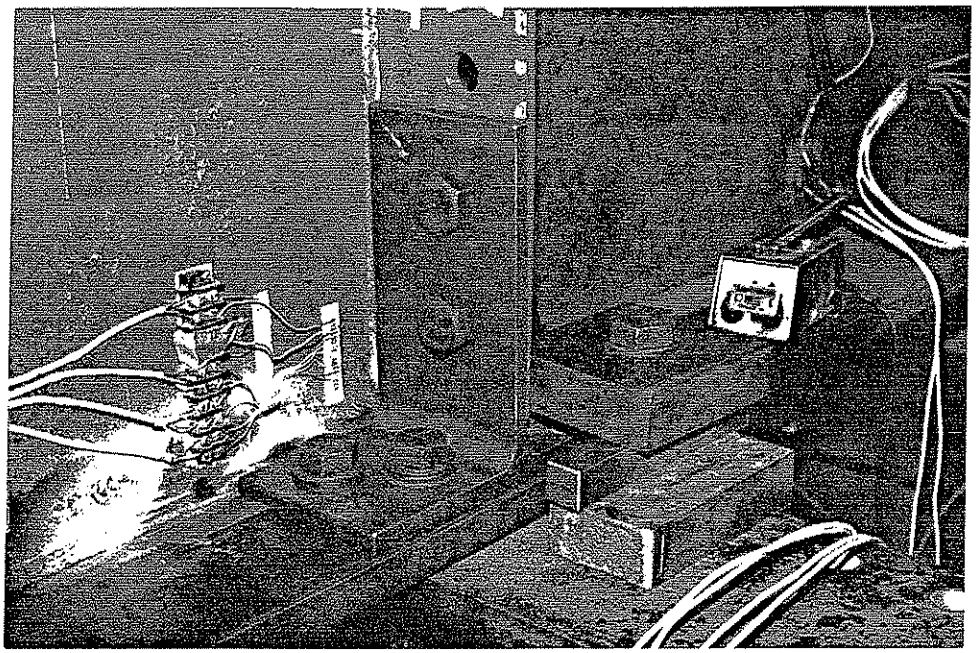

Figure 58: Retrofit Tee bolted to connection plate and flange (T3-I G11)

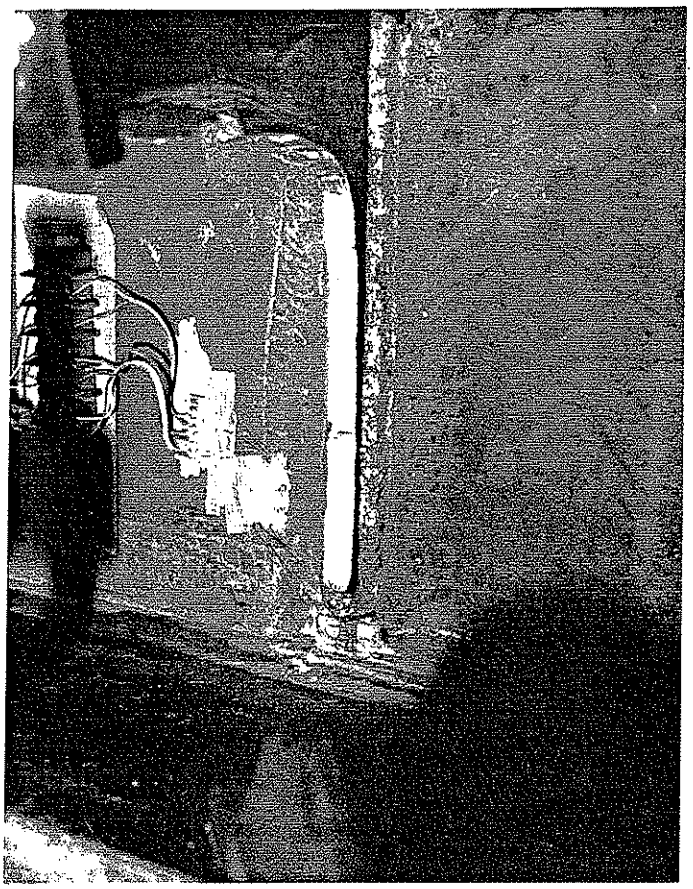

Figure 59: Partial removal of connection plate T1-G7 (1 1/2 in. detail)

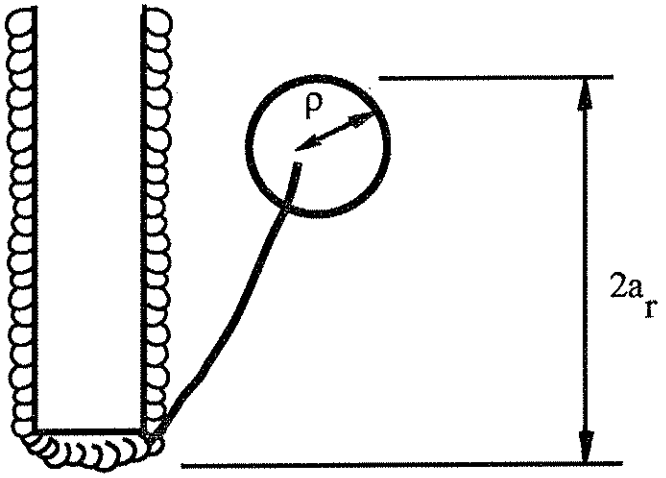

Figure 60: Retrofit hole at transverse connection plate web gap.

APPENDIX A
LATERAL GUSSET PLATE TEST RESULTS

Table A-1: Detail T5-5 (Type B) Web Gaps

	EAST GAP	WEST GAP
NOMINAL GAP SIZE	1½ in.	1½ in.
WELD TOE GAP SIZE	0.35 in.	0.9 in.
EXTRAPOLATED S_R	Not gaged	19.5 ksi
CYCLES TO CRACK		5×10^6
DETECTED CRACK LENGTH		0.13 in.
FIRST RETROFIT		
CYCLES AT RETROFIT		9.4×10^6
CRACK LENGTH AT RETROFIT		6.2 in.
HOLES DRILLED (DIAM.)		1¼ in.
SECOND RETROFIT		
CYCLES AT RETROFIT		11.3×10^6
CRACK LENGTH AT RETROFIT		7.8 in.
RETROFIT PROCEDURES		2 in. hole drilled
THIRD RETROFIT		
CYCLES AT RETROFIT		12×10^6
CRACK LENGTH AT RETROFIT		9.8 in.
RETROFIT PROCEDURES		2 in. hole drilled
TEST TERMINATED AT		20×10^6

Table A-2: Detail T5-9 (Type C) Web Gaps

	EAST GAP	WEST GAP
NOMINAL GAP SIZE	1 in.	1 in.
WELD TOE GAP SIZE	0.2 in.	0.3 in.
EXTRAPOLATED S_R	23.3 ksi	23.3 ksi
CYCLES TO CRACK	1.28×10^6	1.28×10^6
DETECTED CRACK LENGTH	1.0 in.	1.4 in.
FIRST RETROFIT		
CYCLES AT RETROFIT	3.8×10^6	3.8×10^6
CRACK LENGTH AT RETROFIT	2.9 in.	3.3 in.
HOLES DRILLED (DIAM.)	1 in.	1 in.
SECOND RETROFIT		
CYCLES AT RETROFIT	5.0×10^6	5.3×10^6
CRACK LENGTH AT RETROFIT	5.8 in.	4.6 in.
RETROFIT PROCEDURES	1¼ in. holes drilled	Bolted attachment
THIRD RETROFIT		
CYCLES AT RETROFIT	5.3×10^6	
CRACK LENGTH AT RETROFIT	6.4 in.	
RETROFIT PROCEDURES	Bolted attachment	
TEST TERMINATED AT		10×10^6

Table A-3: Detail T5-10 (Type C) Web Gaps

	EAST GAP	WEST GAP
NOMINAL GAP SIZE	1 in.	1 in.
WELD TOE GAP SIZE	0.2 in.	0.2 in.
EXTRAPOLATED S_R	26.3 ksi	26.3 ksi
CYCLES TO CRACK	1.28×10^6	1.28×10^6
DETECTED CRACK LENGTH	1.3 in.	1.0 in.
FIRST RETROFIT		
CYCLES AT RETROFIT	2.9×10^6	2.9×10^6
CRACK LENGTH AT RETROFIT	3.1 in.	2.3 in.
HOLES DRILLED (DIAM.)	3/4 in.	3/4 in.
SECOND RETROFIT		
CYCLES AT RETROFIT	3.8×10^6	5.3×10^6
CRACK LENGTH AT RETROFIT	5.3 in.	3.7 in.
RETROFIT PROCEDURES	1 1/4 in. holes drilled	Bolted attachment
THIRD RETROFIT		
CYCLES AT RETROFIT	5.0×10^6	
CRACK LENGTH AT RETROFIT	6.3 in.	
RETROFIT PROCEDURES	1 in. holes drilled	
FOURTH RETROFIT		
CYCLES AT RETROFIT	5.3×10^6	
CRACK LENGTH AT RETROFIT	8.6 in.	
RETROFIT PROCEDURES	1 1/4 in. holes and bolted attachment	
TEST TERMINATED AT		10×10^6

Table A-4: Detail T5-11 (Type C) Web Gaps

	EAST GAP	WEST GAP
NOMINAL GAP SIZE	3 in.	3 in.
WELD TOE GAP SIZE	2.4 in.	2.6 in.
EXTRAPOLATED S_R	28.3 ksi	Not gaged
CYCLES TO CRACK	1.15×10^6	1.15×10^6
DETECTED CRACK LENGTH	0.85 in.	1.05 in.
RETROFIT		
CYCLES AT RETROFIT	3.3×10^6	3.3×10^6
CRACK LENGTH AT RETROFIT	6.8 in.	2.2 in.
RETROFIT PROCEDURES	1¼ in. holes and bolted attachment	1¼ in. holes and bolted attachment
TEST TERMINATED AT		10×10^6

Table A-5: Detail T5-12 (Type C) Web Gaps

	EAST GAP	WEST GAP
NOMINAL GAP SIZE	3 in.	3 in.
WELD TOE GAP SIZE	2.6 in.	2.3 in.
EXTRAPOLATED S_R	30.0 ksi	31.5 ksi
CYCLES TO CRACK	1.1×10^6	1.1×10^6
DETECTED CRACK LENGTH	0.8 in.	0.6 in.
RETROFIT		
CYCLES AT RETROFIT	3.3×10^6	3.3×10^6
CRACK LENGTH AT RETROFIT	2.35 in.	1.95 in.
RETROFIT PROCEDURES	1¼ in. holes and bolted attachment	1¼ in. holes and bolted attachment
TEST TERMINATED AT		10×10^6

APPENDIX B
TRANSVERSE CONNECTION PLATE TEST RESULTS

Table B-1: Detail T2-L1 G2 Web Gap

	NORTH SIDE OF WEB PLATE	
NOMINAL GAP SIZE	3 in.	
WELD TOE GAP SIZE	1.81 in.	
IN-PLANE S_R	6.0 ksi	
OUT-OF-PLANE S_R	8.9 ksi	Extrapolated at end of connection plate
CYCLES TO CRACK	4.5×10^6	
INITIAL CRACK LENGTH	0.9 in.	Detected at end of connection plate
TEST TERMINATED AT	22.6×10^6	
FINAL CRACK LENGTH	3.8 in.	

Table B-2: Detail T1-L2 G3 Web Gap

	SOUTH SIDE OF WEB PLATE	
NOMINAL GAP SIZE	1½ in.	
WELD TOE GAP SIZE	0.24 in.	
IN-PLANE S_R	6.0 ksi	
OUT-OF-PLANE S_R	32.5 ksi	Extrapolated at end of connection plate
CYCLES TO CRACK	1.8×10^6	
INITIAL CRACK LENGTH	0.6 in.	Detected at end of connection plate
TEST TERMINATED AT	17.0×10^6	
FINAL CRACK LENGTH	3.1 in.	

Table B-3: Detail T2-L2 G4 Web Gap

	SOUTH SIDE OF WEB PLATE	
NOMINAL GAP SIZE	3 in.	
WELD TOE GAP SIZE	2.75 in.	
IN-PLANE S_R	6.0 ksi	
OUT-OF-PLANE S_R	7.7 ksi	Extrapolated at end of connection plate
CYCLES TO CRACK	17.0×10^6	Crack found after completion of test
CRACK LENGTH	0.25 in.	Embedded in transverse connection plate weld
TEST TERMINATED AT	17.0×10^6	

Table B-4: Detail T1-I G5 Web Gap

	NORTH SIDE OF WEB PLATE	
NOMINAL GAP SIZE	1½ in.	
WELD TOE GAP SIZE	0.5 in.	
IN-PLANE S_R	6.0 ksi	
OUT-OF-PLANE S_R	7.5 ksi	Extrapolated at end of connection plate
CYCLES TO CRACK	10.7×10^6	
INITIAL CRACK LENGTH	0.6 in.	Detected at end of connection plate
TEST TERMINATED AT	20.0×10^6	
FINAL CRACK LENGTH	2.5 in.	

Table B-5: Detail T2-I G5 Web Gap

	NORTH SIDE OF WEB PLATE	
NOMINAL GAP SIZE	3 in.	
WELD TOE GAP SIZE	1.93 in.	
IN-PLANE S_R	6.0 ksi	
OUT-OF-PLANE S_R	8.8 ksi	Extrapolated at end of connection plate
CYCLES TO CRACK	8.7×10^6	
INITIAL CRACK LENGTH	0.6 in.	Detected at end of connection plate
TEST TERMINATED AT	20.0×10^6	
FINAL CRACK LENGTH	1.9 in.	

Table B-6: Detail T2-I G6 Web Gap

	NORTH SIDE OF WEB PLATE	
NOMINAL GAP SIZE	3 in.	
WELD TOE GAP SIZE	1.95 in.	
IN-PLANE S_R	6.0 ksi	
OUT-OF-PLANE S_R	19.2 ksi	Extrapolated at end of connection plate
CYCLES TO CRACK	1.11×10^6	
INITIAL CRACK LENGTH	0.3 in.	Detected at end of connection plate
FIRST RETROFIT		
CYCLES AT RETROFIT	3.02×10^6	
CRACK LENGTH AT RETROFIT	1.2 in.	Crack extension in Path I
RETROFIT PROCEDURE	One 3/4 in. hole	
SECOND RETROFIT		
CYCLES AT RETROFIT	8.75×10^6	
CRACK LENGTH AT RETROFIT	1.4 in.	Crack extension in Path II
RETROFIT PROCEDURE	One 3/4 in. hole	
TEST TERMINATED AT	20.0×10^6	
FINAL CRACK LENGTH	2.6 in.	

Table B-7: Detail T1-H G7 Web Gap

	NORTH SIDE OF WEB PLATE	
NOMINAL GAP SIZE	1½ in.	
WELD TOE GAP SIZE	0.50 in.	
IN-PLANE S_R	6.0 ksi	
OUT-OF-PLANE S_R	20.2 ksi	Extrapolated at end of connection plate
CYCLES TO CRACK	0.71×10^6	Detected at end of connection plate
CRACK LENGTH	0.4 in.	
FIRST RETROFIT		
CYCLES AT RETROFIT	3.02×10^6	
CRACK LENGTH AT RETROFIT	1.8 in.	
RETROFIT PROCEDURE	5½ in. connection plate removed	
SECOND RETROFIT		
CYCLES AT RETROFIT	6.96×10^6	
CRACK LENGTH AT RETROFIT	2.1 in.	
RETROFIT PROCEDURE	5½ in. connection plate removed	
TEST TERMINATED AT	11.4×10^6	
FINAL CRACK LENGTH	2.3 in.	

Table B-8: Detail T2-H G8 Web Gap

	NORTH SIDE OF WEB PLATE	
NOMINAL GAP SIZE	3 in.	
WELD TOE GAP SIZE	2.01 in.	
IN-PLANE S_R	6.0 ksi	
OUT-OF-PLANE S_R	23.3 ksi	Extrapolated at end of connection plate
CYCLES TO CRACK	0.52×10^6	
INITIAL CRACK LENGTH	0.45 in.	Detected at end of connection plate
RETROFIT		
CYCLES AT RETROFIT	2.85×10^6	
CRACK LENGTH AT RETROFIT	2.0 in.	Crack extension in Path I
RETROFIT PROCEDURE	One 1 in. hole	
TEST TERMINATED AT	11.4×10^6	
FINAL CRACK LENGTH	2.8 in.	Crack extended 0.8 in. in Path II

Table B-9: Detail T3-L G9 Web Gap

	SOUTH SIDE OF WEB PLATE	
NOMINAL GAP SIZE	1½ in.	
WELD TOE GAP SIZE	1.13 in.	
IN-PLANE S_R	12.0 ksi	
OUT-OF-PLANE S_R	16.4 ksi	Extrapolated in transverse connection plate weld
CYCLES TO CRACK	3.33×10^6	
INITIAL CRACK LENGTH	0.45 in.	Embedded in transverse connection plate weld
TEST TERMINATED AT	6.0×10^6	
FINAL CRACK LENGTH	0.9 in.	

Table B-10: Detail T3-L G10 Web Gap

	NORTH SIDE OF WEB PLATE	
NOMINAL GAP SIZE	1½ in.	
WELD TOE GAP SIZE	0.3 in.	
IN-PLANE S_R	12.0 ksi	
OUT-OF-PLANE S_R	10.2 ksi	Extrapolated at end of connection plate
CYCLES TO CRACK	2.5×10^6	
INITIAL CRACK LENGTH	0.4 in.	Detected at end of connection plate
TEST TERMINATED AT	6.0×10^6	
FINAL CRACK LENGTH	1.1 in.	

Table B-11: Detail T4-L G10 Web Gap

	NORTH SIDE OF WEB PLATE	
NOMINAL GAP SIZE	3 in.	
WELD TOE GAP SIZE	2.02 in.	
IN-PLANE S_R	12.0 ksi	
OUT-OF-PLANE S_R	14.8 ksi	Extrapolated at end of connection plate
CYCLES TO CRACK	0.86×10^6	Detected at end of connection plate
INITIAL CRACK LENGTH	0.3 in.	
RETROFIT		
CYCLES AT RETROFIT	3.33×10^6	
CRACK LENGTH AT RETROFIT	1.7 in.	
RETROFIT PROCEDURE	Bolted attachment	
TEST TERMINATED AT	6.0×10^6	
FINAL CRACK LENGTH		Crack entered the bottom flange

Table B-12: Detail T3-I G11 Web Gap

	NORTH SIDE OF WEB PLATE	
NOMINAL GAP SIZE	1½ in.	
WELD TOE GAP SIZE	0.44 in.	
IN-PLANE S_R	12.0 ksi	
OUT-OF-PLANE S_R	27.5 ksi	Extrapolated at web-flange weld
CYCLES TO CRACK	0.50×10^6	
INITIAL CRACK LENGTH	0.7 in.	Detected at web-flange weld
RETROFIT		
CYCLES AT RETROFIT	1.98×10^6	
CRACK LENGTH AT RETROFIT	5.8 in.	Sum of crack extensions in Path I and II
RETROFIT PROCEDURE	Bolted attachment	
TEST TERMINATED AT	3.04×10^6	
FINAL CRACK LENGTH	7.8 in.	

Table B-13: Detail T3-I G12 Web Gap

	SOUTH SIDE OF WEB PLATE	
NOMINAL GAP SIZE	1½ in.	
WELD TOE GAP SIZE	0.40 in.	
IN-PLANE S_R	12.0 ksi	
OUT-OF-PLANE S_R	15.3 ksi	Extrapolated at web-flange weld
CYCLES TO CRACK	1.13×10^6	
INITIAL CRACK LENGTH	0.9 in.	Detected at web-flange weld
RETROFIT		
CYCLES AT RETROFIT	1.98×10^6	
CRACK LENGTH AT RETROFIT	2.6 in.	Sum of crack extensions in Path I and II
RETROFIT PROCEDURE	Bolted attachment	
TEST TERMINATED AT	3.04×10^6	
FINAL CRACK LENGTH	3.8 in.	

Table B-14: Detail T4-I G11 Web Gap

	SOUTH SIDE OF WEB PLATE	
NOMINAL GAP SIZE	3 in.	
WELD TOE GAP SIZE	2.11 in.	
IN-PLANE S_R	12.0 ksi	
OUT-OF-PLANE S_R	24.7 ksi	Extrapolated at end of connection plate
CYCLES TO CRACK	0.21×10^6	
INITIAL CRACK LENGTH	0.45 in.	Detected at end of connection plate
RETROFIT		
CYCLES AT RETROFIT	1.25×10^6	
CRACK LENGTH AT RETROFIT	1.2 in.	Crack extension in Path I
RETROFIT PROCEDURE	One 1 in. hole	
TEST TERMINATED AT	3.04×10^6	
FINAL CRACK LENGTH	2.1 in.	Crack extended 0.9 in. in Path II

Table B-15: Detail T4-I G12 Web Gap

	NORTH SIDE OF WEB PLATE	
NOMINAL GAP SIZE	3 in.	
WELD TOE GAP SIZE	1.90 in.	
IN-PLANE S_x	12.0 ksi	
OUT-OF-PLANE S_x	27.1 ksi	Extrapolated at end of connection plate
CYCLES TO CRACK	0.14×10^6	
INITIAL CRACK LENGTH	0.35 in.	Detected at end of connection plate
FIRST RETROFIT		
CYCLES AT RETROFIT	1.25×10^6	
CRACK LENGTH AT RETROFIT	3.5 in.	Crack extension in Path I
RETROFIT PROCEDURE	One 1¼ in. hole	
SECOND RETROFIT		
CYCLES AT RETROFIT	1.98×10^6	
CRACK LENGTH AT RETROFIT	2.0 in.	Crack extension in Path II
RETROFIT PROCEDURE	4 in. connection plate removed	
TEST TERMINATED AT	3.04×10^6	
FINAL CRACK LENGTH	6.4 in.	